LEACHING OF HEAVY METALS FROM FLY ASH STABILIZED SOILS USED IN HIGHWAY PAVEMENTS

by

Md Sazzad Bin-Shafique, Craig H. Benson, and Tuncer B. Edil

Final Report

To

Combustion Byproducts Recycling Consortium

West Virginia University

February 2003

EXECUTIVE SUMMARY

This study was conducted to evaluate the potential for leaching of metals from fly ash stabilized subgrade soils used in highway construction. Four different tasks were undertaken: (1) water leach testing (WLT), (2) laboratory column testing, (3) field lysimeter testing, and (4) numerical modeling. Testing was conducted on soil-fly ash mixtures that were prepared with three locally available fly ashes and four subgrade soils representing a range of subgrade soil conditions that might be encountered in Wisconsin.

The WLTS showed that concentrations of metals in the leachate from soil-fly ash mixtures tend to be lower (1.5 to 2.5 times) than those from fly ash alone. The concentration increases non-linearly with increasing fly ash content, and cannot be estimated from a simple dilution calculation. The partitioning of metals between the solid and liquid phases is non-linear because the pH of the leachate increases non-linearly with increasing fly ash content.

Column leaching tests conducted in the laboratory showed that the pH of the effluent and initial effluent concentration from soil-fly ash mixtures increases with increasing fly ash content. The initial effluent concentration depends primarily on the type of fly ash, and the retardation factor depends primarily on the type of soil that is used to prepare the soil-fly ash mixture. The partition coefficient increases slightly for soils having higher CEC. The release pattern for metals from the soil-fly ash mixtures

appears to be adsorption-controlled. The pH of the pore fluid is persistent for at least 30 pore volumes of flow, which corresponds to at least 30-yrs of flow in the field.

Lysimeters installed at the field sites show that the average annual water flux through the stabilized soil layer is approximately 4-6% of the average annual precipitation, and is comparable to that from a control section constructed without fly ash. Concentrations of most of the metals of concern are higher in leachate collected from the fly ash stabilized pavement section than the control pavement section, and decreased slightly over time. Concentrations of metals in the field leachate agree well with concentrations in the effluent from the column leaching tests conducted in the laboratory, which suggests that transport parameters obtained from the column leaching tests can be used to predict field conditions.

A numerical model was developed to simulate typical field scenarios where subgrade is stabilized with fly ash. Simulations conducted using transport parameters obtained from the column tests showed that the maximum concentration decreases by about 5 times within the first meter below a fly ash stabilized layer, and then decreases more gradually at deeper depths. The maximum concentration at a given depth is independent of the retardation factor, and decreases with increasing dispersion coefficient and decreasing thickness of the stabilized layer. The time to reach the maximum concentration at a particular depth is independent of the thickness of the stabilized layer, and increases as the dispersion coefficient decreases and the retardation factor increases.

Design charts based on the results of numerical simulations are presented that can be used to quantify the maximum relative concentration at a particular depth and

the time required to achieve the maximum concentration. The only required parameter is the initial effluent concentration, which depends primarily on the type of fly ash and can be estimated from a water leach test. To determine the time required to achieve the maximum concentration at a given depth, the Darcy flux and the retardation factor are required. The retardation factor depends primarily on the type of soil being stabilized, but does not vary significantly for fine-grained soils. Thus, quick and reasonable predictions can be made using a conservative estimate of the retardation factor and Darcy flux.

ACKNOWLEDGEMENTS

Financial support for this project was provided by the U.S. Department of Energy through the Combustion Byproduct Recycling Consortium (CBRC) and by the Consortium for Fly Ash Use in Geotechnical Applications at the University of Wisconsin-Madison (Mineral Solutions, Inc., Alliant Energy, Inc., and Xcel Energy Services, Inc.). The support of these parties is gratefully acknowledged. The Wisconsin Department of Transportation and D'Onofrio Kottke & Associates, Inc. are acknowledged for their support and cooperation associated with the field tests. The findings and opinions expressed in this report are solely those of the authors. Endorsement by the sponsors is not implied and should not be assumed.

TABLE OF CONTENTS

LIST OF FIGURES

LIST OF TABLES

SECTION 1

INTRODUCTION

The use of fly ash is generally governed by regulations and guidelines promulgated by state environmental regulatory agencies (Kyper 1992). In Wisconsin, fly ash use is regulated by Ch. NR 538 of the Wisconsin Administrative Code. NR 538 encourages beneficial use of industrial byproducts to an extent that is consistent with protection of public health and the environment. According to NR 538, byproducts are classified into "categories" (Categories 1-5) that define applications where the byproducts can be used. Byproducts are assigned into categories based on the concentration of potential contaminants from elemental analysis and/or from water leach tests.

NR 538 defines twelve "methods" in which byproducts can be used, and the categories of byproducts suitable for each method. Using fly ash to stabilize soil in confined geotechnical fill, such as road subbase, is Beneficial Use Method 5. Industrial byproducts falling into Categories 1-4 can be used for Method 5, with Category 4 being the least stringent. To qualify for Category 4, fly ash has to be tested for five species (Cd, Cr, Se, Ag, and SO_4^{-2}) and concentrations of these species must not exceed the limits set in NR 538.

From a regulatory perspective, fly ash only needs to be tested for the required species using a water leach test (WLT) following ASTM D 3987. Site-specific tests, such as properties of the soil, depth to groundwater, and properties of the stabilized subbase, are not required. The primary objective of this study was to

go beyond that required in NR 538, and to conduct an in-depth geoenvironmental assessment of the potential for groundwater contamination by fly ash stabilized soil.

Four different tasks were conducted as part of this assessment: (1) water leach testing, (2) laboratory column testing, (3) field lysimeter testing, and (4) numerical modeling. This report describes the work conducted on these tasks. Section 2 presents a literature review of past research on environmental assessment of fly ash and on the theoretical background of contaminant transport. Section 3 describes the materials used for this study. The experimental methods are described in Section 4. Section 5 describes the experimental results. The numerical simulations and the parametric studies are described in Section 6. Findings of the study are summarized in Section 7.

SECTION 2

BACKGROUND

2.1 FLY ASH

More than 65 million Mg of fly ash is generated in the US each year as a byproduct of burning coal at electric power plants, making fly ash one of the most plentiful of the industrial byproducts (Collins et al. 1992). Fly ash is a pozzolan, that is, a siliceous or siliceous-aluminous material that becomes cementitious when combined with an activator (lime, Portland cement, or kiln dust) in the presence of water. Fly ash has been recycled as an engineering material for many years because of its pozzolanic characteristics (Ghosh and Subbarao 1998). For example, as early as 1914, *Engineering News Record* published research results recognizing that Portland cement concrete can benefit from the addition of fly ash (FHWA 1995).

2.1.1 Origin of Fly Ash

Fly ash is the finely divided mineral residue resulting from combustion of ground or powdered coal at electric generating plants (ASTM C 618). Fly ash consists of organic and inorganic matter present in coal that has been fused during coal combustion. This material is solidified while suspended in the exhaust gases, and is collected by electrostatic precipitators. Since the particles solidify while suspended in the exhaust gases, fly ash particles are generally very fine (silt size, 0.074 - 0.005 mm) and spherical in shape (Ferguson 1993).

2.1.2 Fly Ash Classification

Fly ash is classified into two classes, F and C, based on the chemical composition of the fly ash. The chemical requirements stipulated in ASTM C 618 for classifying fly ashes are shown in Table 2.1. When the chemical composition does not comply with the requirements either for Class C or F that stipulated in ASTM C 610, the fly ash is classified as off-specification fly ash.

Class F fly ash is produced from burning anthracite and bituminous coals. This fly ash has siliceous or siliceous and aluminous material, which itself possesses little or no cementitious value but will, in finely divided form and in the presence of moisture, chemically react with calcium hydroxide at ordinary temperature to form cementitious compounds (Chu et al. 1993). Class C fly ash is normally produced from lignite and sub-bituminous coals, and usually contains a significant amount of calcium hydroxide (CaO), also known as lime (Cockrell et al. 1970). In addition to having pozzolanic properties, Class C fly ash also is cementitious (ASTM C 618-99). After the introduction of the Clean Air Act Amendments of 1990, utilities in the western and mid-western regions of the United States (US) began burning sub-bituminous coal in their power plants to meet more stringent EPA sulfur emission standards. As a result, self-cementing Class C fly ash has become widely available.

Color is useful for estimating the calcium oxide content and organic content of fly ash. Lighter color fly ash generally has a greater percentage calcium oxide. Darker colors suggest higher organic content (Cockrell et al. 1970).

Table 2.1. Chemical Requirements for Fly Ash Classification.

Properties	**Fly Ash Class**	
	Class F	**Class C**
Silicon dioxide (SiO_2), aluminum oxide (Al_2O_3), and iron oxide (Fe_2O_3), min, %	70.0	50.0
Sulfur trioxide (SO_3), max, %	5.0	5.0
Moisture content, max, %	3.0	3.0
Loss on ignition, max, %	6.0	6.0

2.1.3 Fly Ash Applications

Although a majority of fly ash produced in the United States is currently landfilled, 22% of fly ash is used in a variety of beneficial applications (FHWA 1995). The increased cost and potential environmental impacts of landfilling has caused regulatory agencies to encourage more beneficial use of fly ash (Ghodrati et al. 1995). As a result, new and innovative uses of fly ash are continually being researched and developed (Torrey 1978).

Fly ash is frequently used in Portland cement concrete, stabilized roadbase, structural fills, and flowable fills. Fly ash is also used in soil stabilization, in waste stabilization, in asphalt mixes, in cold recycled bituminous pavement, and in grouts for concrete pavement subsealing (Cross and Fager 1993). Land application as an agricultural amendment has also been advocated as a promising large-scale utilization option (Clark et al. 1995, Sikka and Kansal 1995, Adriano et al. 2001).

Fly ash is used in Portland cement concrete to take the advantage of the pozzolanic characteristic of fly ash. Pozzolans in fly ash react with the cementitious material in cement and increase the strength and workability of concrete (Malhotra and Mehta 1996).

Fly ash and lime are combined with aggregates to produce a good quality stabilized roadbase. The resulting material is produced and placed like cement-stabilized aggregate base. Stabilization with fly ash makes a strong and durable base from a locally available material at a lower cost.

Fly ash can be used as bulk fill material in geotechnical fill, such as in construction of embankments, dykes, and road subgrade (DiGioia and Nuzzo 1972,

Gray and Lin 1972). The advantages of using fly ash as a bulk fill material include low cost, low unit weight, and good strength.

Fly ash is used in flowable fill, that is, a mixture of coal fly ash, water, sand, and Portland cement. Flowable fill flows like a liquid, and sets up like a solid. Flowable fill is self-leveling and does not require compaction or vibration to achieve maximum density (FHWA 1995).

Fly ash has been used in soil stabilization to improve the mechanical properties of soils for more than 20 years (Ferguson 1993). Fly ash is mixed with wet soil and then the mixture is compacted and allowed to cure to gain strength. In some cases, an activator (e.g., lime) is added to the mixture. Combustion of sub-bituminous coal produces a fly ash that has higher lime content and shows self-cementing characteristics. Thus, fly ashes from sub-bituminous coals generally do not need an activator.

2.1.4 Regulatory Requirements

Although many beneficial applications exist for fly ash, it can only be used if the fly ash and the application comply with regulatory requirements (Kyper 1992). Use of fly ash in Wisconsin is regulated by Ch. NR 538 of the Wisconsin Administrative Code (a copy of NR 538 is in Appendix A). NR 538 classifies byproducts into “categories” (Categories 1-5) depending on their chemical composition and leachate characteristics, and defines twelve “methods” in which byproducts can be used. The application of fly ash to stabilize soil as confined geotechnical fill, such as road subbase, is Beneficial Use Method 5. Industrial

byproducts falling into Categories 1-4 can be used for Method 5, with Category 4 being the least stringent. To qualify for Category 4, a leaching test (ASTM D 3987-85) has to be conducted on the fly ash. The leachate is analyzed for five species (Cd, Cr, Se, Ag, and SO_4^{-2}) and aqueous concentrations of these species must not exceed the standards set in NR 538. Typically Wisconsin fly ashes are likely to qualify for Category 4 industrial byproduct.

2.1.5 Limitations of Current Leaching Test Methods

A key limitation of current leach testing methods is that the tests do not consider the setting in which the byproducts will be used. NR 538 considers the use of byproducts in bulk form, but not mixtures, such as fly ash and soil. Mixtures may behave differently than the byproduct alone, limiting the validity of tests conducted using only the byproduct (Gustin et al. 1996). For example, water leach testing of fly ash stabilized soil probably provides a more representative estimate of contaminant release for soil stabilization applications than tests solely on fly ash.

Water leach tests do not yield leachate representative of that produced in the field and do not simulate a site-specific leaching condition. The lack of correspondence between test conditions and conditions encountered in the field environment hampers quantitative interpretation of water leach tests (Walton et al. 1997). Water leach tests can provide the potential for contaminant release from soil-fly ash mixtures, but are not adequate to evaluate how a soil-fly ash mixture used as subbase will impact groundwater.

2.2 FLY ASH CHEMISTRY

2.2.1 Chemical Composition of Fly Ash

The chemical constituents of fly ash depend mainly on the chemical composition of the coal. However, fly ashes that are produced from the same source or have very similar chemical composition can have significantly different ash mineralogies depending on the coal combustion technology that was used. Consequently, the ash hydration properties as well as the leaching characteristics can vary significantly between generating facilities (Torrey 1978).

Typical chemical compositions of Class F and Class C fly ash are shown in Table 2.2, along with the chemical composition of Portland cement (FHWA 1995). The primary inorganic chemical constituents of fly ash are the oxides of Si, Al, Fe, and Ca. Fly ash also contains lesser amounts of Mg, S, Na, K, as well as very small quantities (mg/kg) of trace metals (Torrey 1978). Organic compounds in fly ash include unburned carbon and very small quantities (mg/kg) of organic pollutants (see Appendix B).

2.2.1.1 Mineralogy of Fly Ash

The inorganic oxides in fly ash may be in crystalline or glassy phases. The relative amounts of crystalline and glassy phase materials in fly ash depend largely on the combustion and glassification process used at the particular power plant. When the maximum temperature of the combustion process is above 1200^0 C and the cooling time is short, the ash is mostly glassy phase material (McCarthy et al.

Table 2.2. Typical Chemical Composition of Fly Ash.

Chemical Species	Percent of Composition		
	Typical Class C	**Typical Class F**	**Typical Portland Cement**
CaO (lime)	24	9	64
SiO_2	40	55	23
Al_2O_3	17	26	4
Fe_2O_3	6	7	2
MgO	5	2	2
SO_3	3	1	2

1987). When a more gradual cooling of the ash particles occurs, crystalline-phase calcium compounds are formed. The minerals present in the coal dictate the elemental composition of the fly ash, but the mineralogy and crystallinity of the ash are dictated by the boiler design and operation. The primary factors that influence the mineralogy of a coal fly ash are chemical composition of the coal, coal combustion process including coal pulverization, combustion, flue gas clean up, fly ash collection operations, and the additives used during combustion, including oil additives for flame stabilization and corrosion control additives (Baker 1987).

Hydration and leaching properties of fly ash are significantly influenced by the mineralogy of the fly ash, which includes the relative proportion of the spherical glassy phase and crystalline materials, the size distribution of the ash, the chemical nature of glass phase, and the type of crystalline material (Roy et al. 1985).

2.2.1.2 Heavy Metals in Fly Ash

Fly ash contains a small amount of trace metals that can have environmental consequences when fly ash is used in geotechnical applications. The amount and distribution of metals in fly ash depend mainly on the type of coal and the burning process. The heavy metals are more or less uniformly distributed in coal. In the combustion zone, metals or metal species act differently depending on their thermal behavior. Partitioning of metals into the solid and gas phases occurs according to the combustion temperature and the chemical environment in the combustion chamber (Binner et al. 1997).

The volatile metals evaporate at the high temperature of the boiler. The extent of evaporation depends on complex and interrelated factors such as operating temperature, oxidative and reductive conditions, and the presence of scavengers, mainly halogens (Evans et al. 2000). As the gases cool through the post-furnace system, the metal species condense and are trapped into the glassy phase or adsorbed onto ash particles through a range of processes (Barton et al. 1990).

Lithophilic metals, such as Co, Cr, Mn, and V, are usually tightly fixed in the coal and are hardly vaporized. As a result, they tend to be equally distributed between bottom ashes and fly ashes. Heavy metals released into the gas phase during combustion are called volatile metals. Highly volatile elements, such as Hg and Tl, are emitted almost totally in the vapor phase and thus are not found in significant amounts in fly ash. Elements, such as As, Cd, Cu, Pb, and Zn are vaporized at intermediate temperature, and are found primarily in fly ash (Yan et al. 2001). Since the amount and distribution of metals in fly ash remain relatively constant for a particular ash source, leachable materials also remain relatively constant.

2.2.2 Hydration of Fly Ash

Formation of cementitious material by the reaction of CaO (lime) with the pozzolans (AlO_3, SiO_2, Fe_2O_3) in the presence of water is known as hydration of fly ash. The hydrated calcium silicate gel or calcium aluminate gel (cementitious

material) can bind inert material together. The pozzolanic reactions are as follows (TRB 1987):

$$CaO + H_2O \rightarrow Ca(OH)_2 \quad (2.1)$$

$$Ca(OH)_2 \rightarrow Ca^{++} + 2[OH]^- \quad (2.2)$$

$$Ca^{++} + 2[OH]^- + \underset{\text{(silica)}}{SiO_2} \rightarrow \underset{\text{(gel)}}{CSH} \quad (2.3)$$

$$Ca^{++} + 2[OH]^- + \underset{\text{(alumina)}}{Al_2O_3} \rightarrow \underset{\text{(gel)}}{CAH} \quad (2.4)$$

For Class C fly ash, the calcium oxide (lime) in the fly ash reacts with the siliceous and aluminous materials (pozzolans) in the fly ash. A similar reaction can occur in Class F fly ash, but lime must be added because the lime content of the ash is too low. Lime stabilization of soils occurs in a similar manner, where the pozzolanic reactions depend on the siliceous and aluminous materials provided by the soil.

Presence of other chemical constituents in the fly ash can significantly affect the hydration reaction. Hydration of tricalcium aluminate in the fly ash provides one of the primary cementitious products in many fly ashes. The rapid rate at which hydration of tricalcium aluminate occurs results in a rapid set, and is the reason why delays in compaction result in lower strengths of fly ash stabilized soils (Boles 1986).

The effect of stabilization cannot be predicted based solely on the chemical composition of the fly ash (Boles 1986). The hydration chemistry of fly ash depends on the chemical properties of the fly ash and the soil being stabilized.

2.3 LEACHING

If water contacts or passes through a porous media, each constituent present in the matrix dissolves into pore water at some finite rate because there is no such thing as a completely insoluble material (Conner 1990). Permeation of the contaminated pore water out of the porous matrix due to any driving force is called "leaching." The contaminated water that is generated as water passes through a porous matrix is called "leachate." The capacity of the waste material to leach is called its "leachability."

2.3.1 Leaching Mechanisms

The main mechanisms that cause leaching are shown in Fig. 2.1. When a porous matrix containing heavy metals is exposed to an aqueous solution, the pore water becomes contaminated due to desorption of metals or/and dissolution of metal compounds. The process of desorption of metals or dissolution of metal compounds in the pore water is called "solubilization" (Conner 1990). The difference in chemical potential between the pore fluid and the fluid surrounding the porous matrix induces diffusion of metals through pore fluid and causes leaching. When the aqueous solution or water passes through the porous matrix, contaminant

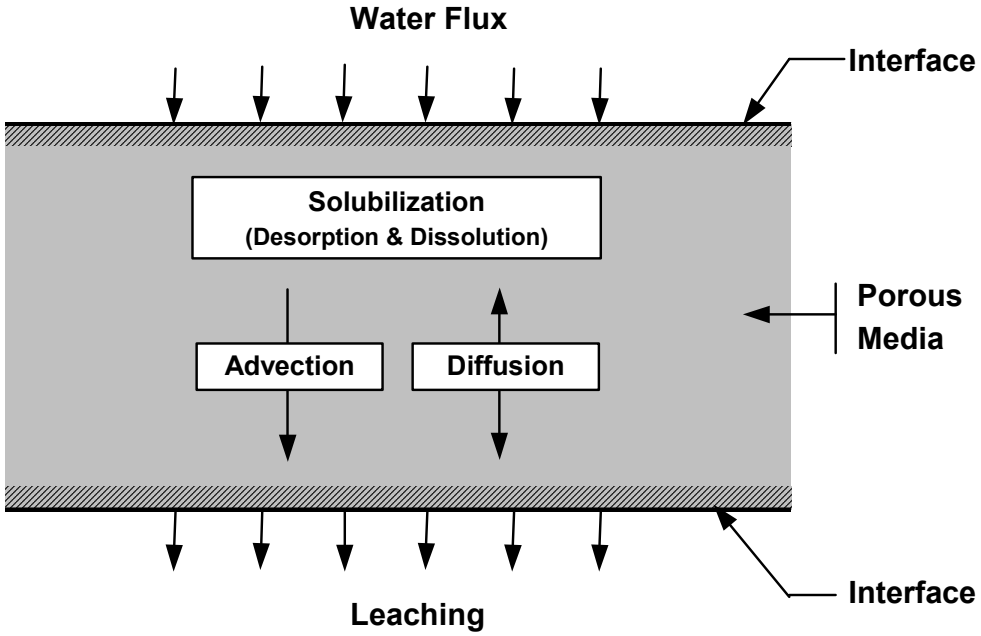

Fig. 2.1. Schematic of Leaching Mechanisms (adapted from Cote et al. 1985).

transport occurs due to advection along with the diffusion of contaminants through pore water.

2.3.2 Factors Affecting Leaching

2.3.2.1 Solubility of Metals

The solubility of heavy metals in water depends on hydrolysis, and the presence of other organic and inorganic ligands, their coordination chemistry, and the pH of the solution. The formation constants for the inorganic ligand-metal complexes are well known for many complexes and can be used to calculate the distribution of metal over its various forms in solution (Allen et al. 1993). However, the formation constants for complexes between metals and natural dissolved organic ligands are not well documented (Allen et al. 1993) because of the absence of reliable physical chemical models that can account for metal binding to natural organic matter. The lack of physical chemical models seriously hinders the theoretical determination of solubility of a metal in water having different organic ligands.

Chemical analyses show that there are so many different types of organic ligands present in fly ash that the speciation of metals is very complex. Regardless of the speciation, solubility of different metal species is highly dependent on pH of the solution. The pH of the pore fluid of soil-fly ash is often very high and the solubility is usually very low at higher pH.

Solubility of the metal (hydr)oxides and carbonates is shown in Fig. 2.2 as a function of pH. The metal (hydr)oxide or carbonate is assumed to be the only ligand present in the solution. The solubility decreases linearly with increasing pH. [Me^{+z}] represents the metal ion concentration in equilibrium with solid phase. Since the pH of pore water in soil-fly ash mixtures is expected to be very high, the release of heavy metals may be solubility-controlled (Murarka 1991).

2.3.2.2 Adsorption of Metals

The adsorption of metals depends on the properties of the solid (particle size, nature of inorganic oxide coating, organic carbon content, and zero point charge of the solid) as well as the properties of the liquid, including pH and total dissolved metal concentrations (i.e., the sum of free metal pool, inorganic ion pairs, as well as the concentration of the complexing ligands). Since the total dissolved concentration reflects the sum of many different components, the total dissolved concentration can be affected by any factor that would impact one of the individual components. The effect of pH on adsorption is generally dominant, because pH has a major influence on solubility of most chemical species (Sauve et al. 2000).

In practical situations, a mixture of metals and other ions is often involved. The relative preference of clay particles to adsorb metal ions depends on the selectivity coefficient for the metal and clay surface. For most clays, the Hofmeister series can describe the affinity of ions for the clay surface (Stumm and Morgan 1996). The Hofmeister series is:

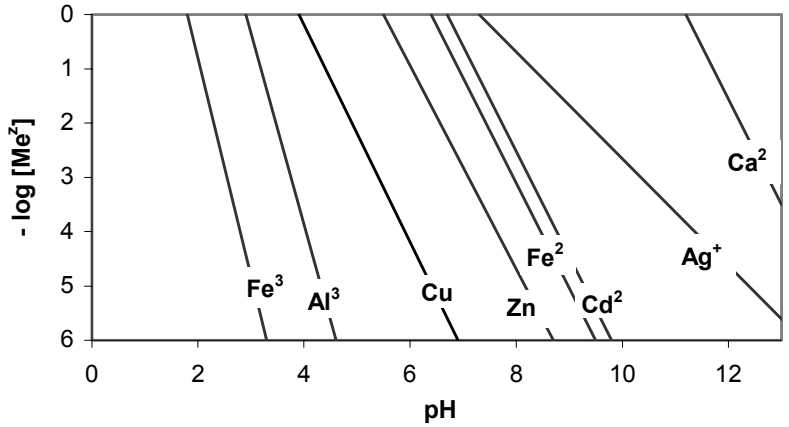

(a)

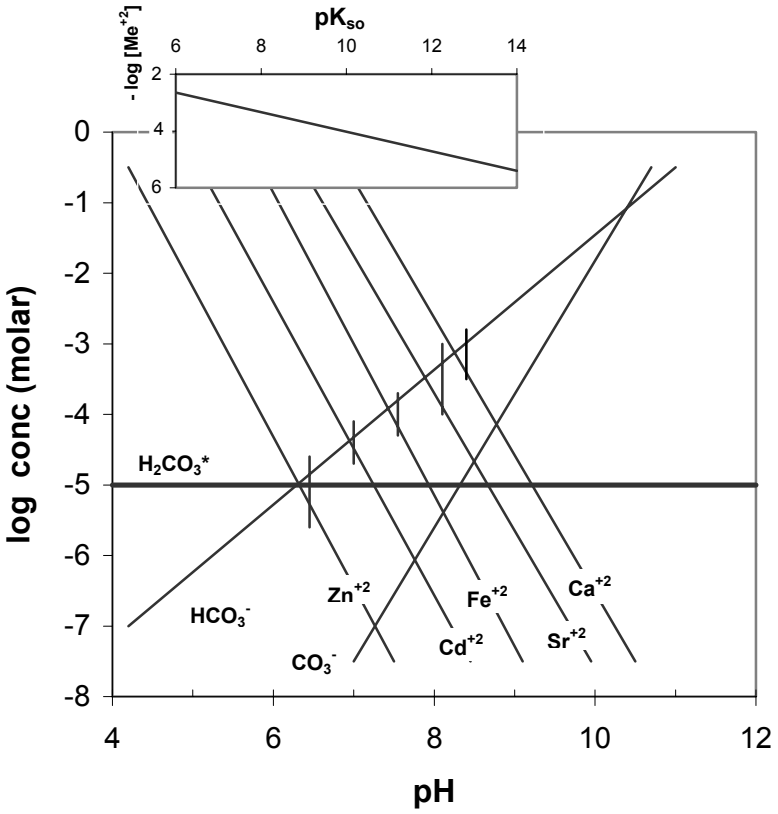

(b)

Fig. 2.2. Solubility of (a) metal oxides and hydroxides and (b) metal carbonates as a function of pH for solutions open to the atmosphere. H_2CO_3* represents the concentration of CO_2 in aqueous phase (from Stumm and Morgan 1995).

$$Ba^{+2} > Sr^{+2} > Ca^{+2} > Mg^{+2} > Cs^{+1} > K^{+1} > Na^{+1} > Li^{+1} > H^{+1}$$

The affinity to adsorb usually is greater for ions of higher valence and smaller hydrated radius at equal concentrations. Ions with higher valance tend to be adsorbed first, as do ions with smaller hydrated radius. Consequently, retardation of a metal in a soil matrix is strongly affected by the composition of the solution.

2.3.2.3 Chemistry of the Pore Water

2.3.2.3.1 pH of Pore Water

pH is the most important parameter influencing metal release during leaching (Brunori et al. 1999). The presence of fly ash in soil-fly ash mixtures can change the pH of the pore water (Theis et al. 1982), and thus affect the composition of the leachate.

Fly ash leachate can be acidic or alkaline (Das et al. 1989), depending on the constituents in the fly ash. Theis et al. (1982) investigated factors affecting the pH of fly ash leachate and found that the relative amounts of lime and amorphous iron in the fly ash define the acidic or basic character of fly ash leachate. Leaching tests were conducted with 11 different fly ash samples by mixing 200 g of each fly ash with 1 L of distilled water in a closed vessel. The mixtures were allowed to equilibrate for 24 hours on a shaker table. At the end of the tests, pH of each leachate was measured and identified as the equilibrium pH of that fly ash. A second series of similar tests was conducted with each of the 11 fly ashes at a controlled pH of 3, where pH was continually adjusted with sodium hydroxide and

perchloric acid as needed. The aqueous concentration of iron and calcium were measured in each leachate.

Equilibrium pH of the leachate from the first series of tests is plotted as a function of iron-to-calcium ratio in the leachate of the controlled pH (3) tests of the second series for each fly ash and shown in Fig. 2.3. Equilibrium pH decreases with the increasing iron-to-calcium ratio. A ratio of 3 to 1 of the concentrations of Fe and Ca in the leachate roughly delineates the acidic or basic character of fly ash leachates. The iron content is a measure of the acid component, whereas soluble calcium, which is associated with the lime fraction, represents the basic component of fly ash.

Solubility and adsorption of metals both are highly affected by the pH of the pore fluid. The solubility of heavy metals in pore water is usually extremely low at high pH. If the concentration of metals is relatively high compared to the solubility, then some of the metals precipitate. Subsequent leaching of metals from the precipitates is governed by solubility-controlled release rather than by adsorption-controlled release (Murarka 1991).

Adsorption of metal ions on the solid surface is strongly influenced by the pH of the pore water (Weng et al. 1990, Brunori et al. 1999, Sauve et al. 2000). This influence is caused primarily by a change in the surface potential of the adsorbent, and also by a change in the competition between protons and metal ions for adsorption sites. A change in surface potential affects metal adsorption through a change in electrostatic attraction or repulsion (Allen et al. 1993). As an example,

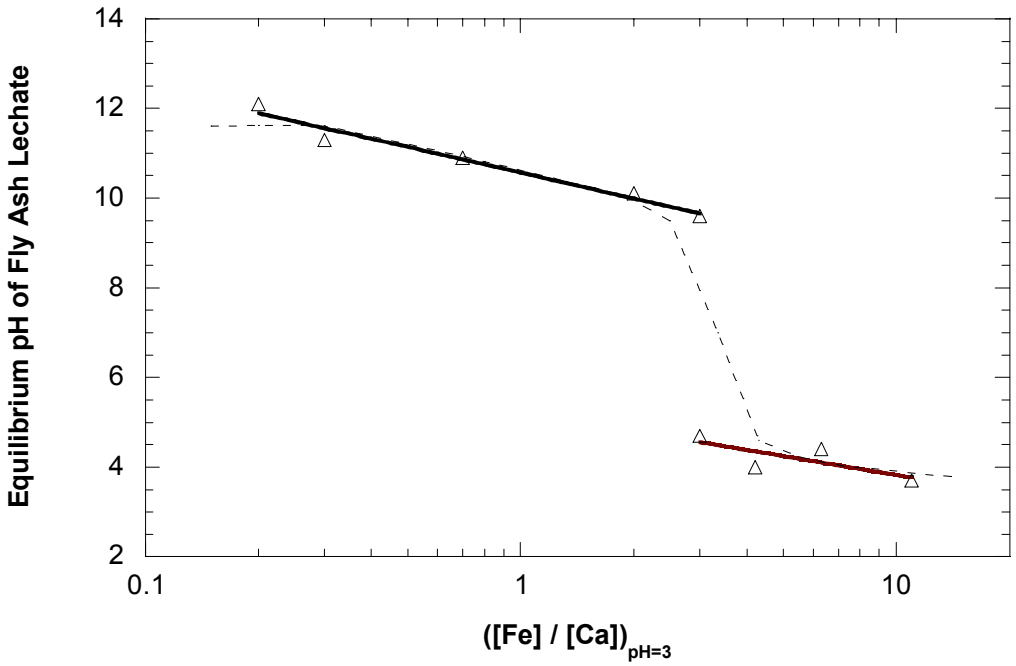

Fig. 2.3. Equilibrium pH of Fly Ash Leachate as a Function of the Ratio of Fe to Ca in the Leachate Obtained from Leaching Tests at Constant pH 3 for same fly ash. (adapted from Theis et al. 1982).

sorption of various metal ions on hydrous ferric oxide at different pH is shown in Fig. 2.4. The fraction of metal adsorbed on solid surface increases with increasing pH. For each metal ion, there is a narrow window of 1-2 pH units where the extent of adsorption rises from zero to almost 100%.

Pore water of the soil-fly ash mixture is expected to have high pH because of its exposure to hydrated calcium silicate (C-S-H) and Portlandite [$Ca(OH)_2$]. However, the lime content in a soil-fly ash mixture is lower than that in fly ash alone, and thus the high pH in pore water of soil-fly ash mixtures may not persist. The persistency of pH in soil-fly ash mixtures needs to be examined, since a small decrease (2 or 3) in pH over time can increase the solubility and decrease the adsorption of metals by many orders of magnitude. If the pH decreases over time, the concentration of heavy metals in the leachate is expected to increase over time as well.

2.3.2.3.2 Dissolved Ligands

The anions or molecules with which a metal forms a coordination compound are referred as ligands. Dissolved ligands have an important influence on leaching since both the solubility of metals in pore water and adsorption of metals on the solid surface are affected by the concentration of dissolved ligands in pore water. Formation of complexes with dissolved ligands increases the solubility of the metal. The presence of soluble metal complexes often reduces metal adsorption (Reed and Nonavinakere 1992), particularly when the metal complexes have less affinity

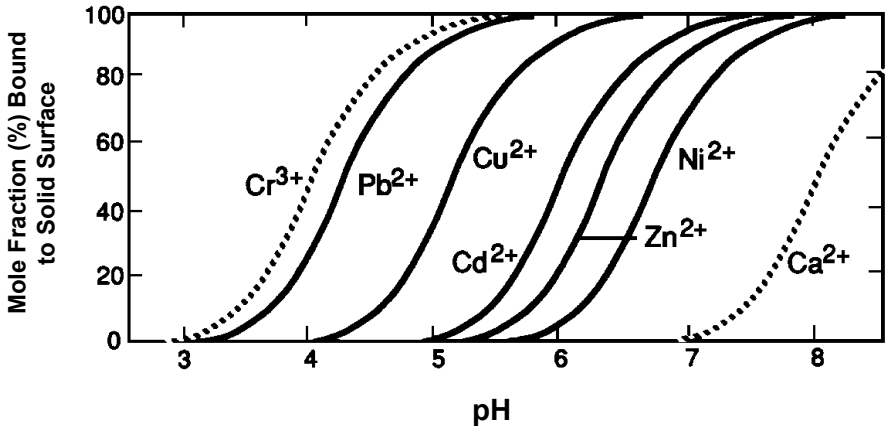

Fig. 2.4. pH Dependence of Metal Adsorption on Hydrous Ferric Oxide (adapted from Stumm and Morgan 1996).

for the sorption sites than the free metal ion. Thus, high concentrations of dissolved ligands can cause high metal concentrations in leachate.

2.3.2.3.3 Total Metal Concentration

The amount of metal adsorbed on solid surfaces and the metal concentration in aqueous phase both increase as the total metal concentration increases. However, the partition coefficient tends to decrease with increasing total concentration (Di Toro et al. 1986). As a result, the fraction of the total metals that adsorbed on a solid surface often decreases when the total concentration increases (Jang et al. 1998), and can cause higher metal concentrations in the aqueous phase.

2.3.2.3.4 Background Electrolyte

Background electrolyte composition and ionic strength can affect metal adsorption by altering the solution chemistry of the metal and the electric double layer associated with the particle surfaces. In systems with more than one adsorbable ion, competition between a metal ion of interest and other species for the same adsorption sites is an important factor that influences metal adsorption (Allen et al. 1993). A concentrated background electrolyte can “swamp” the surface of the solid, limiting metal access to the adsorption sites (Reed and Nonavinakere 1992).

Ayala et al. (1998) varied the ionic strength (10^{-1} to 10^{-4} M) by adding sodium sulfate and potassium sulfate in batch tests, and found no influence of ionic strength

on adsorption of Cu and Cd on fly ash surface. In contrast, adsorption of Co and Ni on chitosan beads (an adsorbent used for water purification) increases with increasing ionic strength when potassium sulfate and potassium chloride are added to the solution in batch tests (Mitani el al. 1995).

2.3.2.4 Chemistry of the Solid Phase

2.3.2.4.1 Distribution of Metals

Distribution of metals on the solid phase is an important factor controlling leaching. For an example, metal leaching from fly ash is affected by the total amount of metals in the fly ash and the relative amounts of metals in the glassy and crystalline phases. Metals locked within the glassy phase are released only through long-term weathering processes, whereas metals or metal compounds deposited on surface of the fly ash during combustion are more active chemically (Theis et al. 1982). DiGioia et al. (1986) also report that the glassy spheres are relatively inert and immune to dissolution due to their elemental composition and glass-like structure.

2.3.2.4.2 Point of Zero Charge

Adsorption of metals on solid surface or mineral components of the solid surface is influenced by the surface charge of the solid surface. The point of zero charge (pzc) is the pH at which the net surface charge of a solid is zero. The pzc of some of minerals and the effect of pH on the surface charge are shown in Fig. 2.5.

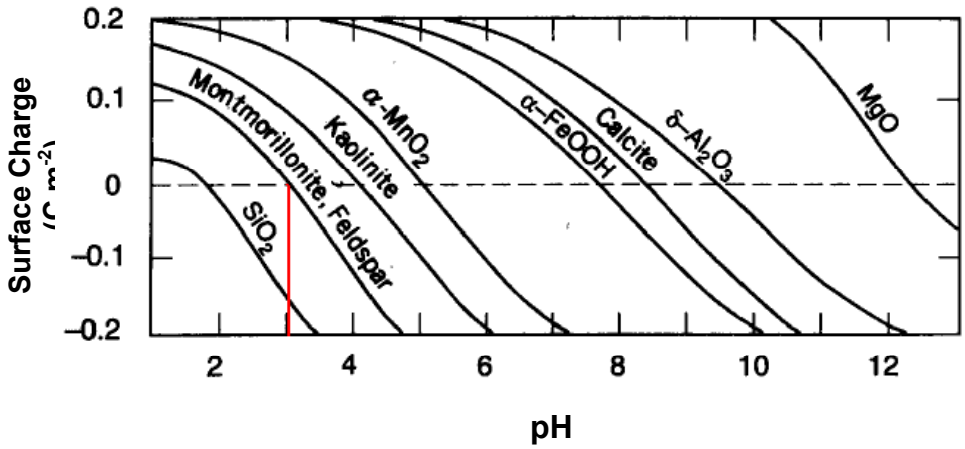

Fig. 2.5. Point of Zero Charge and the Effect of pH on the Surface Charge of Some Common Minerals (adapted from Stumm and Morgan 1996).

The pH at the intersection of the dashed line representing net zero surface charge and the curve for a particular mineral represents its pH_{zpc}. For example, the pzc for montmorillonite is 3. Increasing the pH above the pH_{zpc} results in a more negative surface charge, and increased adsorption of cations on the solid surface (Ricou et al. 1999). The pzc of fly ash is typically varies between 2 and 4 (Weng and Huang 1990, Ricou et al. 1999).

2.3.3 Standard Leaching Tests

Leaching or extraction tests are often used as expedient means to evaluate the potential of a material to release contaminants to the environment. The material is exposed to a leachant (typically water) and the amount of contaminant in the leachate is measured and compared to an established standard. Some of the widely used standard leaching tests with their corresponding extraction conditions are shown in Table 2.2.

2.3.3.1 Water Leach Test (ASTM D 3987-85)

The water leach test defined in ASTM D3987-85 is intended as a rapid means of obtaining an aqueous extract from a solid waste. Site-specific leaching conditions are not simulated in this test. The method is only appropriate for inorganic compounds. The material to be tested is mixed homogeniously and then a representative 70-g sample of the material is added to 1400 mL of Type IV reagent water in a sealed 2-L container. The mixture is agitated continuously for

Table 2.3. Extraction Conditions for Different Standard Leaching Tests.

Test Procedure	Method	Purpose	Leaching Medium	Liquid-to-Solid Ratio	Particle Size	Time of Extraction
Water Leach Test	ASTM D 3987-85	To provide a rapid means of obtaining an aqueous extract	Deionized water	20:1	Particulate or monolith as received	18 hr
TCLP	EPA SW-846 Method 1311	To compare toxicity data with regulatory level. RCRA requirement.	Acetate buffer *	20:1	< 9.5 mm	18 hr
Extraction Procedure Toxicity (EP Tox)	EPA SW-846 Method 1310	To evaluate leachate concentrations. RCRA requirement.	0.04 M acetic acid (pH = 5.0)	16:1	< 9.5 mm	24 hr
Multiple Extraction Procedure	EPA SW-846 Method 1320	To evaluate waste leaching under acid condition	Same as EP Toxicity, then at pH = 3.0	20:1	< 9.5 mm	24 hr extraction per stage
Synthetic Acid Precipitation Leach Test	EPA SW-846 Method 1312	For waste exposed to acid rain	DI water, pH adjusted to 4.2 to 5	20:1	< 9.5 mm	18 hr

* Either an acetate buffered solution with pH = 5 or acetic acid with pH = 3.0

18 ± 0.25 hours at a temperature between 18^0 and 27^0 C. The mixture is then allowed to settle for 5 min, and the aqueous phase is separated by decantation. The decant is filtered through 0.45 μm filter paper and subjected to chemical analysis.

2.3.3.2 Toxicity Characteristic Leaching Procedure (TCLP)

The TCLP test defined in EPA Method 1311 is designed to determine the mobility of both organic and inorganic compounds present in liquid, solid, and multi-phase wastes. Waste samples are crushed to particle size less than 9.5 mm and extracted with an acetate buffer solution with a pH of 5 or an acetic acid solution with a pH of 3, depending on the alkalinity of the waste. The acetate buffer is added only once, at the start of the extraction. A liquid-to-solid ratio of 20:1 is used and the extraction period is 18 hr. The leachate is filtered through a 0.6 μm to 0.8 μm glass fiber filter prior to conducting chemical analyses.

2.3.3.3 Extraction Procedure Toxicity (EP Tox) Test

The EP Tox test defined in EPA Method 1310 is applicable to liquid, solid, and multiphase samples. Waste samples are crushed to a particle size less than 9.5 mm, and then extracted with deionized water maintained at pH 5 with acetic acid. The liquid-to-solid ratio starts at 16:1, and may increase as additional acid solution is added as needed to adjust the pH during the 24-hr test. The leachate is filtered through a 0.45 μm filter paper and then subjected to chemical analysis. Results of the EP Tox test are generally comparable to results of TCLP tests at pH

5, but may differ significantly from a TCLP test conducted at pH 3. The EP Tox test can be used for both inorganic and organic compounds.

2.3.3.4 Multiple Extraction Procedure (MEP)

The MEP test (EPA Method 1320) is intended to simulate leaching caused by repetitive precipitation of acid rain. The repetitive extraction reveals the highest concentration of each constituent that is likely to leach in a natural environment. This test is applicable to liquid, solid, and multiphase samples. Like the EP Tox test, the MEP involves an initial extraction with deionized water acidified to pH 5 with acetic acid. The liquid-to-solid ratio is 16:1. The initial extraction is followed by at least eight extractions with a synthetic acid rain solution (sulfuric/nitric acid adjusted to pH 3) with a liquid-to-solid ratio of 20:1. In every stage, the mixtures are agitated for 24 hr and then the leachate is filtered through a 0.45 μm filter paper prior to conducting chemical analyses. The MEP test can be used for both inorganic and organic compounds.

2.3.3.5 Synthetic Acid Precipitation Leach Test

The Synthetic Acid Precipitation Leach Test defined in EPA Method 1312 is designed to determine the mobility of both organic and inorganic compounds present in liquid, soils, and wastes. This test is similar to the TCLP test, except a different leachant pH is used. Waste samples are crushed to a particle size less than 9.5 mm, and then an extraction is conducted with deionized water (ASTM Type II) adjusted to pH 4.2 to 5 using acetic acid. A liquid-to-solid ratio of 20:1 is used,

and the extraction period is 18 hr. The leachate is filtered through a 0.6 μm to 0.8 μm glass fiber filter paper prior to conducting chemical analyses.

2.4 LEACHING STUDIES

Because fly ash may contain different toxic contaminants, leachate emanating from fly ash or soil-fly ash mixtures may contain toxic metals that can contaminate groundwater (Binner et al. 1997). As a result, leaching of heavy metals is the primary environmental concern when using fly ash in geotechnical applications. Leachability of metals from fly ash and soil-fly ash mixtures has been studied by several investigators.

Gustin and Thomes (1997) conducted Synthetic Precipitation Leach Procedure (SPLP) tests on Class C Eagan fly ash, 12 different soils, and soil-fly ash mixtures (20% fly ash) prepared with those soils and Eagan fly ash. The purpose was to evaluate the leaching characteristics of fly ash stabilized soil. The fly ash was from the Northern States Power Black Dog and High Bridge Plants in Minnesota.

Twelve soils comprising six different soil types, such as poorly graded sand (SP), silty sand (SM), clayey sand (SC), silt (ML), low plasticity clay (CL), and high plasticity clay (CH) were collected from the east and west sides of the Mississippi river (six from each side). The soil samples were saturated with tap water and blended with Eagan fly ash in accordance with ASTM D 3551, and compacted. Following compaction, the mixtures were allowed to cure for 24 hr and were then subjected to leaching using the SPLP following EPA Method 1312.

Concentrations of contaminants of concern from the SPLP tests are shown in Tables 2.4 and 2.5. The concentration of most of the contaminants is higher for fly ash than the soils.

The concentration of barium from all of the soil-fly ash mixtures was much lower than that from fly ash alone. The concentration of thallium and zinc from the soil-fly ash mixtures was also lower than from the fly ash alone, but the concentrations of boron, chromium, and sulfate were higher for most of the soil-fly ash mixtures than the fly ash alone. Gustin and Thomes (1997) report that the lower barium concentration for soil-fly ash mixtures was due to dilution and adsorption on clay particles.

Theis et al. (1982) investigated the sorptive behavior of trace metals on fly ash in an aqueous system. A series of leaching tests was conducted with 11 different fly ash samples (six alkaline and five acidic) by mixing 200 g of each fly ash with 1 L of distilled water in a closed vessel. The mixtures were allowed to equilibrate for 24 hours on a shaker table at constant pH of 3, 6, 9, and 12. pH adjustments were made with sodium hydroxide and perchloric acid as needed. At the end of the tests, the leachates were centrifuged, filtered through 0.45 μm membranes, and analyzed for aqueous concentrations of trace metals. The fly ashes were subjected to an extraction procedure involving dissolution in hydrofluoric acid and aqua regia (digestion) to determine the total metals in the ash. A second extraction was made with ammonium oxalate to determine the metals associated with the surface of the fly ash.

Table 2.4. Concentration of Contaminants from SPLP Tests on Eagan Fly Ash and Six Different Types of Soils (adapted from Gustin and Thomes 1997).

Species	Concentration From Synthetic Precipitation Leach Procedure (μg/L)						
	Fly Ash	SP	SM	SC	ML	CL	CH
Soil Samples Collected East of the Mississippi River							
Barium	15,000	188	431	621	437	1,123	590
Boron	387	32	55	67	92	152	81
Chromium	11	<5	<5	<5	<5	5	<5
Thallium	2	<1	<1	1	<1	<1	<1
Zinc	36	6	2	4	34	61	<1
Sulfate	< 10	<5,000	<5,000	<5,000	<5,000	<5,000	<5,000
Soil Samples Collected West of the Mississippi River							
Barium	15,000	130	544	786	608	973	947
Boron	387	56	99	138	110	209	170
Chromium	11	<5	<5	<5	<5	<5	<5
Thallium	2	<1	<1	<1	<1	<1	<1
Zinc	36	<1	<1	<1	<1	6	2
Sulfate	< 10	<5,000	<5,000	<5,000	<5,000	<5,000	27,333

Note: Detection limits: Thallium = 1 μg/L, Zinc = 1 μg/L, Sulfate (fly ash) = 10 μg/L, and Sulfate (soil) = 5,000 μg/L

Table 2.5. Concentration of Contaminants from SPLP Tests on Eagan Fly Ash and Soil-Fly Ash Mixtures Prepared with Six Different Soils and 20% Eagan Fly Ash (adapted from Gustin and Thomes 1997).

Species	Concentration From Synthetic Precipitation Leach Procedure (μg/L)						
	Fly Ash	SP + FA	SM + FA	SC + FA	ML + FA	CL + FA	CH + FA
Soil Samples Collected East of the Mississippi River							
Barium	15,000	860	1533	520	337	180	190
Boron	387	977	603	717	870	910	950
Chromium	11	96	67	59	60	55	66
Thallium	2	1	1	1	1	<1	<1
Zinc	36	21	23	23	28	20	<20
Sulfate	< 10	60,000	50,000	53,000	64,000	203,000	79,000
Soil Samples Collected West of the Mississippi River							
Barium	15,000	923	690	453	647	213	403
Boron	387	737	707	727	650	917	983
Chromium	11	65	55	56	62	39	<10
Thallium	2	1	<1	<1	<1	<1	<1
Zinc	36	< 20	<20	<20	<20	23	<20
Sulfate	< 10	54,000	50,000	53,000	51,000	77,000	85,000

Note: FA = Fly Ash, Detection limits: Thallium = 1 μg/L, Zinc = 20 μg/L, and Sulfate = 10 μg/L

The available fraction of total metals that was released to the aquatic environment is shown in Table 2.6. The average release of metals (from 11 fly ashes) to water as a fraction of the surface associated metals at different adjusted pH is shown in Fig. 2.6. Theis et al. (1982) found that the leaching of trace metals from fly ash in leachate follows a predictable pattern of decreasing release with increasing pH. They also noticed that the fraction of surface metals released to leachate is not higher than 20% of the surface associated metals at neutral pH.

Kanungo and Mohapatra (2000) conducted batch tests on two Class F fly ashes collected from India to characterize leaching from fly ash at different pH. In a series of 125-mL polyethylene bottles, 2 g of fly ash sample was added to 50 mL of deionized water (1:25 liquid-to-solid ratio). The bottles were securely stoppered to avoid contamination with CO_2 and shaken five times daily for 3 to 4 min for up to 30 d. The solid contents of the bottles were separated by centrifugation and filtration through 0.45 μm membranes. Similar experiments were carried out at constant pH of 3.0, 5.5, and 8.0. The pH was adjusted using 0.1 M HNO_3 and 0.1 M NaOH. The filtrate was analyzed for trace elements (Table 2.7). As in Theis et al. (1982), Kanungo and Mohapatra (2000) found that for most of the trace elements, aqueous phase concentrations increase at lower pH.

Chichester and Landsberger (1996) studied the leaching dynamics of metals from municipal solid waste incinerator (MSWI) fly ash using column leaching tests to simulate leaching from a fly ash landfill. MSWI fly ash was collected from the US Army Waterways Experiment Station in Vicksburg, Mississippi and subjected to

Table 2.6. Fraction of Total Metals Associated with the Surface of Fly Ash Expressed as Percent of Total Metals (adapted from Theis et al. 1982).

Species	Range[1]	Average[1]
Arsenic	65 - 100	93
Cadmium	<2 - 58	25
Chromium	15 - 84	44
Copper	25 - 75	48
Lead	5 - 40	8
Nickel	5 - 42	11
Zinc	10 - 70	30

[1] From all 11 fly ashes.

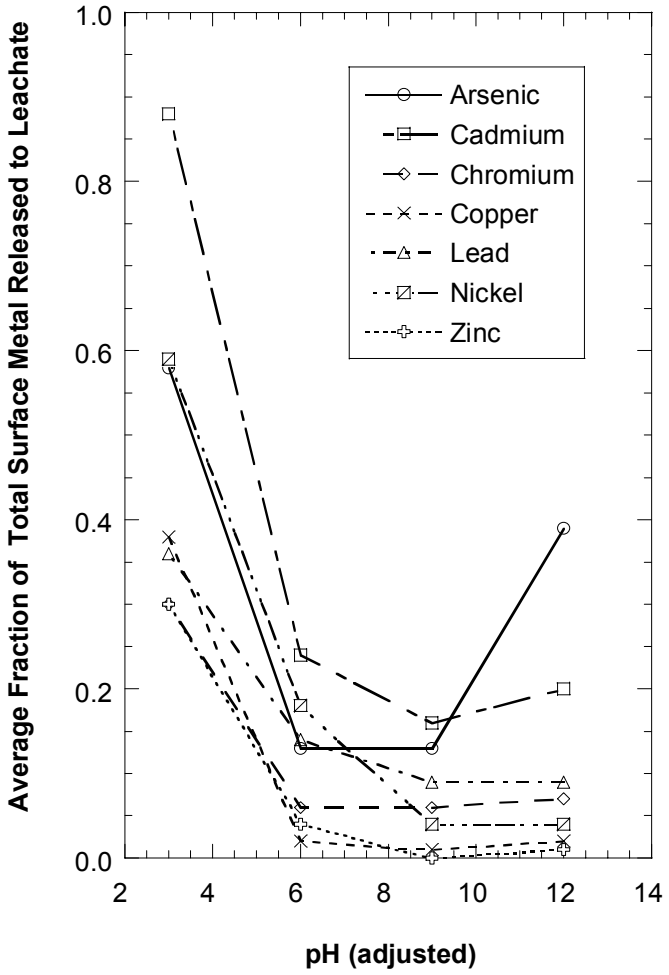

Fig. 2.6. Fraction of the Total Surface Metals that Released to Aqueous Phase from Batch Tests Conducted at Constant pH (adapted from Theis et al. 1982).

Table 2.7. Release of Trace Elements in Leachate During Batch Leaching at Different pH (adapted from Kanungo and Mohapatra 2000).

Period of Leaching (d)	Trace Element Concentration (mg/L)						
	Cd	Cr	Pb	Se	Fe	Co	Ni
pH = 3.0							
1	0.10	0.40	1.00	1.30	15.00	1.00	2.50
8	0.20	0.62	2.20	1.57	26.00	1.80	4.70
14	0.35	0.84	3.80	1.95	40.00	2.60	7.20
21	0.39	0.75	4.50	1.87	62.00	3.30	10.50
30	0.42	0.85	5.00	1.73	70.00	3.50	10.00
pH = 5.5							
1	0.20	0.50	1.00	0.77	12.00	0.90	1.80
8	0.50	0.70	1.50	1.03	16.00	1.00	3.40
14	0.70	1.00	2.00	1.23	22.10	1.60	5.00
21	0.75	0.90	3.00	1.32	28.20	2.00	6.50
30	0.76	0.80	2.50	1.55	25.00	1.60	6.00
pH = 8.0							
1	0.40	0.08	0.50	ND	3.00	0.60	0.08
8	0.30	0.10	0.40	ND	0.15	0.67	1.00
14	0.50	0.10	0.30	ND	0.18	0.60	5.00
21	0.50	0.07	0.20	ND	0.10	0.45	6.00
30	0.00	0.06	0.20	ND	0.07	0.52	4.50

Note: ND = Not detected.

column test in rigid-wall permeameters. The bottom plate of the permeameter was divided into two parts coaxially (inner and outer ring) to monitor for sidewall flow. The column was operated with deionized water (pH = 5.7) at a nearly constant water head having a hydraulic gradient of approximately 4. The effluent samples were collected and analyzed by inductively coupled plasma-atomic emission spectroscopy (ICP-AES). Elution curves reported by Chichester and Landsberger (1996) for Sr and B are shown in Fig. 2.7. Chichester and Landsberger (1996) found that the concentration decreases substantially at higher pore volumes of flow.

Goh and Tay (1993) conducted similar column leaching tests on MSWI fly ash along with MSWI fly ash mixed with lime (5%) to evaluate how leaching can be affected by lime addition. The MSWI fly ash consisted of 42% SiO_2, 15% CaO, 12.5% Al_2O_3, and 3% Fe_2O_3. The specific gravity of the fly ash was 1.71, and the loss on ignition was 15%.

The tests were conducted in a rigid-wall permeameter at a constant head using an average downward flow rate of 50 L/d. Leachates were collected at different time intervals and analyzed for trace metals using an atomic absorption (AA) spectrophotometer (furnace). pH of the effluents was measured immediately after collection. Over 100 d, the average pH over 100 d of the effluent from the fly ash alone was 9.4, and from the mixture was 12.0. Concentrations of trace metals (Cd, Cr, Cu, Ni, and Zn) from the column tests are shown in Fig. 2.8. The concentrations decrease with time, as was reported by Chichester and Landsberger (1996), and are lower in the effluent from the mixture having higher pH.

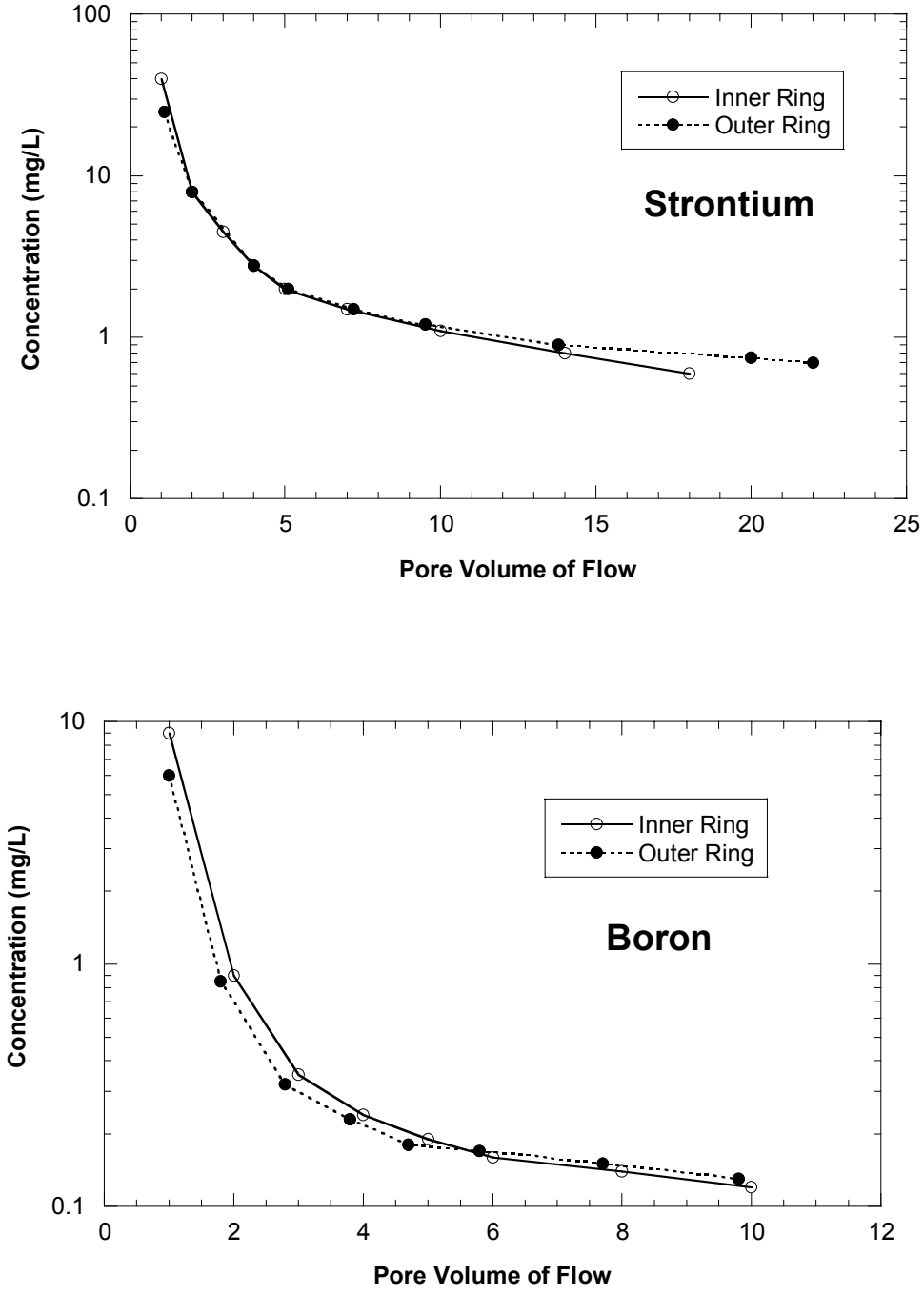

Fig. 2.7. Elution Curves from the Column Leaching Tests on MSWI Fly Ash for (a) Strontium and (b) Boron (adapted from Chichester and Landsberger 1996).

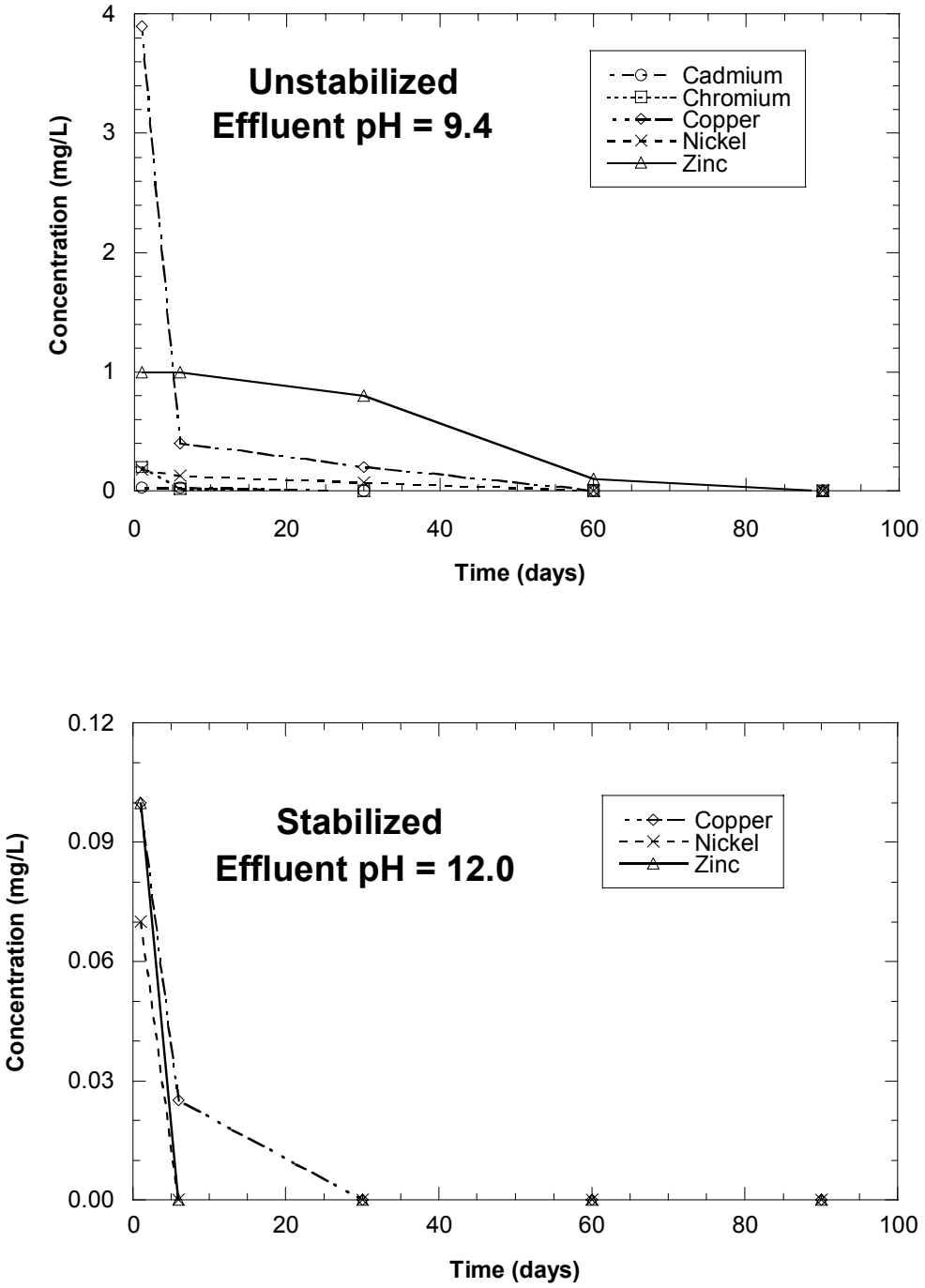

Fig. 2.8. Concentration of Trace Metals from the Column Leaching Tests on (a) MSWI Fly Ash and (b) MSWI Fly Ash Mixed with Lime (adapted from Goh and Tay 1993).

Concentrations of Cd and Cr in the effluent from the stabilized fly ash were below the detection limit (1 μg/L).

Ghose and Subbarao (1998) also conducted similar column leaching tests, but on Class F fly ash and Class F fly ash mixed with lime (4%, 6%, and 10%). Column leaching tests were conducted on compacted mixtures and Class F fly ash alone in rigid-wall permeameters. Tap water (pH = 7) was used as influent and a constant hydraulic gradient of approximately 10 was applied. The leachate was analyzed using atomic absorption (AA) spectrophotometry (flame) for Cd, Cr, Cu, Fe, Mg, Ni, Pb, and Zn. pH and concentrations of the trace metals in the effluent collected on the 7^{th} day are shown in Table 2.8. As in Goh and Tay (1993), Ghose and Subbarao (1998) found that the concentration of trace metals generally decreases with increasing pH of the effluent.

Biliski and Alva (1995) conducted column leaching tests on agriculture soil amended with fly ash to evaluate the impact on groundwater when using fly ash for agricultural uses. Candler fine sand (pH = 5.5, sand content = 96%, organic matter = 1.3%) was sampled from a citrus grove near Lake Alfred, Polk County, FL. The soil was air-dried, ground to pass a 2-mm sieve, and packed in plexiglass columns (30-cm long, 7-cm inner diameter) to a height of 28 cm. Fly ash from Tampa Electric Company (TECO, Tampa, FL) was mixed uniformly within the top 10 cm of soil in the column at application rates of 0, 10, 20, 30, 40, and 50%. The columns were operated with distilled water at a constant flow rate of 1 mL/min using a peristaltic pump. Leachates were collected at each half pore volume for a total of 5

Table 2.8. Concentrations in Leachate on 7th Day from the Column Leaching Test (adapted from Ghose and Subbarao 1998).

Parameter	pH	Cd (mg/L)	Cr (mg/L)	Cu (mg/L)	Fe (mg/L)	Mn (mg/L)	Ni (mg/L)	Pb (mg/L)	Zn (mg/L)
RF + 0% L	8.85	0.060	0.068	0.260	0.120	9.530	-	1.300	0.135
RF + 4% L	12.2	ND	0.050	0.180	ND	0.013	-	1.630	0.508
RF + 6% L	12.3	0.009	-	-	-	-	-	1.070	-
RF + 10% L	12.4	0.009	0.011	0.195	-	0.272	0.082	0.237	0.134

Note: RF = Raw fly ash; L = Lime; ND = Not detected

pore volumes and were analyzed for Cu, Mn, Fe, Zn, Cr, and Se using inductively coupled plasma-atomic emission spectroscopy (ICP-AES). The total amounts of trace metals that leached in a total of five pore volumes of leachate are shown in Table 2.9.

Biliski and Alva (1995) found that the total mass leached increases significantly with increasing fly ash content. Elution patterns of various elements from the Candler fine sand amended with 50% fly ash are shown in Fig. 2.9. The highest concentration of most elements was observed in the leachate corresponding to 1.5 pore volumes, except for Fe and Cu. The Fe and Cu concentrations reached a maximum within one pore volume. The concentration decreased considerably for all elements beyond three pore volumes of flow.

Das et al. (1989) conducted column leaching tests on a large variety of acidic and alkaline fly ashes to evaluate leaching patterns. The fly ashes were compacted in acrylic columns and operated in an up-flow mode at a constant flow rate using a peristaltic pump. The leachate was analyzed for Al, Na, K, Br, Ca, Cr, Cs, Mo, Sb, Se, Si, and W using atomic adsorption spectrophotometry. Concentrations of trace metals were graphed as a function of pore volumes and a mass balance curve was fitted to column test data to find release pattern. Das et al. (1989) proposed the following mass balance equation for column leaching test:

$$v\,(c_0 - c) + G\,F(t) = V\,dc/dt \qquad (2.1)$$

where v is the average flow velocity, c_0 is the influent concentration (=0 for distilled

Table 2.9. Quantities of Various Elements Leached in a Total of Five Pore Volumes of Leachate from Soil-Fly Ash Mixture at Different Fly Ash Contents (adapted from Biliski and Alva 1995).

Fly Ash Content (% of Soil)	Total Quantities of Elements Leached for 5 Pore Volumes								
	Ca (mg)	K (mg)	Na (mg)	Mn (μg)	Zn (μg)	Fe (μg)	Se (μg)	Cu (μg)	Cr (μg)
0	39	3.2	2.9	126	73	113	120	229	6.9
10	61	3.1	4.4	139	105	388	144	185	8.5
20	91	6.2	7.0	510	180	583	145	142	11.6
30	83	8.0	8.0	1171	242	698	144	164	13.9
40	140	8.0	12.0	883	387	494	176	159	15.4
50	231	16.8	21.4	1074	737	375	171	134	12.4

Note: Leachates were collected at the bottom of the 30-cm soil column where only top 10-cm was amended with fly ash.

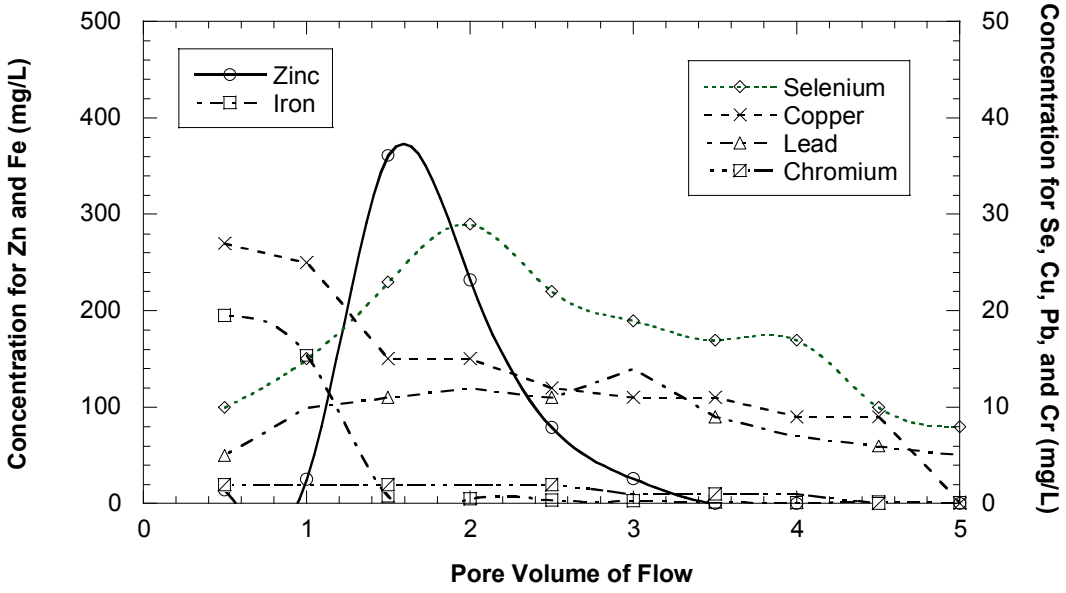

Fig. 2.9. Concentration of Trace Metals from the Column Leaching Tests on Agricultural Soil Amended with Fly Ash. Leachates were Collected at the Bottom of the 30-cm Soil Column. Only the Top 10-cm was Amended with Fly Ash (adapted from Biliski and Alva 1995).

water), c = concentration after many pore volumes (long-term equilibrium), G = mass of fly ash in the column, V is the volume of column expressed in pore volumes, and F(t) is specific mass transfer function. Das et al. (1989) also report that the possible functions F(t) are: (1) instantaneous dissolution upon wetting (F(t) = 0); (2) exponentially decreasing release ($F(t) = ke^{\alpha n}$); (3) slow dissolution (F(t) = k); and (4) precipitation and adsorption governed dissolution ($F(t) = k_1 e^{\alpha n} - k_2 [c(t) - c]$), where n = number of free volumes led through, and k, k_1, k_2 and α are metal release rate constants. After fitting the curves with the column test data, Das et al. (1989) report that instantaneous dissolution occurs for Na, Cr, Se, Mo, and W. However, the fitted curve with the column test data was not included in the publication.

Kaminsky and Landsberger (2000) conducted column leaching tests on contaminated soil and used the same mass balance equation (Eq. 2.1) proposed by Das et al. (1989) for modeling metal release from contaminated soil. Typical elution curves (for Cd and Zn) from Kaminsky and Landsberger (2000) are shown in Fig. 2.10. The instantaneous dissolution function fits the best for Cd and the slow dissolution function fits the best for Zn. Kaminsky and Landsberger (2000) also report that instantaneous dissolution occurs for S and Ca, slow dissolution occurs for Pb, and exponential leaching occurs for Cu.

Edil et al. (1992) conducted column leaching test on sand-fly ash mixtures to evaluate leaching from a fly ash liner material. Class C fly ash was mixed with coarse Portage sand (50% fly ash and 50% sand, by dry weight) and compacted in

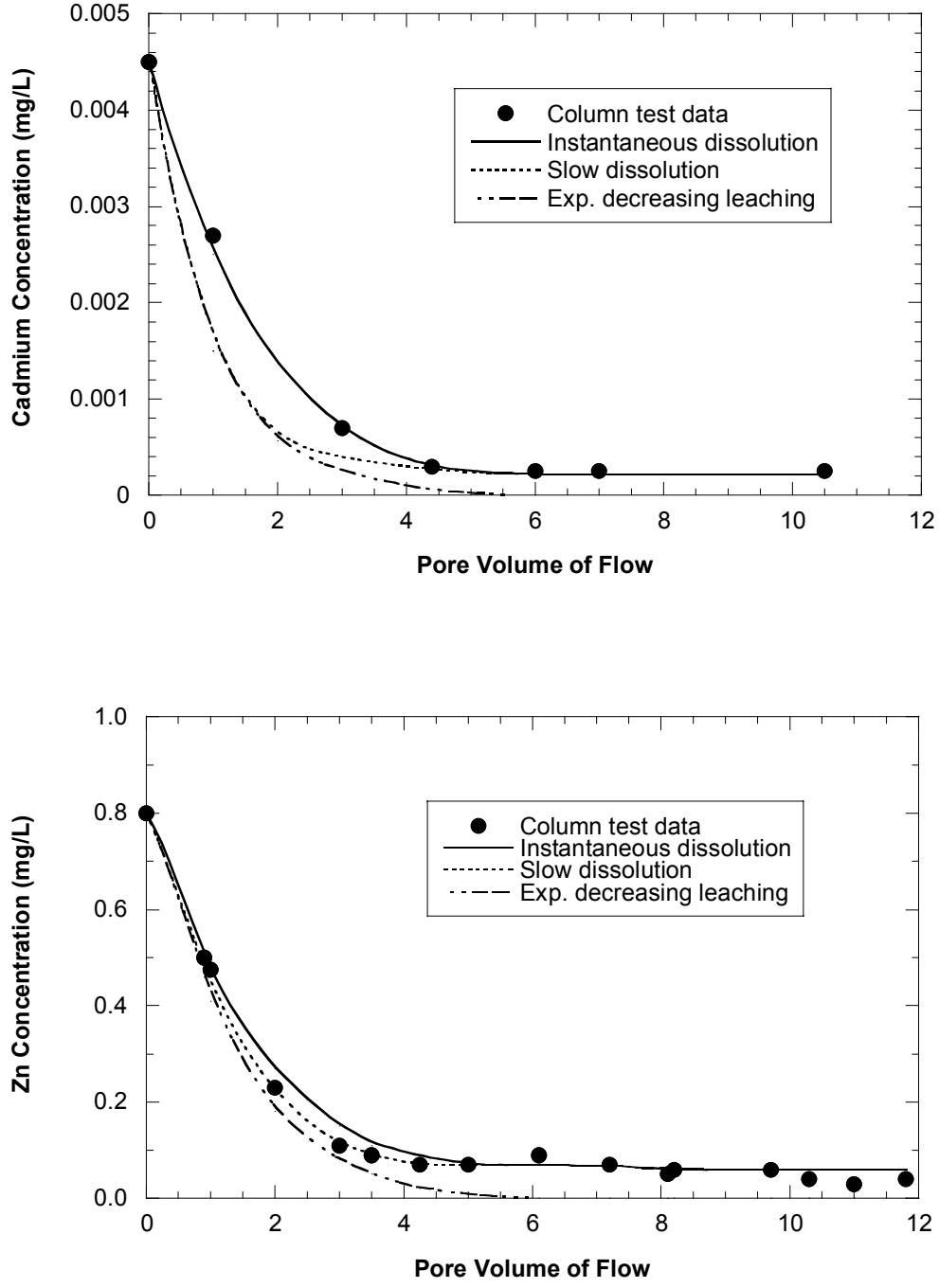

Fig. 2.10. Concentrations of Metals from Column Leaching Tests on Contaminated Sandy Alluvial Sediment Collected from the Bank of Mississippi River (adapted from Kaminsky and Landsberger 2000).

a Proctor mold using a static method. Two different compaction pressures were used to prepare specimens with two different hydraulic conductivities. Column tests were conducted in flexible-wall permeameters with a constant head and using a synthetic leachate as the feed solution. The synthetic leachate consisted of calcium, sulfate, cadmium, zinc, and boron with sodium and chloride added to achieve comparable ionic strength to a leachate collected from a fly ash storage facility. pH of the effluent was measured immediately after collection. The effluent samples were analyzed using inductively coupled plasma-atomic emission spectroscopy (ICP-AES). The initial pH was 12-12.5, but decreased to an apparent steady state level slightly above pH 11.5.

The leachate quality was measured in terms of the chemical species that were in the feed solution and for elements of special interest that were expected to leach from the fly ash (Al, As, Cr, Se, Si, and Sr). Edil et al. (1992) propose that the release pattern from fly ash follows two basic shapes (Fig. 2.11). These release patterns are described as the first-flush response and the lagged flush response. Edil et al. found that most metals show the first-flush leaching pattern. The exceptions were strontium and chromium for the test specimen having low hydraulic conductivity.

Creek and Shackelford (1992) studied the effect of flow rate on leaching characteristics of compacted soil-fly ash mixtures. Column leaching tests were conducted on Class F fly ash and three mixtures of fly ash (50% fly ash + 45% sand + 5% bentonite; 75% fly ash + 15% sand + 10% bentonite; 75% fly ash + 22.5%

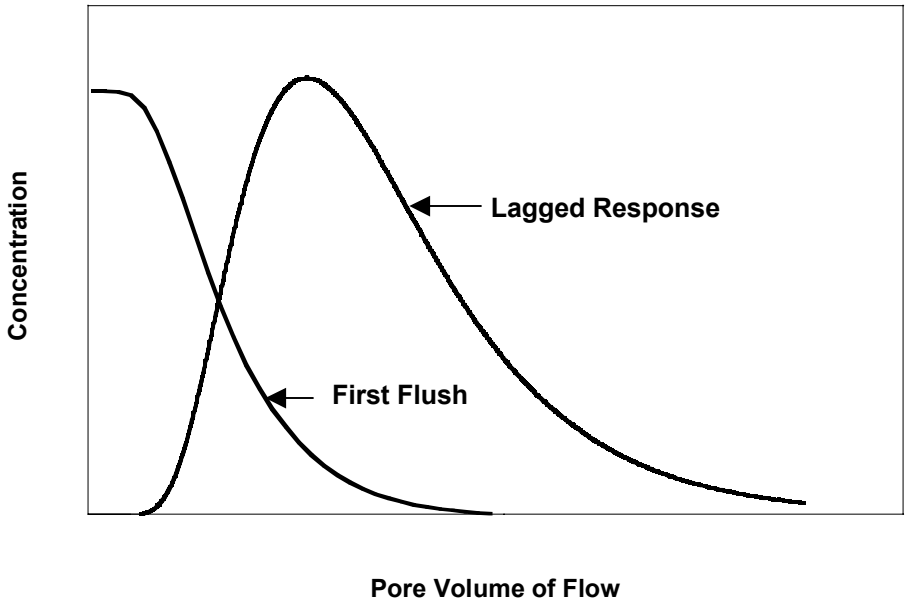

Fig. 2. 11. The Typical Leaching Curves of Metals from Class C Fly Ash as Discussed by Edil et al. 1992: (a) First Flush Response and (b) Lagged Flush Response.

sand + 2.5% bentonite) at four different hydraulic gradients (25, 50, 100, and 150) using tap water as the permeant fluid. Leachate was collected every quarter pore volume for a total of three pore volumes of effluent. The leachates were analyzed for the 13 trace metals (Al, B, Ba, Ca, Cd, Cr, Cu, Fe, Mn, Mo, Pb, Sr, and Zn). As in Biliski and Alva (1995), Creek and Shackelford (1992) found that an increase in fly ash content tends to increase the leaching of most of metals. As described in Edil et al. (1992), Creek and Shackelford (1992) found early and delayed leaching patterns, and most of the leached metals showed the early leaching pattern. The exceptions were barium, calcium, and strontium, which showed delayed leaching pattern. The effect of flow rate had no noticeable effect on leaching of metals.

SECTION 3

MATERIALS

3.1 SOILS

Soil samples were collected from four different locations in Wisconsin. Locations of the sampling sites are shown in Fig. 3.1. Two of the locations are the field test sites described in Edil et al. (2002), where the subgrade has been stabilized with fly ash (Scenic Edge site in Cross Plains, WI and STH 60 site near Lodi, WI). The third site is near the intersection of STH 13 and CTH “H” near Cloverland in Douglas County, WI. The fourth site is on STH 28, 50 m west of the intersection with TW-North at Mayville, WI. These sites were selected so that soft subgrade soils having a broad range of properties could be tested. Personnel from the Wisconsin Department of Transportation assisted in locating the sampling sites. The samples were collected from a depth of 0.2 to 0.3 m along the roadway at each site.

Index properties, compaction characteristics, classifications, and California bearing ratio (CBR) are shown for each soil in Table 3.1. Joy silt loam and Plano silt loam are low plasticity clays. Lacustrine red clay is a highly plastic clay and Theresa silt loam is an organic highly plastic clay. The CBR tests were performed at the natural water content for all soils following ASTM D 1883. The dry unit weight of the CBR specimens is also shown in Table 3.1. The CBR ranges from 1 to 3, which indicates that all are very soft soils.

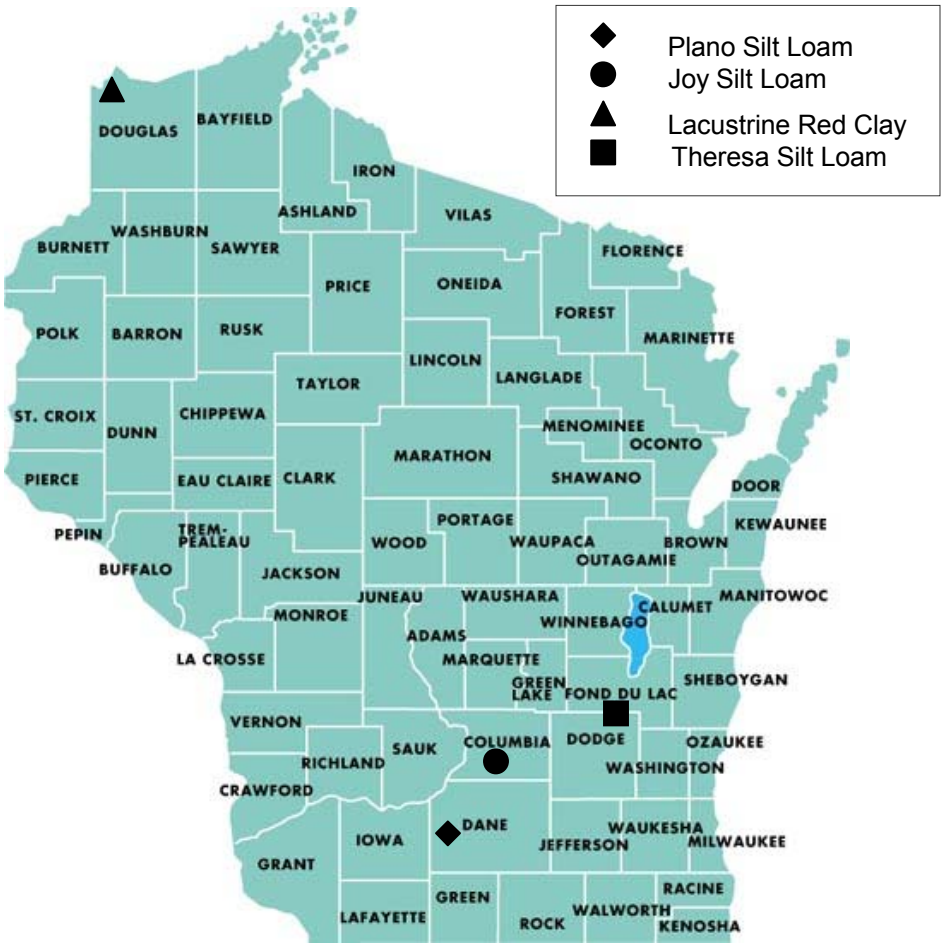

Fig. 3.1. Locations of Soil Sampling Sites.

Table 3.1. Index Properties, Compaction Characteristics, Classifications, and CBRs of Soils.

Soil	Sampling Location	Liquid Limit	Plasticity Index	Specific Gravity	LOI (%)	Classification		CBR	w_N (%)	$\gamma_{d(CBR)}$ (kN/m^3)	w_{OPT} (%)	γ_{dmax} (kN/m^3)
						USCS	AASHTO					
Joy Silt Loam	STH 60 near Lodi, WI	39	17	2.70	1	CL	A - 6	3	25	15.1	19	16.5
Plano Silt Loam	Scenic Edge in Cross Plains, WI	44	20	2.71	2	CL	A -7- 6	1	27	14.6	19	16.2
Lacustrine Red Clay	STH 13 near Cloverland, WI	69	38	2.71	2	CH	A-7-6	2	35	13.3	24	15.7
Theresa Silt Loam	STH 28 near Mayville, WI	61	19	2.24	10	OH	A-7-5	1	35	12.8	29	13.5

Notes: LOI = Loss on ignition, w_N = Natural water content, $\gamma_{d(CBR)}$ = Dry unit weight for CBR samples, w_{OPT} = Optimum water content, and γ_{dmax} = Maximum dry unit weight.

Particle size distribution curves for the soils are shown in Fig. 3.2. The particle size distributions are similar for the Joy silt loam, Plano Silt loam, and Theresa silt loam. The Lacustrine red clay is finer than the other soils. The percent fines (P_{200}) varies between 94 and 97%, and the 2 μm clay fraction varies between 20 and 65%.

The maximum dry unit weight and optimum water content, determined using standard Proctor compaction, range between 13.5 and 16.5 KN/m^3 and 19-29%, respectively. The compaction curves are provided in Appendix C. Similar maximum dry unit weights were obtained for the Joy silt loam, Plano Silt loam, and Lacustrine red clay. The maximum dry unit weight for Theresa silt loam is appreciably lower than that of the other soils, due to its higher organic content.

Cation exchange capacity (CEC) and paste pH of the soils are shown in Table 3.2. Joy silt loam has the lowest pH (6.9) and also the lowest cation exchange capacity (9.9 meq/100g). Lacustrine red clay has the highest pH (7.4) as well as the highest cation exchange capacity (35.3 meq/100g).

3.2 FLY ASH

Three different fly ashes were used for this study: Columbia, Dewey, and King. Columbia fly ash is from the Columbia Power Station (Unit 2) in Portage, Wisconsin, and was used for soil stabilization at the field sites at Scenic Edge and STH 60. King fly ash is from the Allen S. King Plant in Bayport, Minnesota and Dewey fly ash is from the Nelson Dewey Power Station in Cassville, Wisconsin.

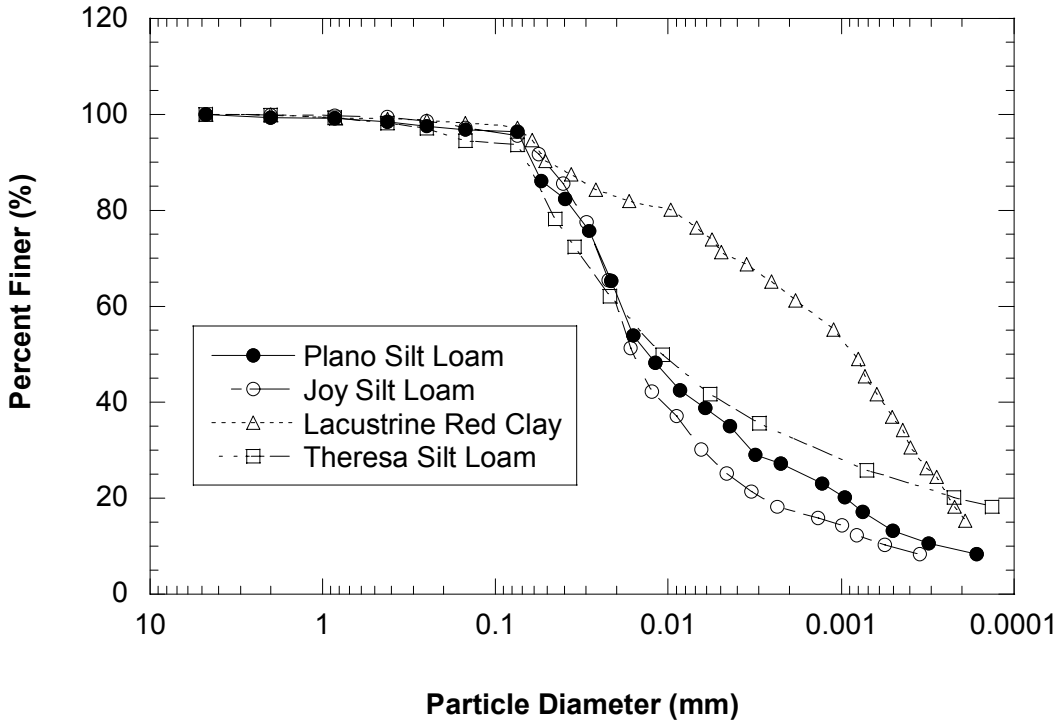

Fig. 3.2. Particle Size Distribution Curves for Soils.

Table 3.2. Adsorption Related Chemical Properties of Soils and Fly Ashes.

Sample	pH	CEC (meq/100g)
Joy silt loam	6.9	9.9
Plano silt loam	7.1	14.2
Lacustrine red clay	7.4	35.3
Theresa silt loam	7.1	27.6
Columbia fly ash	11.7	102.2
Dewey fly ash	10.1	49.3
King fly ash	11.0	77.5

Note: Cation exchange capacity (CEC) is estimated at the corresponding pH. Chemical analyses were conducted by Soil and Plant Analysis Laboratory at UW-Madison.

Physical properties and chemical composition of the fly ashes are shown in Table 3.3. Columbia fly ash classifies as Class C fly ash following ASTM C 618 (see Sec. 2.2.1). Columbia fly ash contains 23% lime and has self-cementing capabilities. Dewey fly ash has high organic content (16%) and classifies as an "off-specification" fly ash, implying that it does not meet the Class C criteria in C 618 and is not suitable for use in concrete. Dewey fly ash has 10% lime and has self-cementing properties. King fly ash also classifies as off-specification because its organic content (5.4%) and SO_3 content (6.4%) exceed the criteria in ASTM C 618. King fly ash has 24% lime content and has self-cementing capabilities.

Chemical compositions of the fly ashes are compared with the composition of typical Class C and F fly ashes in Table 3.4. The Columbia and King fly ashes have lime contents similar to typical Class C fly ash. The lime content of Dewey fly ash is close to that of typical Class F fly ash. The SO_3 content, which causes rapid hydration, is much higher (12%) for Dewey fly ash than any of the other fly ashes, including typical Class C (3.3%) and F fly ashes (0.6%). All three fly ashes have Al_2O_3 and Fe_2O_3 contents comparable to that of Class C fly ash, and SiO_2 content lower than the typical Class C and F fly ashes.

Paste pH and CEC of the fly ashes are shown in Table 3.2. Dewey fly ash has the lowest pH (10.1) as well as the lowest cation exchange capacity (49.3 meq/100g), and Columbia fly ash has the highest pH (11.7) and the highest cation exchange capacity (102.2 meq/100g). The pH and the cation exchange capacity of King fly ash fall between those for the Columbia and Dewey fly ashes.

Table 3.3. Physical Properties and Chemical Composition of Fly Ashes.

Fly Ash	Classification (ASTM 618)	Specific Gravity	Moisture Content (%)	Loss on Ignition (%)	Lime (CaO) Content (%)	Other Oxides (SiO_2 + Al_2O_3 +Fe_2O_3) (%)	Sulfur Trioxide Content (%)
Columbia	C	2.70	0.09	0.7	23.0	55.5	3.7
Dewey	Off-spec	2.53	0.23	16.2	9.8	38.7	11.8
King	Off-spec	2.68	0.44	5.4	23.7	49.5	6.4

NA = Not available

Table 3.4. Chemical Compositions of Fly Ashes.

Chemical Species	Percent of Composition				
	Columbia Fly Ash [1]	Dewey Fly Ash [1]	King Fly Ash [2]	Typical Class C [3]	Typical Class F [3]
CaO (lime)	23.1	9.8	23.7	24	9
SiO_2	31.1	19.8	27.3	40	55
Al_2O_3	18.3	13.0	16.3	17	26
Fe_2O_3	6.1	6.0	5.9	6	7
MgO	3.7	3.1	1.8	5	2
SO_3	3.7	11.8	6.4	3	1

[1] From chemical analyses provided by Alliant Energy (see Appendix B)
[2] From chemical analyses provided by Xcel Energy
[3] From *Fly Ash Facts for Highway Engineers* (1995)

Particle size distributions of the fly ashes are shown in Fig. 3.3. All three ashes contain a broad range of particle sizes in the silt and clay range. Particle size distributions of the King and Dewey ashes are more widely distributed, and these ashes contain coarse as well as fine particles. Columbia fly ash contains some uniform silt size particles and a wide range of smaller particles. The percent fines (P_{200}) varies from 64 to 98%. Columbia fly ash has the highest percent fines (98%) and Dewey fly ash has the lowest (64%). King fly ash has an intermediate fines content (85%).

3.3 STABILIZED SOIL

Compaction curves for the soil-fly ash mixtures were determined using the Harvard Miniature Compaction procedure (ASTM D 4609-94). The compaction effort was intended to simulate standard Proctor effort (ASTM D 698). The first set of mixtures was compacted immediately after mixing with water (no delay). Another set of mixtures was compacted two hours after mixing with water (2-hr delay) to simulate the typical duration between mixing and compaction that occurs in the field. Mixtures were prepared with fly ash contents of 10, 15, and 20% with Joy silt loam and 12, 16, and 20% with Plano silt loam. The compaction curves are provided in Appendix C.

Compaction characteristics of the soil-fly ash mixtures prepared with Plano silt loam and Joy silt loam are shown in Table 3.5. The maximum dry unit weight and optimum water content for the soils alone are also shown in Table 3.5. For

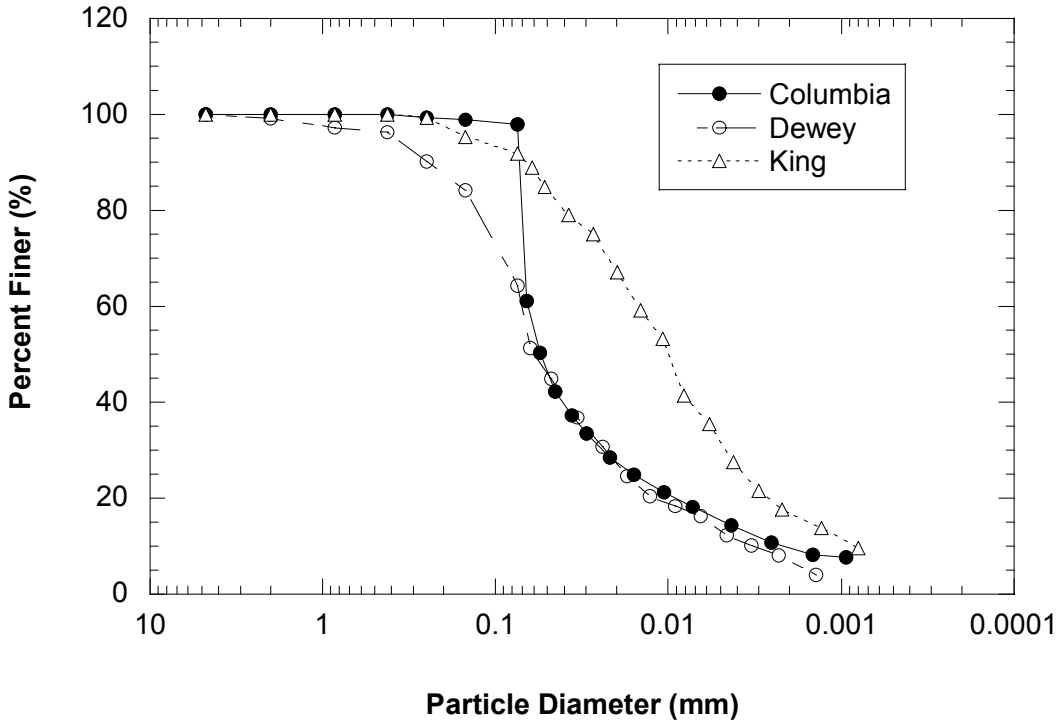

Fig. 3.3. Particle Size Distribution Curves of Fly Ashes.

Table 3.5. Compaction Characteristics of Fly Ash Stabilized Soils.

Soil Type	Fly Ash Type	Fly Ash Content (%)	Stabilized Soil-No delay		Stabilized Soil- 2-hr delay		Soil Alone	
			γ_{dmax} (kN/M^3)	W_{opt} (%)	γ_{dmax} (kN/M^3)	W_{opt} (%)	γ_{dmax} (kN/M^3)	W_{opt} (%)
Plano Silt Loam	Columbia	12	16.2	19	15.6	21	16.2	20
		16	16.2	20	15.5	21		
		20	16.0	20	15.5	22		
Joy Silt Loam	Columbia	10	16.6	18	16.1	20	16.5	19
		15	16.5	19	15.9	20		
		20	16.4	20	15.8	21		

Note: First set of soil-fly ash mixtures was compacted immediately after mixing with water and indicated as “no delay” samples. A second set of soil-fly ash mixtures was compacted two hrs after mixing with water and indicated as “2-hr delay” samples.

both soils, the maximum dry unit weight and optimum water content for the “no delay” soil-fly ash mixtures are comparable with that for the soil alone. In contrast, the maximum dry unit weight for the “2-hr delay” soil-fly ash mixtures is lower than that for the soil alone, and optimum water content of the soil-fly ash mixtures is slightly higher (1%) for both soils. Additionally, the maximum dry unit weight decreases and the optimum water content increases as the fly ash content increases.

The maximum unconfined strength of design mixtures was obtained at 1% wet of optimum water content (Edil et al. 2002). Thus the water content used in the field was specified as optimum water content $\pm$ 2%.

SECTION 4

METHODS

4.1 WATER LEACH TESTS

Water leach tests (WLTs) were conducted on fly ashes to assess their leaching behavior and to determine if the fly ashes were suitable for soil stabilization in accordance with NR 538. The WLTs were conducted following ASTM D 3987-85. Water leach tests were also conducted on soil alone, soil-fly ash mixtures having different fly ash contents, fly ashes spiked with known amounts of different metals, and soil-fly ash mixtures prepared with spiked fly ash.

4.1.1 Water Leach Tests on Fly Ash, Soil Alone, and Soil-Fly Ash Mixtures

The WLTs were conducting by adding 70 g of crushed solid (soil or fly ash alone or soil-fly ash mixture) passing a US No. 4 Standard sieve to 1400 ml of ASTM Type II deionized water in a 2 L sealed container. The mixture was then agitated continuously in a tumbler at a rate of 29 rotations/min for 18 hr at room temperature (25^0 C). Afterwards, the mixture was allowed to settle for 5 min, and then the aqueous phase was separated by decantation. pH of the aqueous phase was measured immediately. The leachate was then filtered through a 0.45 μm filter paper, and stored for chemical analysis. Preservation of the leachate samples and subsequent chemical analyses of leachates are described in Sec. 4.4.

Soil-fly ash mixtures were also prepared for the WLTs using each of the soils and fly ashes, and with different fly ash contents (by dry weight). The mixtures that

were used for the WLTs are shown in Table 4.1. These fly ash contents were also used for column testing. To prepare the soil-fly ash mixtures, the soil was air dried and crushed to pass a US No. 4 Standard sieve. Then a 2 kg sample of soil and fly ash (the proportion depends on fly ash content) was mixed homogeneously on a tray, and the required amount of tap water was sprayed on the mixture to achieve a molding water content 2% dry of optimum water content (see Sec. 4.2.1). The molding water was mixed into the dry soil-fly ash mixture until the mixture appeared homogeneous. A portion of each mixture was used to prepare a column leaching test specimen. The remainder was stored in a sealed plastic bag for seven days before the WLT.

4.1.2 Water Leach Tests on Spiked Fly Ash and Soil-Spiked Fly Ash Mixtures

WLTs with spiked fly ash were conducted to determine how higher metal concentrations affect leaching of metals. WLTs were conducted on the spiked fly ash and soil-spiked fly ash mixtures using the procedure described in Sec. 4.1.1. Only Columbia fly ash was used for the tests on spiked fly ash and soil-spiked fly ash mixtures. The fly ash was spiked by dissolving the mass of metal salts required to achieve the target concentration (Table 4.2) in 1400 ml of ASTM Type II deionized water. WLTs were then conducted using this water as the leachant. Four different sets of metal concentrations were used to simulate different levels of metals in the fly ash.

All tests conducted on soil-spiked fly ash mixtures had a fly ash content of 10% so that all other chemical constituents would remain unchanged. The soil was

Table 4.1. Soil-fly ash mixtures used for WLTs.

Type of Soil	Type of Fly Ash	Fly Ash Content (%)
Low plasticity clay (Joy silt loam)	Columbia	5
		10
		15
		20
	King	10
		20
	Dewey	10
		20
High plasticity clay (Lacustrine red clay)	Columbia	10
		20
	King	10
		20
	Dewey	10
		20
Organic clay (Theresa silt loam)	Columbia	10
		20
	King	10
		20
	Dewey	10
		20
Silica sand	Columbia	10
		20
	King	10
		20
	Dewey	10
		20

Table 4.2. Targeted Concentration of Fly Ash Spiked with Metals.

Species	Spike-A Concentration (mg/kg)	Spike-B Concentration (mg/kg)	Spike-C Concentration (mg/kg)	Spike-D Concentration (mg/kg)
Cadmium	0.5	1.0	2.0	3.0
Chromium (T)	5.0	10.0	20.0	40.0
Selenium	3.0	6.0	12.0	30.0
Silver	1.0	2.0	3.0	5.0

T = Total chromium

air dried and crushed to pass a US No. 4 Standard sieve, and 2 kg of soil and fly ash sample was mixed homogeneously on a tray. The metals were added to fly ash by dissolving the mass of metal salts required to achieve the target concentration in water, and then the water was sprayed on the mixture to achieve a molding water content of 2% dry of optimum (see Sec. 4.2.1). The molding water was mixed into the dry soil-fly ash mixture until the mixture appeared homogeneous. A portion of each mixture was then used to prepare a column test specimen. The remainder was stored in a sealed plastic bag for seven days before the WLT.

4.2 COLUMN TESTS

4.2.1 Preliminary Hydraulic Conductivity Tests

Prior to conducting the column tests, hydraulic conductivity tests were conducted on soil and soil-fly ash mixtures to identify molding water contents that resulted in specimens permeable enough to permit convenient sample collection. The hydraulic conductivity of a soil-fly ash mixture prepared with 10% Columbia fly ash and Joy silt loam from the STH 60 site is shown in Fig. 4.1 for molding water contents ranging between 17.6% and 21.6%. The specimens for the hydraulic conductivity tests were prepared in standard Proctor mold using standard Proctor compaction effort. The hydraulic conductivity decreases sharply as the molding water content is increased beyond optimum water content (19%) of the soil. Thus, all specimens were prepared at molding water content approximately 2% dry of optimum water content so that sufficient volumes of effluent could be collected in a reasonable time frame.

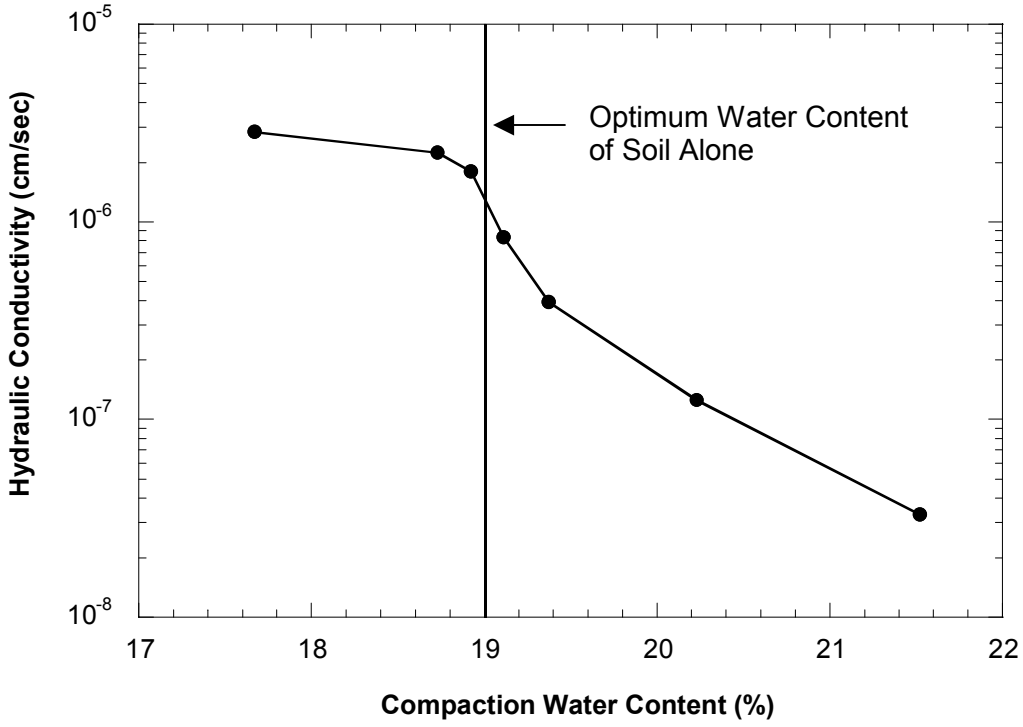

Fig. 4.1. Hydraulic Conductivity of Soil-Fly Ash Mixtures at Different Compaction Water Contents (10% Columbia Fly Ash).

4.2.2 Experimental Setup

4.2.2.1 Column Leaching Tests

Column leaching tests were conducted to provide a more realistic assessment of leaching from soil-fly ash mixtures and to determine leaching and transport parameters, such as initial effluent concentration (i.e., initial pore fluid concentration), effective porosity, partition coefficient, and dispersion coefficient for the soil-fly ash mixtures. Column leaching tests were also conducted on soil alone. The specimens were placed in flexible-wall permeameters operated in an up-flow mode (Das et al. 1989). A photograph of the experimental set-up is shown in Fig. 4.2.

Hydraulic gradients between 7 and 10 were applied to make sample collection convenient. These gradients are larger than exist in the field (typically about 1). However, Creek et al. (1992) report that metal leaching from fly ashes is independent of flow rate. Thus, the larger gradients are believe to have little impact on the test results. The cell pressure was 15 kPa and the pore water pressure ranged from 8-12 kPa.

A 0.1 M LiBr solution was used as the influent liquid to provide an influent with comparable ionic strength to percolating water (Karczewska et al. 1996, Papini 1999). The solution was prepared with LiBr salts (99.9% pure) dissolved in ASTM Type II water. Bromide was used as an independent tracer. Lithium was selected because it is not considered in the environmental analysis, is unlikely to be present in the soil, and has a lower preference for adsorption compared to the metals of

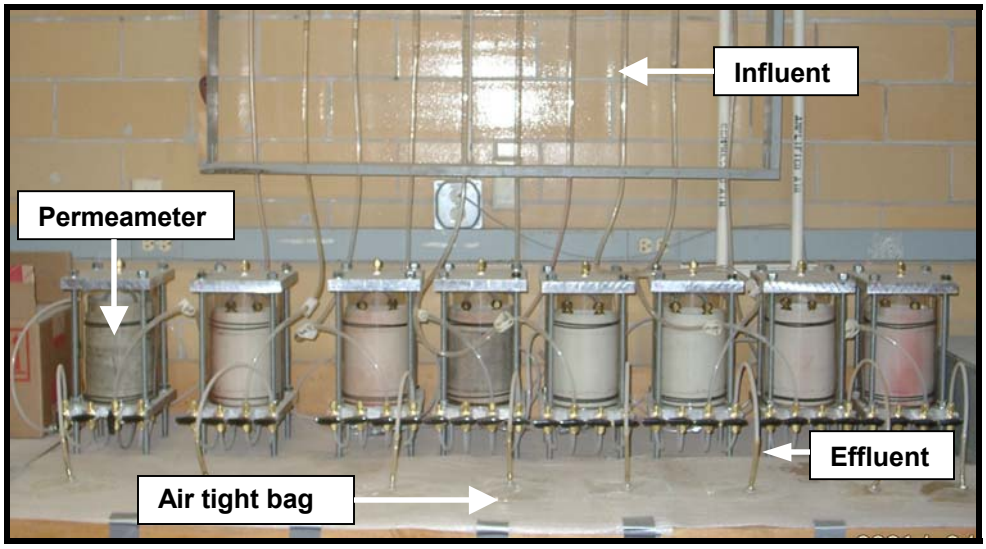

Fig. 4.2. Experimental Setup for Column Test.

concern in this study (Cd, Cr, Se, and Ag). The influent solution was exposed to the atmosphere for several days to achieve pH 6 prior to use, which is comparable to the pH of water in the natural environment (Chichester and Landsberger 1996, Huang et al. 1998).

Effluent from the column test (i.e., leachate) was collected in airtight sampling bags. Leachate was removed from the bags every 0.4 to 0.6 pore volumes of flow and a portion of leachate (50-55 ml) was collected for chemical analysis. The pH, volume, and time of collection of the leachate were recorded. Leachate samples were preserved and subjected to chemical analysis following the methods described in Sec. 4.4.

4.2.2.2 Column Tests on Subgrade Soils

Column tests were also conducted on subgrade soils using the set up described in Sec 4.2.2.1, except with an influent liquid simulating effluent from fly ash stabilized soil. The purpose of these tests was to evaluate transport through an underlying unstabilized subgrade above the groundwater table. Transport parameters of the subgrade soil are necessary to estimate the concentration of metals at the groundwater table.

The synthetic leachate used as the influent liquid was prepared by adding metals (Cd = 20 μg/L, Cr = 200 μg/L, Se = 100 μg/L, Ag = 20 μg/L) to a 0.1 M LiBr solution. This solution simulates the typical initial leachate obtained from the soil-fly ash mixtures. The pH of the influent solution was adjusted to 9.5 using calcium hydroxide and hydrochloric acid to simulate the high pH of the effluent from the soil-

fly ash mixtures. Readjustment of the pH was required several times during the column tests.

4.2.3 Type of Specimens

4.2.3.1 Column Leaching Tests

Two types of specimens were tested in the column leaching tests: Type-F and Type-S. Type-F specimens were prepared with conventional soil-fly ash mixtures and soil alone. Type-S specimens were prepared with soil-fly ash mixtures using fly ash spiked with metals. Type-F specimens were tested to determine transport parameters for soil-fly ash mixtures as well as the subgrade soil. Type-S specimens were tested for three reasons: (i) to determine if a relationship exists between the initial effluent concentration from the column leaching tests and the concentration from the water leach test, and (ii) to examine if the release pattern still follows instantaneous desorption at higher metal concentrations.

Type-F specimens were prepared with soil-fly ash mixtures at the fly ash contents shown in Table 4.1. Specimens with 0% fly ash were also tested to evaluate leaching from soil alone. The soil-fly ash mixtures were prepared and moistened following the method described Sec. 4.1.1. The moistened mixtures were compacted within one hour after mixing with water using standard Proctor effort (ASTM D 698). After compaction, the specimens were extruded from the compaction molds, sealed in polyethylene, and cured for 7 days at room temperature. The column leaching tests were initiated immediately after the curing period.

Four Type-S specimens were prepared using the four metals concentrations used for WLTs the tests (Table 4.2). Type-S specimens were prepared only with Columbia fly ash at a fly ash content of 10%. Type-S specimens were prepared following essentially the same procedures used for the Type-F specimen, except the compaction water was spiked with metals to achieve the target concentrations in Table 4.2.

4.2.3.2 Column Tests on Subgrade Soils

Four specimens were prepared with four different subgrade soils (Joy, Plano, Lacustrine, and Theresa) for the column tests conducted with subgrade soil alone using synthetic leachate as the influent liquid. These specimens were prepared using the same procedures used for the Type-F specimen described in Sec. 4.2.3.1.

4.2.4 Data Processing

Effective porosities and dispersion coefficient were obtaining by fitting the Ogata-Banks (1961) equation to bromide concentrations in effluent of from column leaching test. The Ogata-Banks solution of the advection-dispersion-retardation equation is:

$$\frac{C_e(L,T)}{C_i} = \frac{1}{2}\left\{ \operatorname{erfc}\left(\frac{R-T}{2(TR/P_L)^{1/2}} \right) + \exp(P_L)\ \operatorname{erfc}\left(\frac{R-T}{2(TR/P_L)^{1/2}} \right) \right\} \qquad (4.1)$$

where C_e is the effluent concentration, C_i is the influent concentration, R is the retardation factor, T is the pore volume leached, P_L (= vL/D) is the column Peclet

number, and erfc is the complimentary error function. Transport properties of metals in subgrade soils were also obtained by fitting the Ogata-Banks equation to the metal concentrations in the effluent of the column tests.

Retardation factors for the metals (Cd, Cr, Se, and Ag) were obtained by fitting van Genuchten's (1981) analytical leaching model to the metal concentration in the effluent of the column leaching tests:

$$\frac{C_e(L,T)}{C_o} = 1 - \frac{1}{2}\left\{ \operatorname{erfc}\left(\frac{R-T}{2(TR/P_L)^{1/2}} \right) + \exp(P_L)\ \operatorname{erfc}\left(\frac{R-T}{2(TR/P_L)^{1/2}} \right) \right\} \qquad (4.2)$$

where C_o is the initial concentration in the pore fluid of the porous matrix equilibrium with the solid phase concentration. A derivation of Eqn. 4.2 is described in Appendix G.

Concentrations were assigned to the average pore volumes of flow between the time when the sample was collected and the time when the previous sample was collected, as recommended by Shackelford (1994).

4.3 FIELD TESTS

Lysimeters were installed at the STH 60 and Scenic Edge field sites to determine the amount of liquid passing through the stabilized layer and to characterize the concentrations of Cd, Cr, Se, and Ag in leachate under field conditions. A photograph of the lysimeters being installed at STH 60 is shown in Fig. 4.3. The lysimeters were constructed with 1.5-mm thick textured HDPE

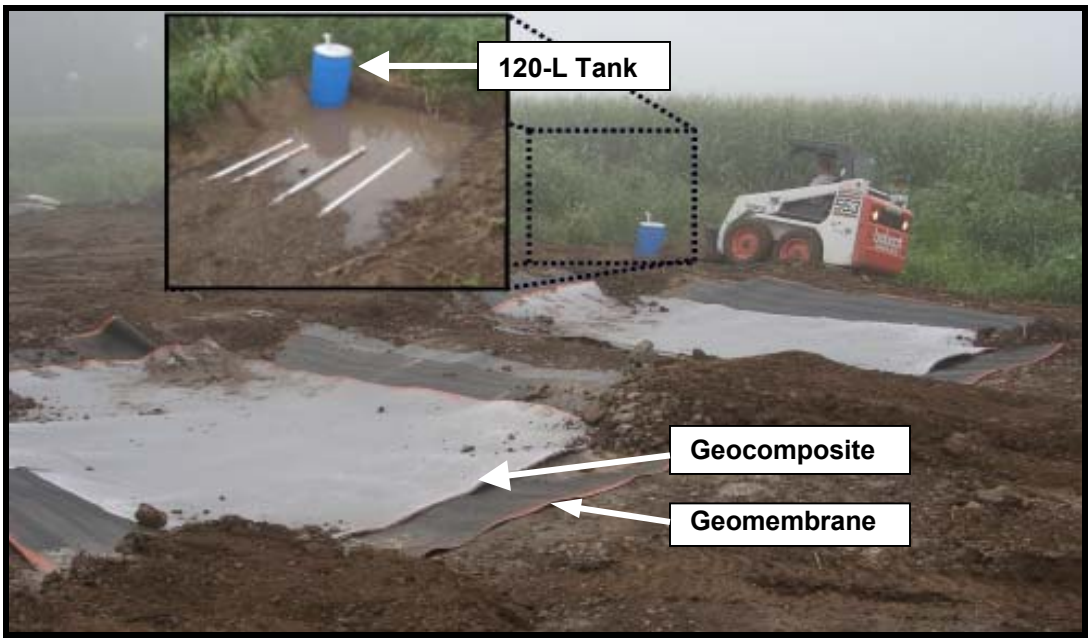

Fig. 4.3. Construction of Lysimeters at STH 60 Site.

geomembrane overlain by a geocomposite drainage layer (geonet with a non-woven geotextile heat bonded to both sides) used to direct the leachate to a sump. Schedule 40 PVC pipe (31 mm diameter) was used to connect the sump in each lysimeter to a 120-L tank buried adjacent to the pavement and below the frost depth. The tank was insulated with extruded polystyrene insulation to prevent freezing of the leachate during the winter.

Leachate is removed from the tanks every 3-5 weeks using a suction pump. The volume of leachate is measured in a 20-L bucket during pumping. Leachate samples for chemical analysis are collected from the outlet pipe when approximately 40-50% of the leachate has been pumped from the tank. After pumping each tank, the pump and the associated hoses are washed by allowing the pump to run with deionized water for 2 to 3 min to prevent cross-contamination. Preservation and chemical analyses of the leachate samples are described in Sec. 4.4.

4.3.1 Lysimeters at STH 60 Site

Two equal size (3.50 m x 4.75 m) lysimeters were installed in the fly ash stabilized test section at the STH 60 site. The layout of these lysimeters is shown in Fig. 4.4. Cross-sections showing placement of the lysimeters in the pavement profile are shown in Fig. 4.5. One lysimeter was installed along the centerline of the roadway; the other was along the shoulder. Two other lysimeters having the same size were installed at similar locations in a control section where no fly ash stabilization was employed.

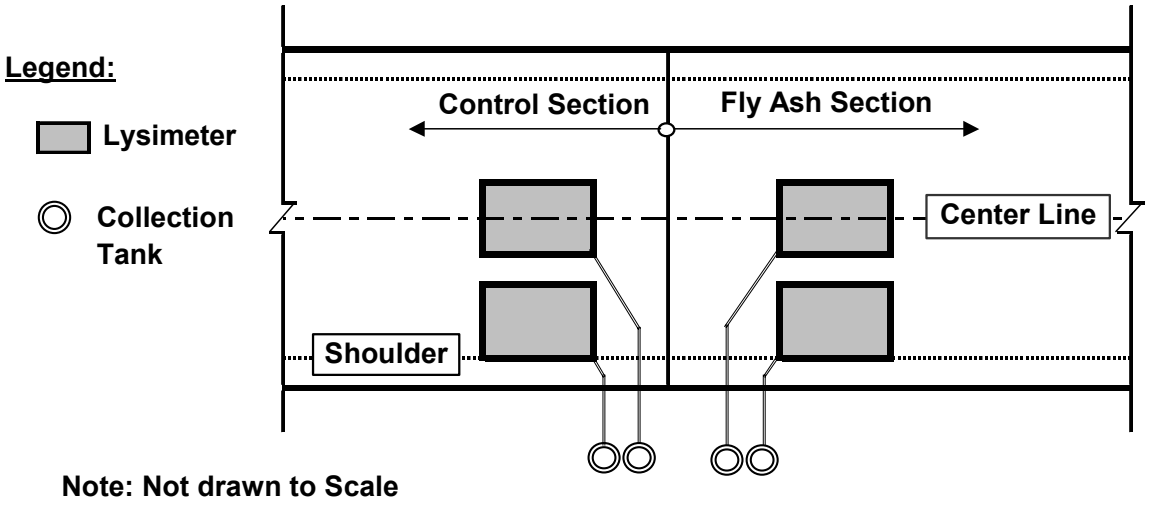

Fig. 4.4. Layout of Lysimeters at STH 60 Site.

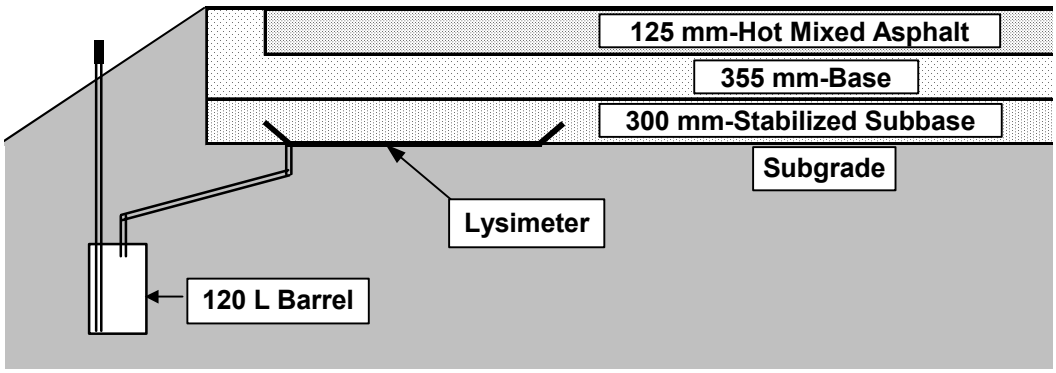

Note: Not drawn to scale

(a)

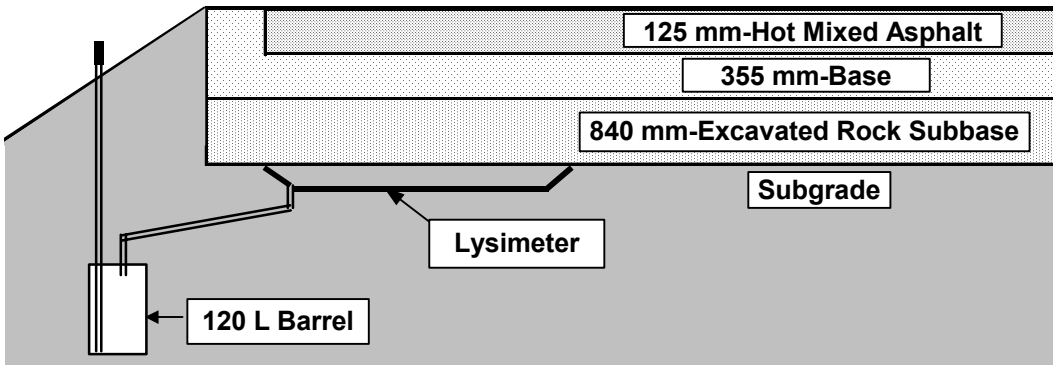

Note: Not drawn to scale

(b)

Fig. 4.5. Cross Section of the Lysimeters at STH 60 Site: (a) Stabilized Subbase Section and (b) Control Section.

In the fly ash section, the pavement profile consisted of three layers: asphalt concrete, base course, and fly ash stabilized subbase. The base course was 255 mm thick, and was constructed with a 140-mm-thick layer of salvaged crushed asphalt concrete overlain by 115-mm-thick layer of crushed aggregate. The subbase was a 300-mm-thick layer of Joy silt loam stabilized with 10% Columbia fly ash. The lysimeters were installed just beneath the stabilized subbase. To prevent damage during stabilization, the lysimeters were filled with soil-fly ash mixture that had been mixed at an adjacent location. The soil-fly ash mixture was placed in the lysimeter immediately after mixing, and then was compacted following the same procedure used for the remaining stabilized section.

The pavement profile in the control section also consisted of three layers: asphalt concrete, base course, and subbase course. The asphalt concrete and base course layers were the same as those used in the fly ash stabilized section. The subbase layer was constructed with excavated rock consisting of cobbles (75 to 350 mm in diameter) and a finer fraction containing gravel, sand, and fines. The particle size distribution of the subbase consisted of approximately 20% cobble size particles, 25% gravel, 50% sand, and 5% fines.

The lysimeters in the control section were installed 0.3 m below the existing subgrade elevation. The lysimeters were filled with 0.30 m of subgrade soil (instead of soil-fly ash mixture) and compacted similar to the other part of the section before the pavement profile was constructed.

4.3.2 Lysimeter at Scenic Edge Site

One lysimeter (2.75 m x 2.75 m) was installed beneath the pavement at the Scenic Edge site. The layout of the lysimeter and a cross-section showing placement of the lysimeter in the pavement profile are shown in Fig. 4.6. The lysimeter was installed 300 mm below the surface elevation of the subgrade so that it would be just beneath the stabilized layer. Similar to the fly ash stabilized section in STH 60, the soil and fly ash were not mixed in situ above the lysimeters to prevent damage during construction. Instead, the lysimeter was filled with soil-fly ash mixtures that had been mixed at an adjacent location. The soil-fly ash mixture was placed in the lysimeter immediately after mixing, and then was compacted following the same procedures used for the remaining stabilized section.

4.4 CHEMICAL ANALYSIS

Leachate samples collected from the field, water leach tests, column leaching tests on soil-fly ash mixtures, and column tests on subgrade soils were stored in the laboratory and subjected to chemical analysis. Concentrations of Cd, Cr, Se, and Ag were determined by furnace atomic absorption (AA) spectrometry following EPA Standard Methods 213.2, 218.2, 270.2, and 272.2. All analyses were conducted using a Varian SpectrAA-800 Atomic Absorption (AA) Spectrometer controlled using a computerized Varian SpectrAA-880 Data Station. The SpectrAA-800 was equipped with a graphite tube atomizer (GTA 100) and an automated sample dispenser for the GTA.

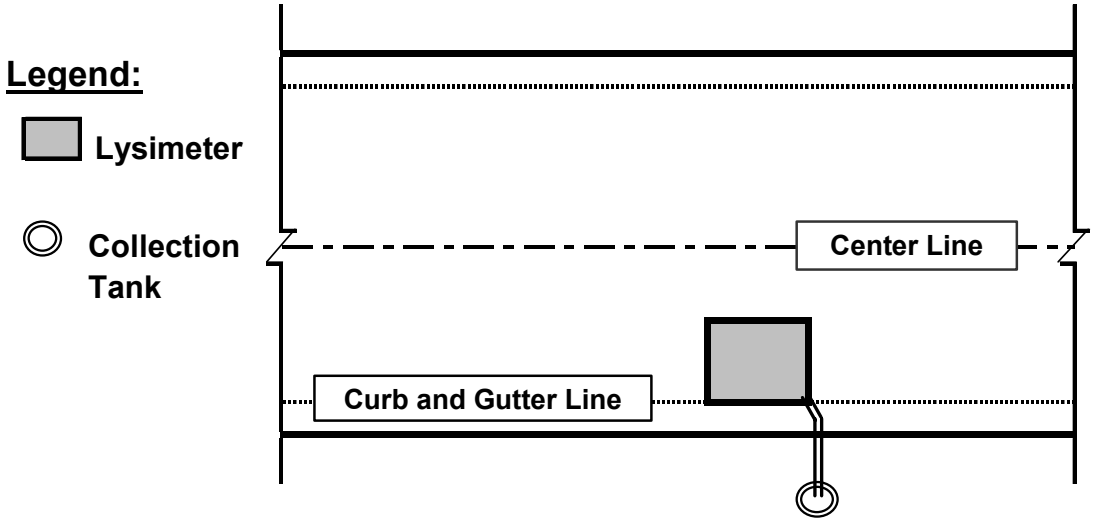

(a)

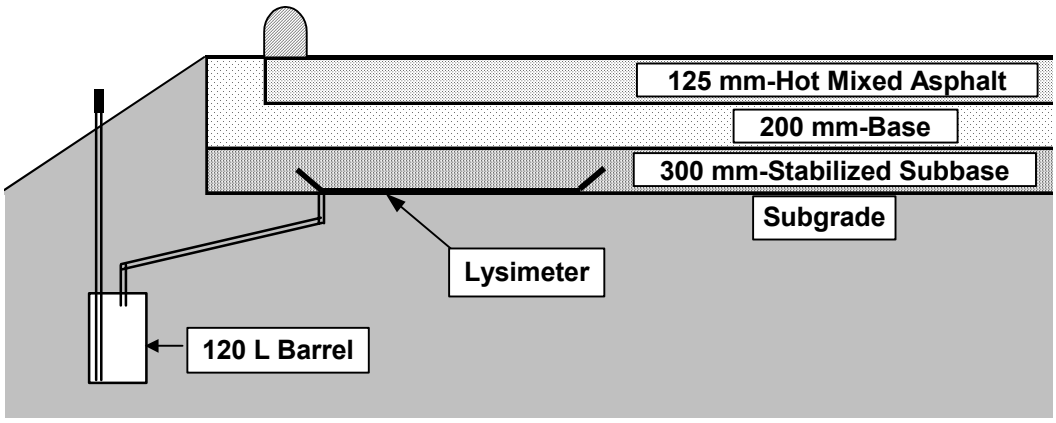

(b)

Fig. 4.6. Lysimeter at Scenic Edge Site (a) Layout and (b) Cross Section.

Concentrations of bromide were determined by ion chromatography (IC) following the instructions provided with the instrument. A Dionex-600 Ion Chromatographer equipped with an ED 50 Electrochemical Detector, GP50 Gradient Pump, and a LC 25 Chromatography Oven, was used for bromide analysis.

4.4.1 Summary of Method for Analysis of Metals

4.4.1.1 Sample Collection, Filtration, and Preservation

EPA Method 1669 was followed for sample collection, filtration, and preservation. To avoid contamination and interferences, several measures were taken according to Part 4.0 (Method 1669), such as minimizing exposure, wearing gloves, using metal-free apparatus, and ensuring a clean environment. Immediately after leachate collection, samples were filtered through a 0.45 μm filter paper and acidified with concentrated 0.5% HNO_3 to bring the sample pH <2. Samples were collected in new 60 ml high-density polyethylene bottles that were washed with acid solution (2% HNO_3) before use. The sampling bottles were sealed to prevent volume change and evaporation. All samples were preserved at 4^{o}C before chemical analysis.

4.4.1.2 Preparation of Standard Solution

Stock solutions obtained from Aldrich Chemical Company were used for all calibrations. The stock solution was diluted using ASTM Type I water containing

0.5% HNO_3. Calibration standards were prepared fresh each time. A blank and at least three standards were prepared within the appropriate range.

4.4.1.3 Instrument Parameters

Instrument parameters such as drying time, ashing time, and wavelength were adapted from the standard method for each element. Other operating parameters, such as atomizing time and temperature and purge gas atmosphere, were chosen as suggested by the instrument manufacturer.

4.4.1.4 Analysis

Chemical analysis was performed according to methods corresponding to specific elements. Before each use of the AA spectrometer, the instrument was configured, tuned, and calibrated for the metals of interest. A separate graphite tube was used for each element. Laboratory blanks were tested along with standard solutions. Equipment blanks and bottle blanks were also tested. Three replicates of each sample were measured.

4.4.2 Calibration Method for Metals Analysis

The instrument was optimized and initialized at zero before calibration. A standard solution was measured for five times for a stability check of the instrument. The instrument was assumed to be stable when the relative standard deviation (RSD) of the absorbance signals was <5% for all 5 replicates. The calibration points were obtained from the calibration blank and calibration standards, and a

new rational curve was fit (automatically by the data station) to the data, which was used as a calibration curve. A new calibration curve was created after measuring 20 samples.

Three replicates of each sample were measured. The RSD of the concentrations estimated from the calibration curve for replicates was calculated automatically by the data station. If the RSD was higher than 10%, the measurement was discarded and another measurement was made. After measuring two samples, a calibration blank was analyzed to ensure no carryover of the metal of interest and to check if the analytical system was free from contamination. The calibration curve was also verified with a standard solution after analyzing four samples. After measuring 10 samples, the calibration curve was re-sloped by analyzing the calibration blank and the midpoint calibration standard. A new calibration curve was created if the re-slope varied 10% of the original slope.

SECTION 5

RESULTS AND ANALYSIS

5.1 WATER LEACH TESTS

Water leach tests (WLTs) were conducted on bulk fly ash, soil-fly ash mixtures, and soils alone to estimate the leaching potential of metals. The purpose of these tests was to estimate the leaching potential from fly ashes as well as from soil-fly ash mixtures. Water leach tests were also performed on fly ashes that were spiked with metals and on soil-fly ash mixtures prepared with spiked fly ash.

5.1.1 Tests with Fly Ash and Soil-Fly Ash Mixtures

Aqueous phase concentrations of Cd, Cr, Se, and Ag from the WLTs are summarized in Table 5.1 along with the standards for NR 538 Category-3 and Category-4 byproducts. As noted in Sec. 2, Category 4 byproducts can be used in confined geotechnical fills, such as pavement subbases. Category-3 is a more stringent standard and refers to uses in unconfined geotechnical fills and capped transportation embankments.

Aqueous concentrations from the tests on bulk fly ash are lower than the Category-4 standards for each of the four species for all three fly ashes. Aqueous concentrations of Cd and Ag are also lower than the Category-3 standard, except for Cd from Dewey fly ash, which is (3.2 μg/L) approximately 50% higher than the Category-3 standard (2.5 μg/L). The concentrations of Cd and Ag in leachate from

Table 5.1. Aqueous Concentration of Metals from WLTs on Fly Ashes, Soil-Fly Ash Mixtures, and Soils.

Fly Ash	Soils	Fly Ash Content (%)	Leachate pH	Metal Concentration (μg/L)			
				Cd	Cr	Se	Ag
NA	Joy silt loam	0	7.0	0.8	23.8	11.0	1.6
	Lacustrine clay	0	7.5	1.1	40.4	10.0	3.1
	Theresa silt loam	0	7.2	1.4	46.9	6.0	4.4
	Silica sand	0	7.5	0.0	0.0	0.0	0.0
Columbia	Joy silt loam	10	11.0	0.6	46.0	16.2	1.8
		20	11.6	0.5	56.2	17.3	1.7
	Lacustrine clay	10	10.9	0.8	52.0	13.0	2.2
		20	11.6	0.8	63.1	14.0	2.4
	Theresa silt loam	10	10.7	0.9	66.0	11.0	2.6
		20	11.4	1.0	73.0	13.0	2.5
	Silica sand	10	11.4	0.4	41.1	13.8	1.1
		20	11.7	0.4	58.4	18.0	1.8
Dewey	Joy silt loam	10	9.7	1.7	32.4	35.0	2.9
		20	10.4	1.7	36.8	45.4	2.7
	Lacustrine clay	10	9.3	1.6	47.0	25.0	2.8
		20	10.1	1.8	50.0	36.0	3.1
	Theresa silt loam	10	9.0	1.8	56.0	32.0	3.6
		20	9.4	2.3	65.8	47.0	3.2
	Silica sand	10	10.4	1.3	29.8	42.0	2.3
		20	10.5	1.8	38.9	53.0	2.8
King	Joy silt loam	10	10.9	0.7	74.6	24.0	3.2
		20	11.5	1.0	86.0	32.0	3.3
	Lacustrine clay	10	10.8	1.2	76.0	20.0	3.3
		20	11.4	1.2	84.0	24.0	3.2
	Theresa silt loam	10	9.9	1.0	83.0	22.0	3.6
		20	11.1	1.3	93.5	30.0	3.5
	Silica sand	10	11.2	1.0	62.8	28.4	2.2
		20	11.5	1.1	79.0	33.0	2.8
Columbia	NA	100	11.8	0.7	95.0	26.0	2.2
Dewey		100	10.5	3.2	59.0	82.0	6.2
King		100	11.5	1.7	123.2	41.0	4.5
Category-3 Standard		100	NA	2.5	50	25	25
Category-4 Standard		100	NA	25	500	250	250

Note: 1. T = Total chromium.
2. Category-3 standards for other species are shown in Appendix A.
3. Detection limits are: Cd = 0.1 μg/L, Cr = 2.0 μg/L, Se = 2.0 μg/L, and Ag = 0.2 μg/L.

the WLTs on fly ashes are also similar to those for the soils alone, except for silica sand. For example, the aqueous concentration of Cd ranged between 0.7 μg/L and 3.2 μg/L for fly ashes and between 0.8 μg/L and 1.4 μg/L for the fine-grained soils. The aqueous concentration of Cd from Columbia fly ash is even slightly lower than those from all soils, except for silica sand. In contrast, the aqueous concentrations of Cr and Se from the WLTs are higher than Category-3 standard for all three fly ashes, and are significantly higher than those from soils. For example, the concentration of Cr in leachate from WLTs ranged between 59 μg/L and 123 μg/L for fly ashes and 24 μg/L and 47 μg/L for soils.

The concentrations of Cr and Se in leachate from WLTs with soil-fly ash mixtures are lower than those from the corresponding fly ash. For example, the concentration of Cr in leachate from soil-fly ash mixture prepared with 10% Dewey fly ash and Joy silt loam is approximately 50% of that from the Dewey fly ash alone, which reflects the effects of dilution and adsorption. Thus, when the aqueous concentration of metals in the leachate from fly ash is higher than that from the soil, the effect of dilution is pronounced in a soil-fly ash mixture.

5.1.1.1 pH of the Leachate from WLTs

pH of the leachate from WLTs is shown in Fig. 5.1 as a function of fly ash content. pH of the leachate increases with increasing fly ash content. The total amount of lime in the soil-fly ash mixtures increases with increasing fly ash content,

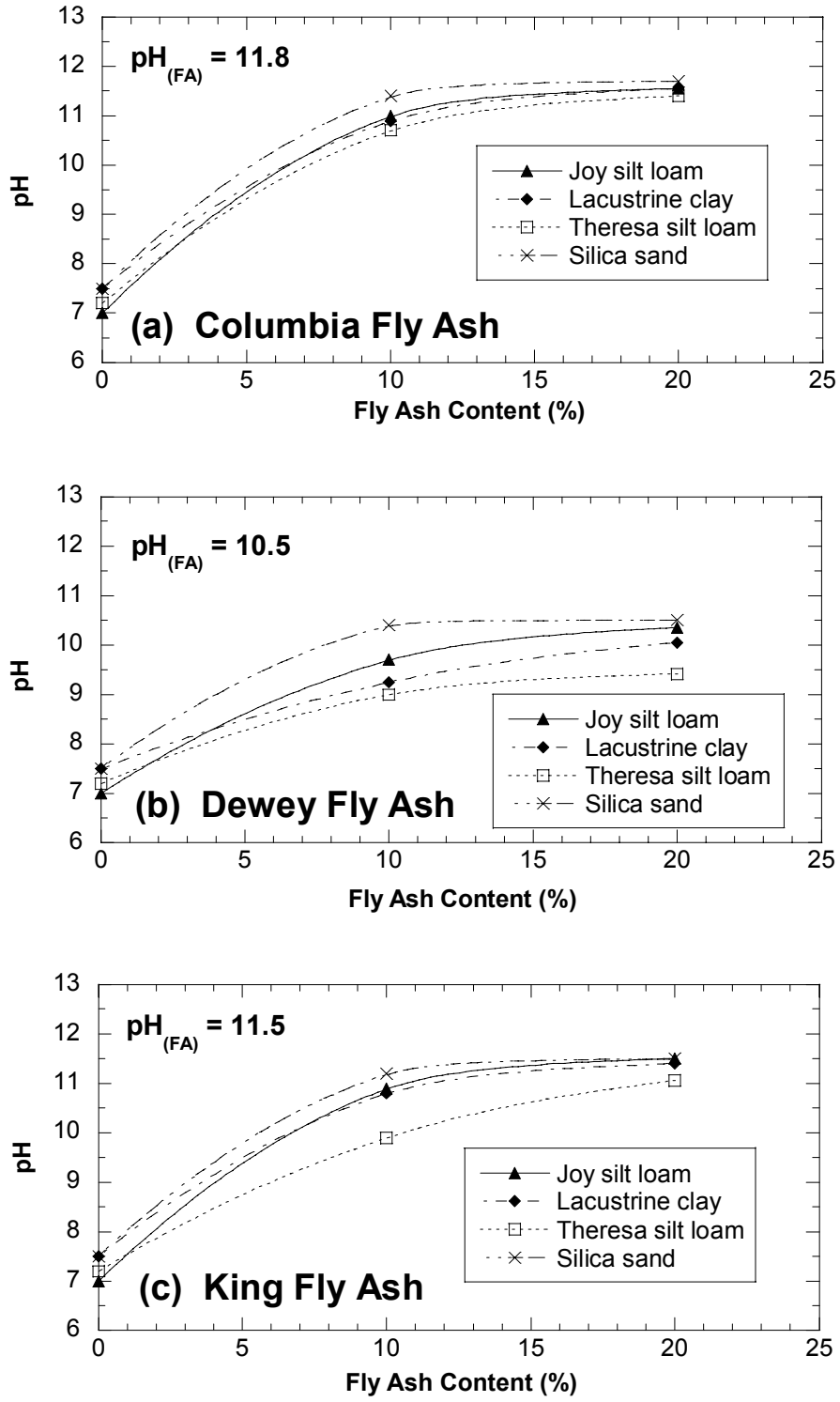

Fig. 5.1. pH of Soil-fly Ash Mixtures at Various Fly Ash Contents for: (a) Columbia Fly Ash (b) Dewey Fly Ash and (c) King Fly Ash.

which is primarily responsible for higher pH at higher fly ash content (Theis el al. 1982). The average pH of the leachate (for all soils) was highest for Columbia fly ash and lowest for Dewey fly ash at a particular fly ash content, which is consistent with the lime content of the fly ashes (see Table 3.4). For most cases, pH of the leachate increases appreciably when the fly ash content increases from 0% to 10%, but increases less as the fly ash content is increased from 10% to 20%. The pH of the leachate from fly ash alone is essentially similar to that from soil-fly ash mixtures prepared with 20% fly ash content.

For all fly ashes, the pH of the leachate is the highest for silica sand and lowest for Theresa silt loam. The pH of the leachate from Joy silt loam and Lacustrine red clay is similar for all fly ashes, except for Dewey fly ash, where the pH is slightly higher for Joy silt loam. The pH of the leachate from Theresa silt loam is the lowest among all soils for all fly ashes, probably because of its high buffering capacity due to presence of weak acids in the organic matter in the soil (McBride 1994).

5.1.1.2 Effect of Fly Ash Content on Concentration of Metals from WLTs

Aqueous concentrations of Cd and Ag from the WLTs are shown in Fig. 5.2 as a function of fly ash content. For Cd and Ag, the aqueous concentrations are very low regardless of the fly ash content and are comparable to those for the soil alone. Adding fly ash to the fine-grained soils, causes the concentrations of Cd and Ag to decrease because the pH of the leachate increases (Fig. 5.2a), which

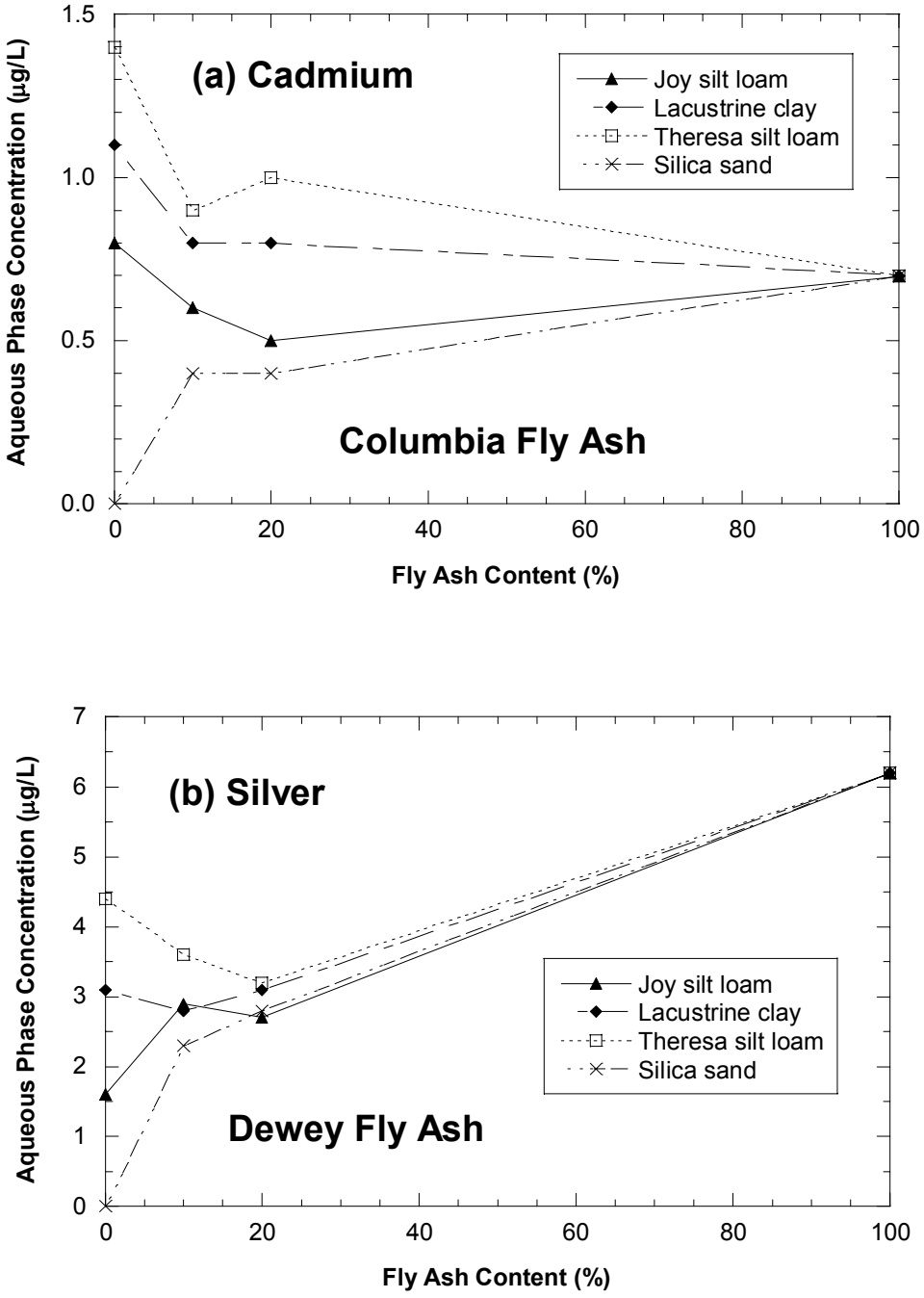

Fig. 5.2. Aqueous Concentration from Water Leach Tests For: (a) Cadmium form Soil-Fly Ash Mixtures Prepared with Columbia Fly Ash and (b) Silver form Soil-Fly Ash Mixtures Prepared with Dewey Fly Ash.

leads to greater adsorption of metals on the solid surface. Because leaching of Cd and Ag from soil-fly ash mixtures is lower than that of soil alone, leaching of Cd and Ag from all three fly ashes should not be an issue of environmental concern. Other graphs for the aqueous phase concentration of Cd and Ag are shown in Appendix D.

Typical graphs showing how aqueous concentrations of Cr and Se vary with fly ash content are shown in Fig. 5.3. The aqueous concentrations of Cr and Se are much higher for the fly ash alone than the soil alone, and thus the concentrations from the soil fly ash mixtures increase with increasing fly ash content. However, the increase in concentration is not linear with fly ash content, even though the mass of metals in soil-fly ash mixture increases approximately linearly with increasing fly ash content. The higher pH associated with the higher fly ash content (Fig. 5.1) increases partitioning, which results in diminished leaching (Brunori et al. 1999, Sauve et al. 2000).

The concentration of metals in the leachate from the soil-fly ash mixtures also depends on the metal content of the soil itself. Soil is the major component (80-90%) of the soil-fly ash mixtures, and the amount of metals in soils has significant contribution to the metal concentration in leachate. To understand the effect of adding fly ash on the aqueous concentration of metals in leachate from soil-fly ash mixtures, the increase in metal concentration due to fly ash was estimated by subtracting the metal concentration from the soil alone from the metal

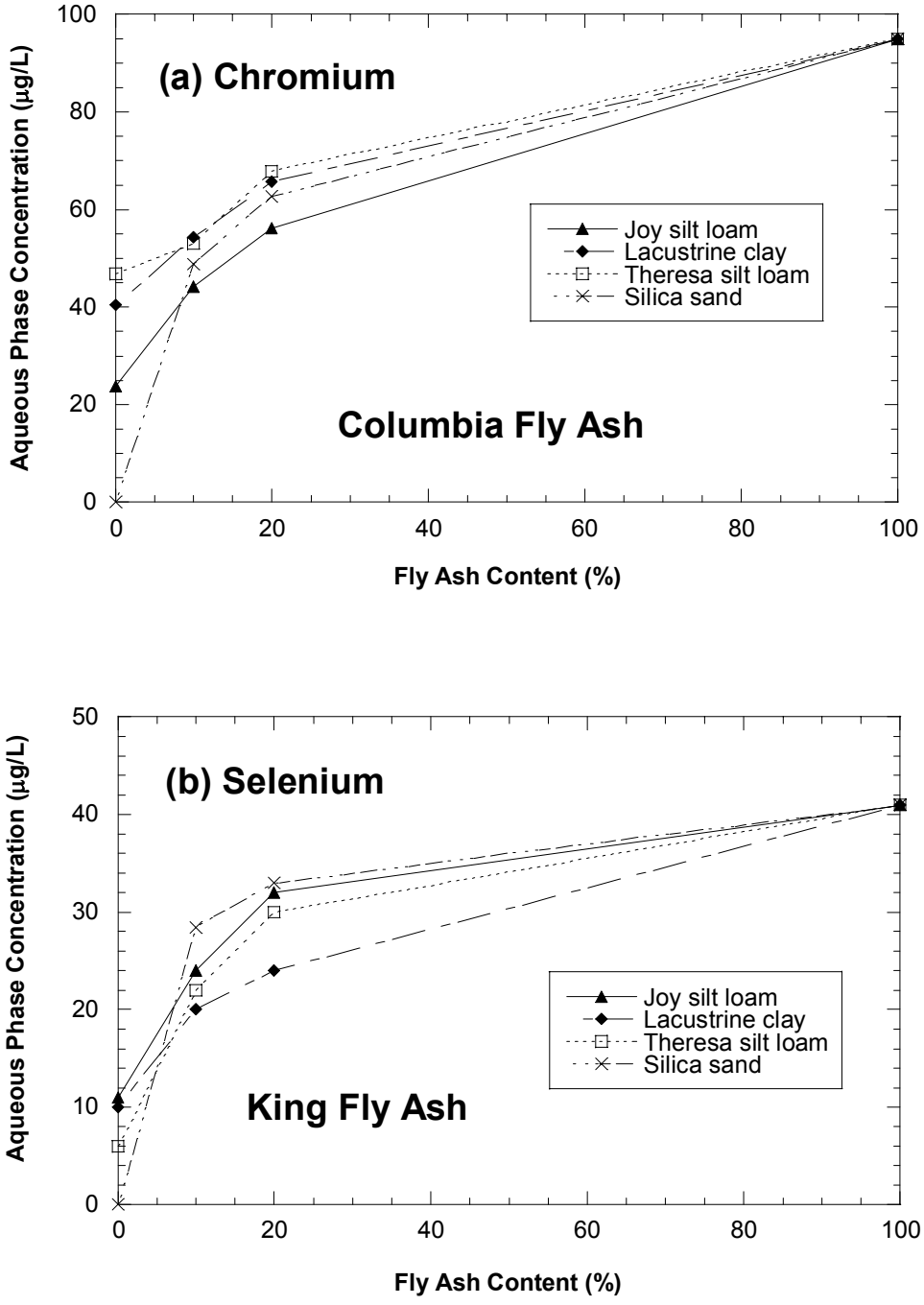

Fig. 5.3. Aqueous Concentration from Water Leach Tests For: (a) Chromium form Soil-Fly Ash Mixtures Prepared with Columbia Fly Ash and (b) Selenium form Soil-Fly Ash Mixtures Prepared with King Fly Ash.

concentration obtained from the soil-fly ash mixture. This increase in metal concentration is shown in Fig. 5.4 as a function of fly ash content. In Fig. 5.4, the increase in concentration has been normalized by the concentration obtained from fly ash alone.

The normalized concentration increases with increasing fly ash content, but the rate of increase diminishes as the fly ash content increases. The normalized increase in aqueous concentration is also inversely proportional to the CEC of the soil (Fig. 5.4a). For example, the normalized increase in aqueous concentration is the highest for silica sand, because it has the lowest CEC (0 meq/100g). In contrast, the normalized increase in aqueous concentration is the lowest for Lacustrine clay, because it has the highest CEC (33 meq/100g). However, pH also plays an important role. For example, the aqueous concentration of selenium (Fig. 5.4a) for Theresa silt loam (CEC = 27 meq/100g) is slightly higher than that for Joy silt loam (CEC = 9 meq/100g), because the pH is lower for the Theresa silt loam (9.9) relative to Joy silt loam (10.9).

The relationship between the aqueous concentrations of Cr and Se from WLTs for fly ash alone and soil-fly ash mixtures (10% and 20% fly ash content) are shown in Fig. 5.5. In general, higher aqueous concentrations from soil-fly ash mixtures are obtained where there are more metals in the fly ash, and more fly ash in the soil-fly ash mixture. The relationship is not linear, because the pH of the leachate from fly ashes and soil-fly ash mixtures varies significantly and the partitioning of metals in the leachate of fly ash varies non-linearly with the pH (Ricou et al. 1998).

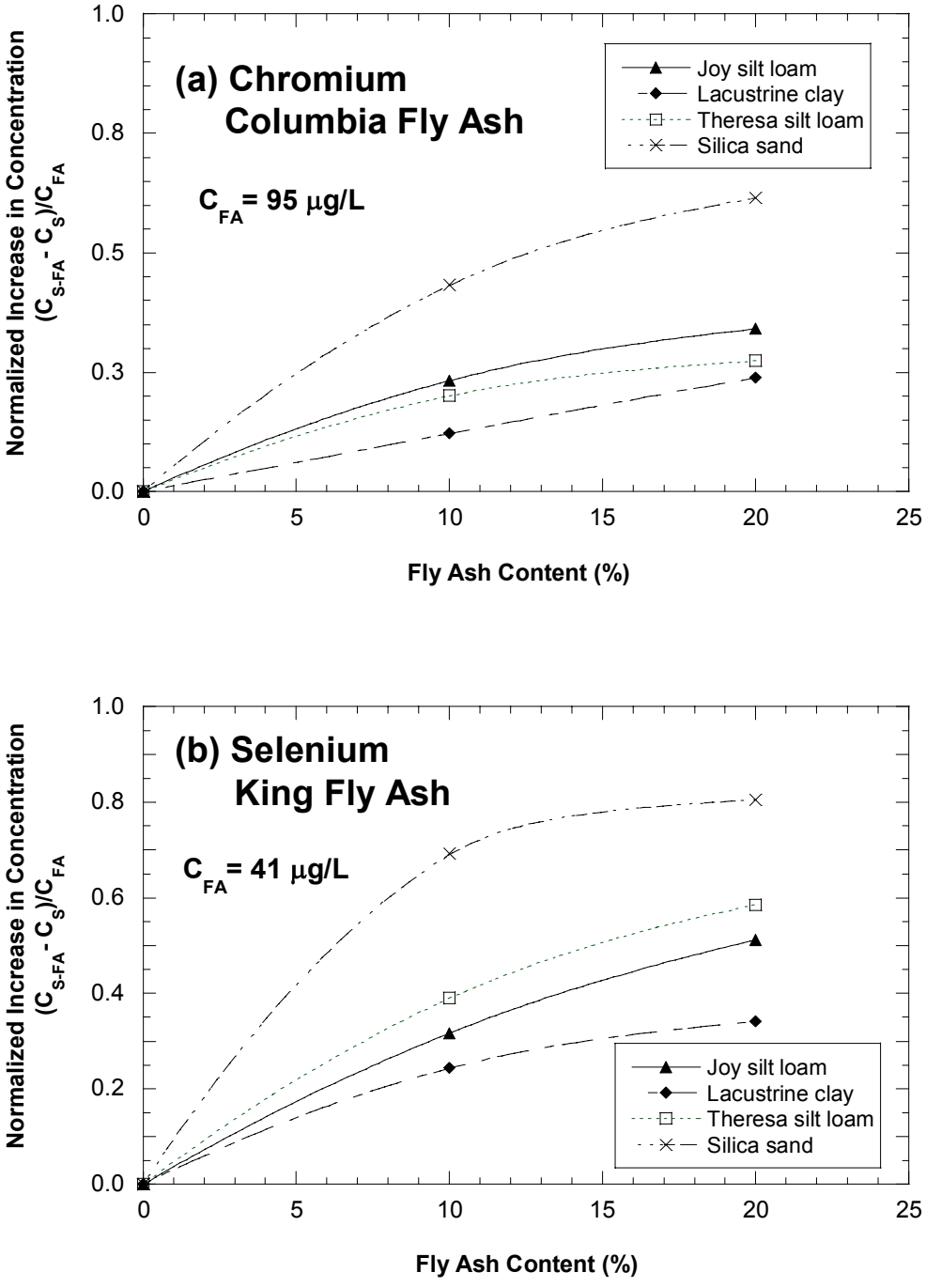

Fig. 5.4. Aqueous Concentration form Water Leach Tests for: (a) Chromium from Soil-Fly Ash Mixtures Prepared with Columbia Fly Ash and (b) Selenium form Soil-Fly Ash Mixtures Prepared with King Fly Ash.

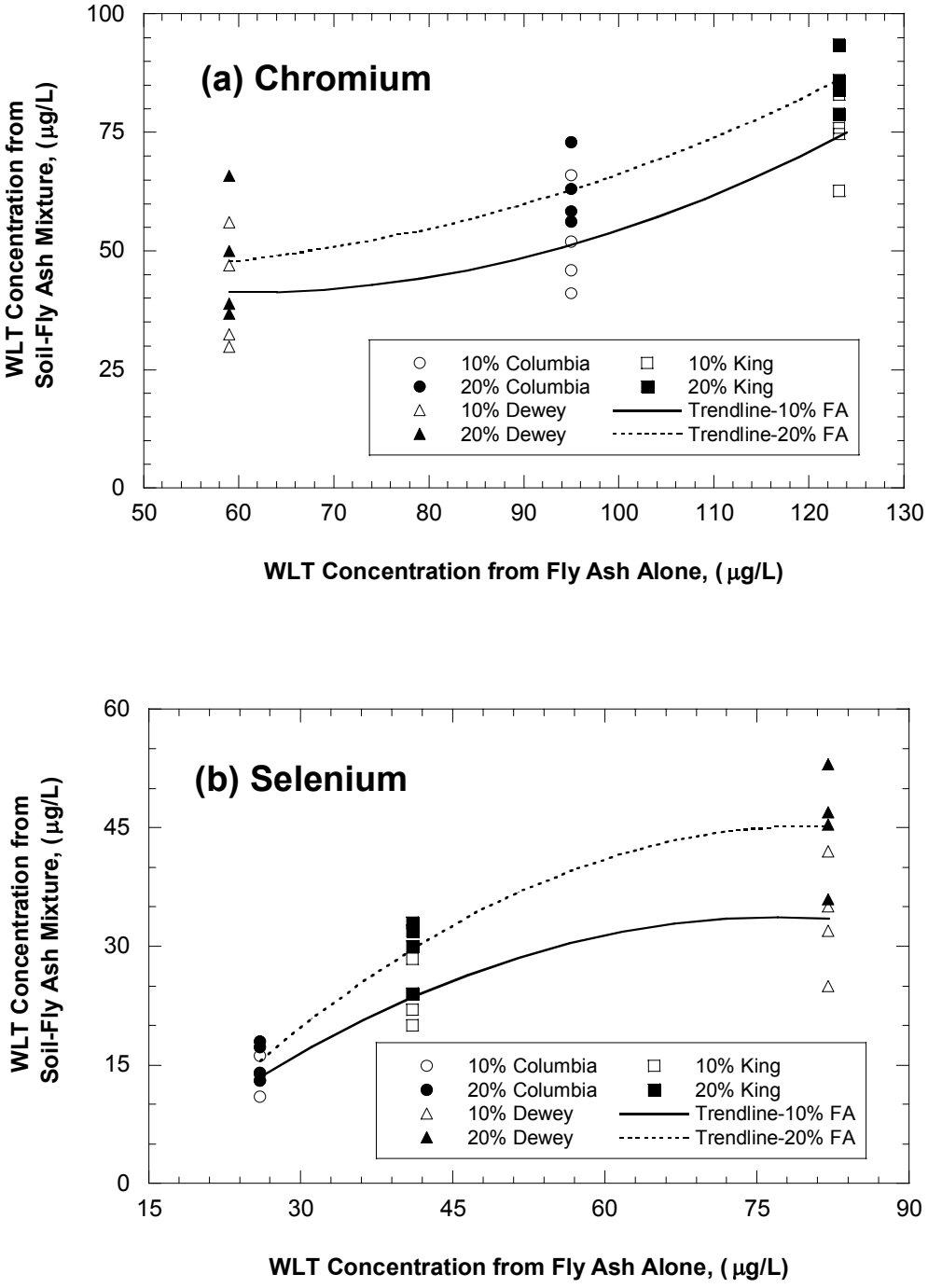

Fig. 5.5. Water Leach Test Concentrations for Fly Ash Alone and Soil-Fly Ash Mixtures (10% and 20% Fly Ash Content): (a) Chromium and (b) Selenium.

5.1.2 Tests with Spiked Fly Ash

Water leach tests with spiked fly ash were conducted to determine how higher metal concentrations in fly ash may affect leaching of metals. As described in Sec. 4, concentrations of metals in the fly ash were varied by adding metal salts to the fly ash. All other chemical constituents were kept the same. Water leach tests were conducted on spiked fly ash and soil-fly ash mixtures prepared with 10% spiked fly ash. Only Columbia fly ash was used for the WLTs with spiked fly ash. Thus, the pH of the leachate for all four tests with spiked fly ash (11.8 ± 0.1) was similar to that of the unspiked Columbia fly ash (11.8). Similarly, the pH of the leachate for all four tests on soil-fly ash mixtures prepared with 10% spiked fly ash (11.0 ± 0.1) was similar to that prepared with unspiked Columbia fly ash (11.0).

The aqueous concentration of metals from the WLTs with spiked fly ashes and soil-fly ash mixtures prepared with spiked fly ashes are summarized in Table 5.2. The concentration of metals increases as the metal mass is increased by spiking. However, the aqueous concentration does not increase in proportion to the amount of metal added, and the very small portion of the metal that is in the aqueous phase suggests that the partition coefficients for the metals are large.

Partition coefficients of each metal for the fly ash were computed using the aqueous concentrations and the sum of the metal mass in the fly ash (obtained from total elemental analysis) and the metal mass added for spiking. Partition coefficients for the soil-fly ash mixtures were computed assuming that the concentration of metals on the soil solid was 50% of that in unspiked fly ash. This

Table 5.2. Aqueous Concentrations and Partition Coefficient of Metals from WLTs on Spiked Fly Ashes and Soil-Fly Ash Mixtures Prepared with Spiked Fly Ash.

Parameters	Spike Type	WLT Material	Cd	Cr (T)	Se	Ag
Aqueous Concentration (μg/L)	Unspiked	Fly Ash Alone	0.7	95	26	2.2
		Soil-Fly Ash Mixture	0.6	41	15	1.7
	Spike-A	Fly Ash Alone	0.9	111	56	2.7
		Soil-Fly Ash Mixture	0.7	40	32	2.0
	Spike-B	Fly Ash Alone	1.0	123	61	3.2
		Soil-Fly Ash Mixture	0.6	56	35	2.4
	Spike-C	Fly Ash Alone	1.1	148	64	3.6
		Soil-Fly Ash Mixture	0.7	64	43	3.1
	Spike-D	Fly Ash Alone	1.4	185	71	4.1
		Soil-Fly Ash Mixture	0.8	68	47	3.8
Average Partition Coefficient (L/kg)	All	Fly Ash Alone	1255	514	440	855
		Soil-Fly Ash Mixture	770	497	402	670

Note: 1. T = Total chromium.

2. Detection limits are: Cd = 0.1 μg/L, Cr = 2.0 μg/L, Se = 2.0 μg/L, and Ag = 0.2 μg/L.

assumption for the metal concentration on the soil solid is arbitrary; however, the initial mass of metals on the soil solid is significantly lower than the mass added during spiking. Thus, the initial mass assumed be on the soil solids has little effect on the partition coefficient. The partition coefficients are summarized in Table 5.2. The partition coefficients for both soil and fly ash are large because of the high pH of the leachate. Generally, adsorption of trace metals on soil solids and on mineral oxides on the soil surfaces increases at higher pH (McBride 1994).

Aqueous concentrations of metals from WLTs on the soil-fly ash mixtures (10% fly ash) prepared with spiked fly ash are graphed versus those from spiked Columbia fly ash alone in Fig. 5.6 and 5.7. The solid symbol (lowest concentration among the five points) represents the concentration obtained from the WLTs with unspiked Columbia fly ash. The remaining four points were obtained from the WLTs on spiked Columbia fly ash.

The relationship between aqueous concentration from fly ash and soil-fly ash mixture is linear, since spiking did not affect the pH of the leachate. The pH of all five tests (spiked and unspiked) on fly ash is similar (11.8) and the pH of all five tests on soil-fly ash mixtures is also similar (11.0). After adding significant amounts of metal salts to the fly ash, the concentration of metals initially on the soil surface can be assumed to be negligible compared to that in spiked fly ash, and thus the linear relationship can be assumed to pass through the origin.

The total amount of metal in the soil-fly ash mixtures (10% fly ash) is approximately one-tenth of that in a comparable amount of bulk fly ash. A simple

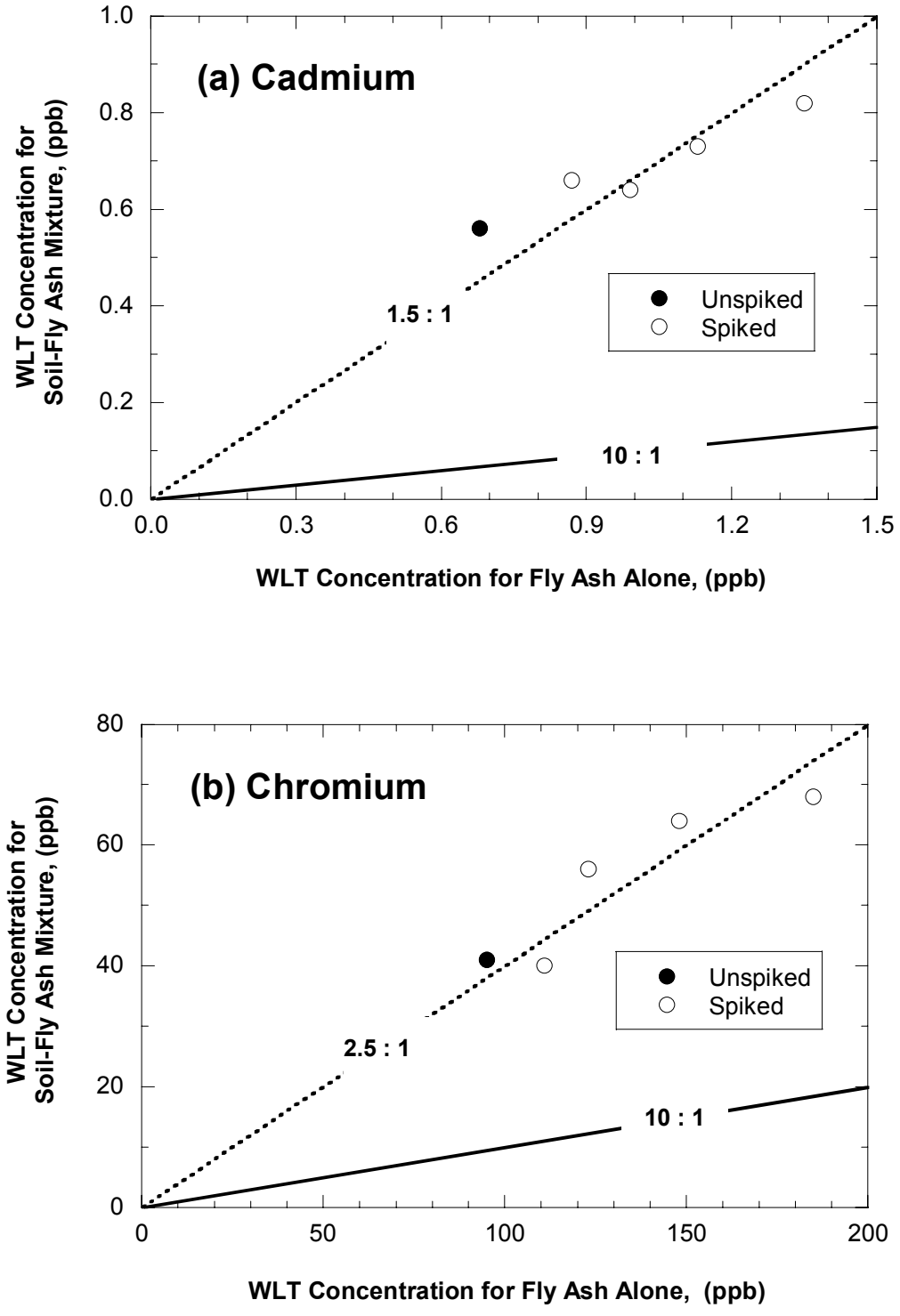

Fig. 5.6. Water Leach Test Concentrations for Columbia Fly Ash Alone and Soil-Fly Ash Mixtures (10% Fly Ash) Prepared with Joy Silt Loam and Columbia Fly Ash: (a) Cadmium and (b) Chromium.

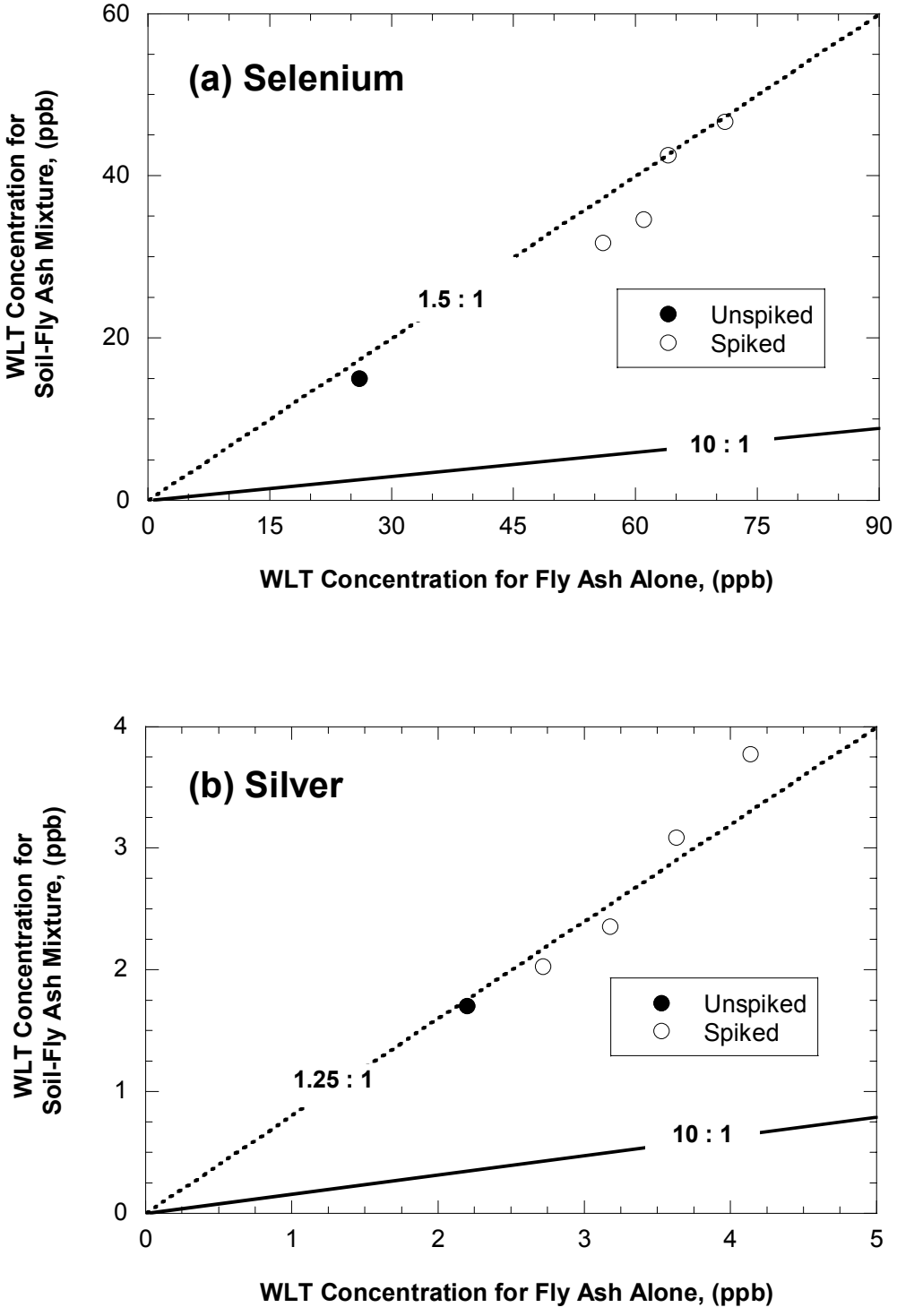

Fig. 5.7. Water Leach Test Concentrations for Columbia Fly Ash Alone and Soil-Fly Ash Mixtures (10% Fly Ash) Prepared with Joy Silt Loam and Columbia Fly Ash: (a) Selenium and (b) Silver.

dilution calculation based on the relative masses of soil and fly ash in the mixtures would indicate that the aqueous concentration from the soil-fly ash mixtures should be ten times lower than that from fly ash alone, and the points on Fig. 5.6 and 5.6 should fall close to the 10:1 line. However, for all metals, the points are between the 1:1.25 and 1:2.5 lines, which indicates that the partition coefficient for the soil-fly ash mixtures is much lower than that of bulk fly ash.

The total amount of lime in the soil-fly ash mixtures (10% fly ash) is also approximately ten times lower than that in a comparable mass of bulk fly ash. The lower fraction of lime in the soil-fly ash mixtures resulted in lower pH (11.0) than that of fly ash alone (11.8). This reduction in pH is probably responsible for the higher concentration of metals in the leachate from the WLTs on the soil-fly ash mixtures, because the partition coefficient changes significantly with pH (Sauve et al. 2000) (i.e., the mass of metals is diluted in a soil-fly ash mixture, but the lower pH of the leachate from soil-fly ash mixture may decrease the partition coefficient, and increase the aqueous concentration). Thus the potential of metal leaching from soil-fly ash mixtures cannot be estimated from the leaching potential of fly ash alone using a simple dilution calculation.

5.2 COLUMN TESTS

Column leaching tests were conducted on soil-fly ash mixtures to provide realistic estimates of the leaching and transport parameters for the metals of concern. Column leaching tests were also conducted on soil-fly ash mixtures prepared with spiked fly ash to estimate the initial effluent concentration as a

function of metal loading. Metals that leach from stabilized subbases also pass through the vadose zone before entering groundwater. Thus, column tests were also conducted on subgrade soils to estimate transport parameters needed for evaluating impacts on groundwater when using fly ash for soil stabilization.

5.2.1 Column Leaching Tests on Soil-Fly Ash Mixtures

Column leaching tests were conducted on soil-fly ash mixtures prepared with different soils and fly ashes to estimate leaching and transport parameters as a function of fly ash content. Concentrations of metals and bromide in the effluent from the column leaching tests were analyzed following the methods described in Sec. 4.4. Physical properties, such as effective porosity and dispersivity were estimated by fitting an analytical solution to the solute transport equation (Eqn. 4.1) with the breakthrough data for of bromide. Retardation factors for the metals were estimated by fitting an analytical leaching model (Eqn. 4.2) to the elution data for the metals. A 0.1 M LiBr solution was used as the influent liquid. A summary of the leaching and transport parameters obtained from the column leaching tests is shown in Tables 5.3 - 5.5.

5.2.1.1 Persistency of Effluent pH

pH of the effluent from column leaching tests on some of the soil-fly ash mixtures is shown in Fig. 5.8 as a function of pore volume of flow. Most of the column leaching tests were allowed to run for at least 12 pore volumes of flow,

Table 5.3. pH and Initial Effluent Concentration from Column Leaching Tests on Soils and Soil-Fly Ash Mixtures.

Fly Ash	Soils	Fly Ash Content (%)	Avg. Effluent pH	Initial Effluent Concentration (μg/L)			
				Cd	Cr	Se	Ag
No	Joy silt loam	0	7.1	6.0	13.1	14.1	3.1
	Lacustrine clay	0	7.6	9.2	23.9	8.8	5.6
	Theresa silt loam	0	7.3	11.8	31.2	7.2	7.2
	Silica sand	0	7.5	0.0	0.0	0.0	0.0
Columbia	Joy silt loam	10	9.9	4.0	60.1	32.1	6.2
		20	11.0	5.5	83.3	48.7	6.3
	Lacustrine clay	10	10.0	8.3	102.0	35.6	NA
		20	10.9	6.3	NA	38.9	5.1
	Theresa silt loam	10	9.6	9.1	254.4	NA	8.2
		20	10.3	10.6	223.1	37.8	9.8
	Silica sand	10	11.4	19.2	297.0	109.6	28.6
		20	11.9	22.1	NA	151.8	26.4
Dewey	Joy silt loam	10	9.4	22.1	81.8	106.0	21.6
		20	10.2	28.4	216.8	143.1	19.2
	Lacustrine clay	10	9.2	NA	107.2	96.2	16.2
		20	9.9	24.6	111.2	187.6	21.3
	Theresa silt loam	10	8.9	36.1	NA	121.6	24.1
		20	9.6	35.1	233.5	162.2	25.6
	Silica sand	10	10.6	38.4	237.4	237.4	61.5
		20	11.2	42.1	288.8	289.1	72.0
King	Joy silt loam	10	9.6	9.8	263.4	105.5	12.6
		20	10.9	11.2	192.3	132.0	15.1
	Lacustrine clay	10	9.8	9.6	136.2	NA	14.1
		20	10.9	9.2	156.2	87.4	21.2
	Theresa silt loam	10	9.2	13.5	188.6	122.2	16.5
		20	10.3	15.1	296.5	102.3	15.9
	Silica sand	10	11.1	NA	546.2	NA	NA
		20	11.6	26.9	684.5	202.7	46.4

Note: 1. T = Total chromium, L = Length of the specimen, NA = Not available.

2. Detection limits are: Cd = 0.1 μg/L, Cr = 2.0 μg/L, Se = 2.0 μg/L, Ag = 0.2 μg/L, and bromide = 10 μg/L.

Table 5.4. Retardation Factor of Metals from Column Leaching Tests on Soil-Fly Ash Mixtures.

Soil	Fly Ash	Retardation Factor			
		Cd	Cr (T)	Se	Ag
Joy silt loam	10% Columbia	5.2	5.7	3.5	5.0
	20% Columbia	4.8	4.8	3.2	4.4
	10% Dewey	5.1	5.1	3.8	5.2
	20% Dewey	5.3	5.4	4.0	5.9
	10% King	5.4	5.4	4.2	5.3
	20% King	5.8	6.1	3.7	5.5
Lacustrine clay	10% Columbia	5.3	5.2	4.1	NA
	20% Columbia	5.4	5.3	4.0	5.8
	10% Dewey	4.4	NA	3.6	4.8
	20% Dewey	6.3	5.2	4.0	6.0
	10% King	5.5	5.7	NA	5.4
	20% King	4.9	5.3	3.9	5.4
Theresa silt loam	10% Columbia	5.3	5.3	3.5	5.2
	20% Columbia	6.1	5.1	4.0	5.1
	10% Dewey	5.2	5.3	3.4	4.5
	20% Dewey	5.3	4.7	3.6	4.7
	10% King	5.2	4.9	3.7	4.8
	20% King	5.3	5.0	3.9	5.0
Silica sand	10% Columbia	2.1	2.0	1.6	2.5
	20% Columbia	2.3	NA	1.9	2.9
	10% Dewey	2.2	2.0	1.6	2.2
	20% Dewey	2.2	1.9	1.9	2.4
	10% King	NA	NA	NA	NA
	20% King	2.3	1.8	1.7	2.4

Note: 1. T = Total chromium, NA = Not available.

2. Retardation factors are obtained by fitting an analytical model of leaching with the effluent concentrations. Effective porosity and dispersivity obtained for each of the specimen from bromide analysis were used while fitting the model curve to estimate retardation factor.

Table 5.5. Partition Coefficient of Metals from Column Leaching Tests on Soil-Fly Ash Mixtures.

Soil	Fly Ash	Partition Coefficient (L/kg)			
		Cd	Cr (T)	Se	Ag
Joy silt loam	10% Columbia	0.96	1.08	0.57	0.92
	20% Columbia	0.95	0.95	0.55	0.85
	10% Dewey	0.99	0.99	0.67	1.01
	20% Dewey	1.22	1.25	0.85	1.39
	10% King	1.10	1.10	0.80	1.07
	20% King	1.22	1.30	0.69	1.14
Lacustrine clay	10% Columbia	1.34	1.31	0.97	NA
	20% Columbia	1.41	1.38	0.96	1.54
	10% Dewey	1.08	NA	0.83	1.21
	20% Dewey	1.88	1.49	1.07	1.78
	10% King	1.47	1.54	NA	1.44
	20% King	1.32	1.45	0.98	1.48
Theresa silt loam	10% Columbia	1.54	1.54	0.90	1.51
	20% Columbia	1.91	1.53	1.12	1.53
	10% Dewey	1.67	1.71	0.95	1.39
	20% Dewey	1.80	1.55	1.09	1.55
	10% King	1.53	1.42	0.98	1.39
	20% King	1.64	1.53	1.11	1.53
Silica sand	10% Columbia	0.21	0.19	0.12	0.29
	20% Columbia	0.24	NA	0.17	0.36
	10% Dewey	0.24	0.20	0.12	0.24
	20% Dewey	0.25	0.19	0.19	0.29
	10% King	NA	NA	NA	NA
	20% King	0.24	0.15	0.13	0.26

Note: 1. T = Total chromium, NA = Not available.

2. Partition coefficient is calculated from total porosity, bulk density, and retardation factor. The retardation factor accounts for linear, reversible, and instantaneous equilibrium sorption of reactive solute.

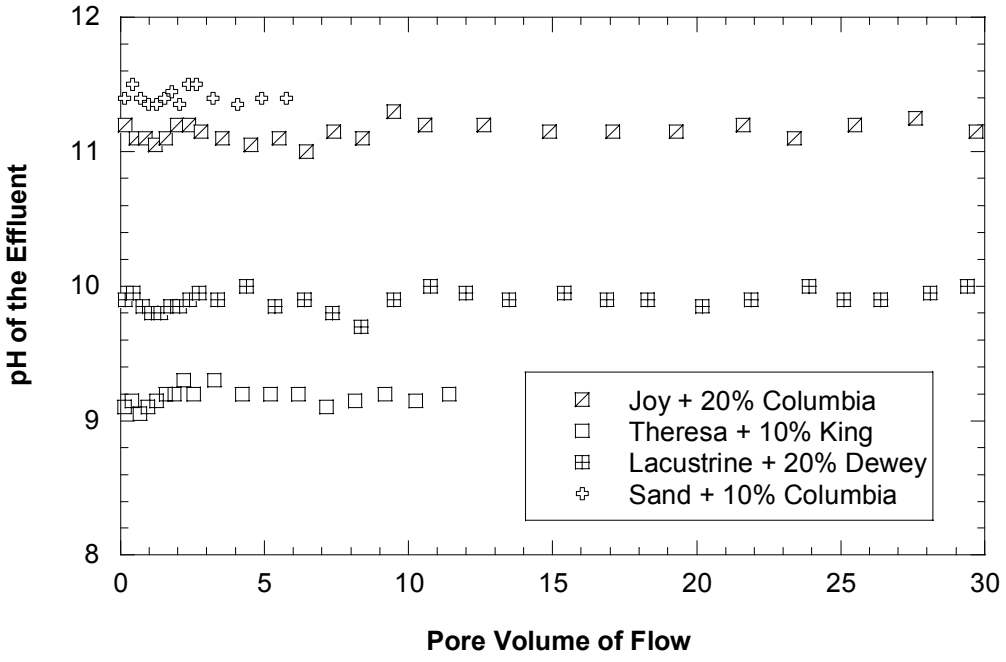

Fig 5.8. pH of Effluent from Column Leaching Tests on Soil-Fly Ash Mixtures.

and two of the tests (Joy + 20% Columbia, and Lacustrine + 20% Dewey) were allowed to run for 30 pore volumes of flow to examine the persistency of the effluent pH. In all cases, the pH of the effluent remained essentially unchanged throughout the test.

Approximately 1 pore volume of flow passed annually through the stabilized layer at STH 60. If the Darcy flux does not vary over time, then the data in Fig. 5.8 suggest that the pH in the field should persist for at least 30 years.

5.2.1.2 pH of the Effluent

pH of the effluent from the column leaching tests was measured immediately after collecting the leachate samples. pH was measured with an Accumet pH meter (Model 50) equipped with a standard glass body electrode. The average pH of the effluent from soil-fly ash mixtures prepared with different soils and fly ashes is shown in Fig. 5.9 as a function of fly ash content. pH of the effluent increases with increasing fly ash content for all cases.

The average pH of the leachate (for all soils) was highest for Columbia fly ash and lowest for Dewey fly ash at a particular fly ash content, which is consistent with the pHs obtained from the WLTs. Similar to the WLTs, pH of the leachate increases rapidly as the fly ash content increases from 0% to 10%, but increases slowly as the fly ash content increases from 10% to 20%. However, the pH of the effluent from column leaching tests was slightly lower (~1 pH unit) than that of the leachate from WLTs for all cases.

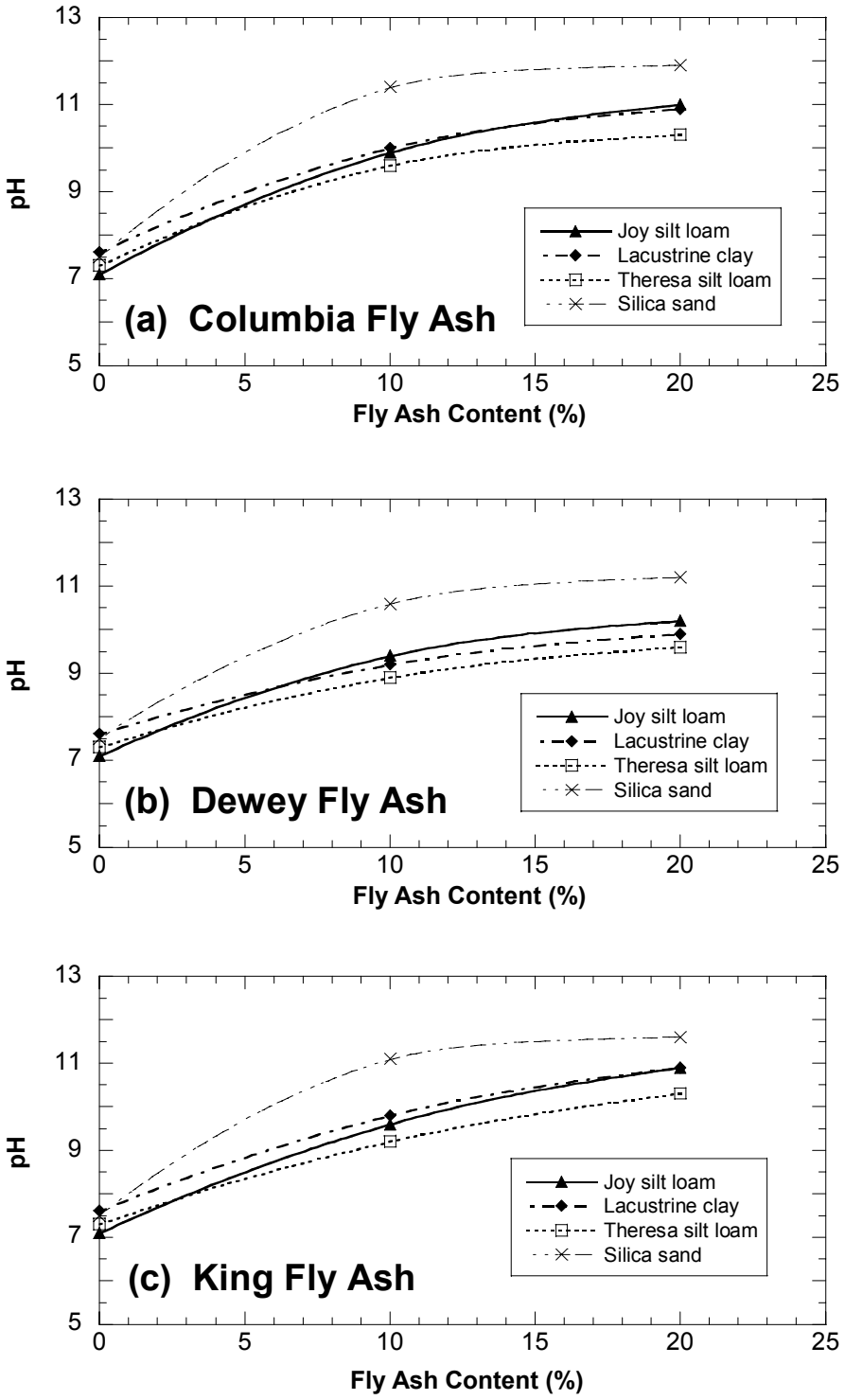

Fig. 5.9. pH of Effluent from Column Leaching Tests on Soil-Fly Ash Mixtures prepared with (a) Columbia Fly Ash (b) Dewey Fly ash, and (c) King Fly Ash.

For all fly ashes, the pH of the effluent is significantly higher for silica sand compared to other soils. In addition, similar to WLTs, the soil-fly ash mixtures prepared with Theresa silt loam have the lowest pH, and the soil-fly ash mixtures prepared with Joy silt loam and Lacustrine red clay have similar pH.

5.2.1.3 Effective Porosity

Effective porosity of soil-fly ash mixtures was estimated by fitting Eqn. 4.1 to the breakthrough data for bromide. A retardation factor of 1 was assumed since bromide is a conservative tracer.

Typical breakthrough curves for bromide from column leaching tests on soil-fly ash mixtures along with the fitted analytical model are shown in Fig. 5.10. The estimated effective porosity of the specimens prepared with different soils and fly ashes at different fly ash contents are shown in Table 5.6 along with the dry unit weight, water content, and total porosity. Total porosity was calculated from the phase relationships.

The effective porosity varies between 0.28 and 0.51, and is lower than the total porosity for most of the soil-fly ash mixtures. The effective-to-total porosity ratio varies between 0.65 and 1.08. Effective porosity higher than total porosity may result from error of calculating total porosity or error associated with the breakthrough data. Effective porosity can be lower than total porosity because of non-interconnected and dead-end pores (Fetter 1992), as well as the bound water associated with the clay surface (Prammer et al 1996). The estimated effective

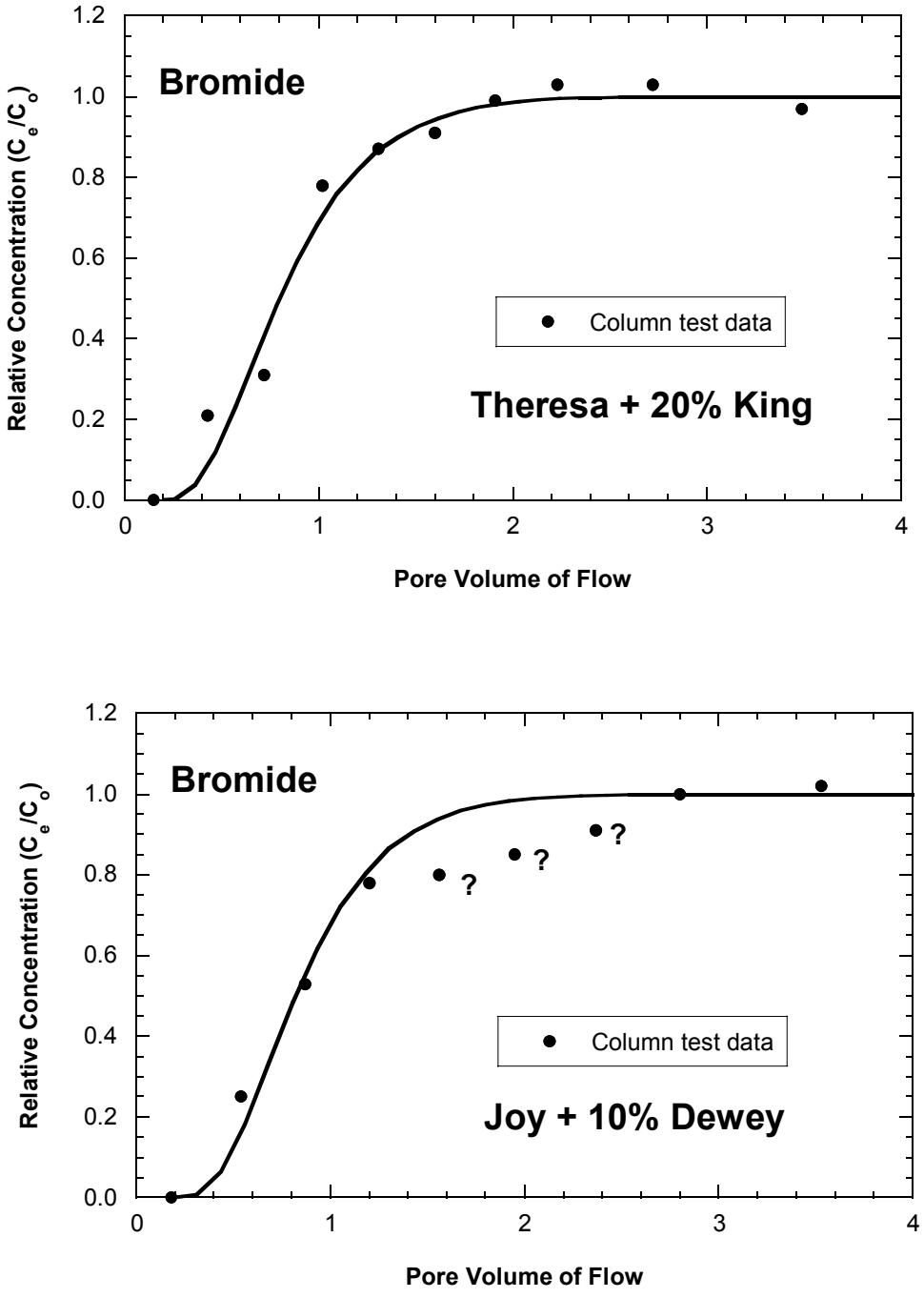

Fig. 5.10. Breakthrough Curves for Bromide from Column Leaching Tests on Soil-Fly Ash Mixtures Prepared with (a) Theresa Silt Loam and 20% King Fly Ash (b) Joy Silt Loam and 10% Dewey Fly Ash. Curves Correspond to the Fit of the Analytical Solution Shown in Eqn. 4.1.

Table 5.6. Porosity and Related Properties of Specimens Used for Column Leaching Tests.

Soil	Fly Ash	Total Porosity	Effective Porosity	Effective-to-Total Porosity Ratio	Dry Unit Weight (kN/m^3)	Water Content (%)
Joy Silt loam	10% Columbia	0.38	0.33	0.87	16.4	17.3
	20% Columbia	0.41	0.31	0.76	15.6	17.6
	10% Dewey	0.39	0.32	0.82	16.1	18.3
	20% Dewey	0.44	0.34	0.77	14.7	16.9
	10% King	0.39	0.42	1.08	16.1	17.4
	20% King	0.41	0.29	0.71	15.6	18.2
Lacustrine clay	10% Columbia	0.49	0.48	0.98	13.6	22.3
	20% Columbia	0.50	0.37	0.74	13.3	22.1
	10% Dewey	0.49	0.51	1.04	13.5	21.1
	20% Dewey	0.54	0.39	0.72	12.1	21.6
	10% King	0.51	0.41	0.80	13.1	22.4
	20% King	0.52	0.34	0.65	12.7	21.4
Theresa silt loam	10% Columbia	0.48	0.36	0.75	11.7	26.1
	20% Columbia	0.50	0.34	0.68	11.5	25.2
	10% Dewey	0.51	0.33	0.78	10.9	26.7
	20% Dewey	0.53	0.43	0.81	10.6	25.3
	10% King	0.48	0.40	0.83	11.6	25.2
	20% King	0.51	0.42	0.82	11.1	25.9
Silica Sand	10% Columbia	0.32	0.29	0.91	17.7	12.5
	20% Columbia	0.31	0.27	0.87	18.1	14.2
	10% Dewey	0.33	0.31	0.94	17.3	11.6
	20% Dewey	0.34	0.29	0.85	17.0	13.9
	10% King	0.32	NA	NA	17.7	13.2
	20% King	0.31	0.28	0.90	17.9	13.8

Note: 1. NA = Not available.

2. Effective porosity is estimated by fitting the analytical model (Eqn. 4.1) with the data for bromide from the column leaching tests. Total porosity is determined from the weight-volume phase relationship.

porosity, and the effective-to-total porosity ratio for all specimens falls within ranges reported by Kim et al. (1997) and Yeh (2000).

5.2.1.4 Dispersion Coefficient and Dispersivity

In one dimensional flow system, such as in column test, the hydrodynamic dispersion coefficient is represented as follows (Freeze and Cherry 1979):

$$D_h = D_L + D^* \quad (5.1)$$

$$D_L = \alpha_L v_s \quad (5.2)$$

$$D^* = \tau D_m \quad (5.3)$$

$$D_h = \alpha_L v_s + \tau D_m \quad (5.4)$$

where D_h = hydrodynamic dispersion coefficient, D_L = longitudinal mechanical dispersion coefficient (L^2/T), D^* = molecular diffusion coefficient (L^2/T), α_L = longitudinal dispersivity (L), v_s = seepage velocity, τ = tortuosity (L/L), and D_m = molecular diffusion coefficient in free water (L^2/T).

The flow and transport properties used for the column leaching tests are shown in Table 5.7. The column Peclet number (v_s L/D_h) varies between 4.9 and 18.4. Mass transport in column tests is usually dominated by advection when the column Peclet number is higher than 50, and by diffusion when the column Peclet number is lower than 1 (Shackelford 1994). The estimated column Peclet number in this study suggests that both advection and diffusion played a significant role in solute transport.

Table 5.7. Flow and Transport Related Properties of Specimens Used for Column Leaching Tests.

Soil	Fly Ash	v_s (cm/s)	D (cm^2/s)	Peclet Number	α (*L) (when τ = 0.1)	α (*L) (when τ = 0.5)
Joy silt loam	10% Columbia	4.03×10^{-5}	6.82×10^{-5}	6.75	0.14	0.13
	20% Columbia	8.77×10^{-5}	2.39×10^{-4}	4.19	0.24	0.23
	10% Dewey	8.21×10^{-5}	1.04×10^{-4}	9.02	0.11	0.10
	20% Dewey	7.93×10^{-5}	9.10×10^{-5}	9.96	0.10	0.09
	10% King	8.08×10^{-5}	6.10×10^{-5}	15.14	0.06	0.06
	20% King	8.78×10^{-5}	1.90×10^{-4}	5.28	0.19	0.18
Lacustrine clay	10% Columbia	5.69×10^{-5}	9.10×10^{-5}	7.15	0.14	0.12
	20% Columbia	5.97×10^{-5}	3.91×10^{-5}	17.45	0.05	0.04
	10% Dewey	5.45×10^{-5}	7.91×10^{-5}	7.88	0.12	0.11
	20% Dewey	7.24×10^{-5}	6.11×10^{-5}	13.54	0.07	0.06
	10% King	6.04×10^{-5}	4.56×10^{-5}	15.14	0.06	0.05
	20% King	8.02×10^{-5}	1.56×10^{-4}	5.88	0.17	0.16
Theresa silt loam	10% Columbia	7.33×10^{-5}	5.61×10^{-5}	14.93	0.06	0.05
	20% Columbia	7.17×10^{-5}	4.61×10^{-5}	17.78	0.05	0.04
	10% Dewey	8.68×10^{-5}	1.11×10^{-4}	8.94	0.11	0.10
	20% Dewey	7.40×10^{-5}	1.60×10^{-4}	5.29	0.19	0.18
	10% King	6.79×10^{-5}	1.16×10^{-4}	6.69	0.15	0.14
	20% King	6.90×10^{-5}	1.02×10^{-4}	7.73	0.13	0.12
Silica sand	10% Columbia	5.69×10^{-5}	8.12×10^{-5}	8.01	0.12	0.11
	20% Columbia	6.22×10^{-5}	6.12×10^{-5}	11.62	0.08	0.07
	10% Dewey	4.65×10^{-5}	5.60×10^{-5}	9.49	0.10	0.09
	20% Dewey	5.78×10^{-5}	3.61×10^{-5}	18.30	0.05	0.04
	10% King	5.69×10^{-5}	NA	NA	NA	NA
	20% King	6.26×10^{-5}	1.16×10^{-4}	6.17	0.16	0.15

Note: v_s = Seepage velocity, D = Dispersion coefficient, α = Longitudinal dispersivity, L= Length of the column, τ = Tortuosity, and NA = Not available.

The dispersion coefficient is a function of seepage velocity (v_s), especially for the Peclet numbers used for this study. The coefficient of proportionately between D_L and v_s is the dispersivity, α_L. The dispersivity is often expressed as a fraction of the column length (L) so that it can be used for any seepage velocity and for any scale (Gelhar et al. 1992). Dispersivity is often considered to be a physical property of the porous media, and does not depend on flow parameters.

The molecular diffusion coefficient of bromide is needed to estimate the longitudinal dispersivity. The molecular diffusion coefficient of bromide in free water is a known parameter; however, to estimate the molecular diffusion coefficient of bromide in soil-fly ash mixtures, the tortuosity (τ) of the mixtures must also be known (Eqn. 5.3).

An attempt to estimate the average tortuosity was made by graphing the dispersion coefficient vs. seepage velocity for all soil-fly ash mixtures, as shown in Fig. 5.11. The dispersion coefficient is linearly related to seepage velocity (Eqn. 5.4), where α is the slope of the trend line and D* is the intercept with the ordinate. The D* from the Fig. 5.11 is higher than molecular diffusion in free water, which is not valid (i.e., τ <1). This may have occurred because Fig. 5.11 was created using data from a variety of test specimens (each with unique α) rather than from a single specimen where v_s was varied systematically. Nevertheless, the slope of the trend line suggests that the dispersion coefficient increases with increasing seepage velocity, and advection is a significant contributor to dispersion.

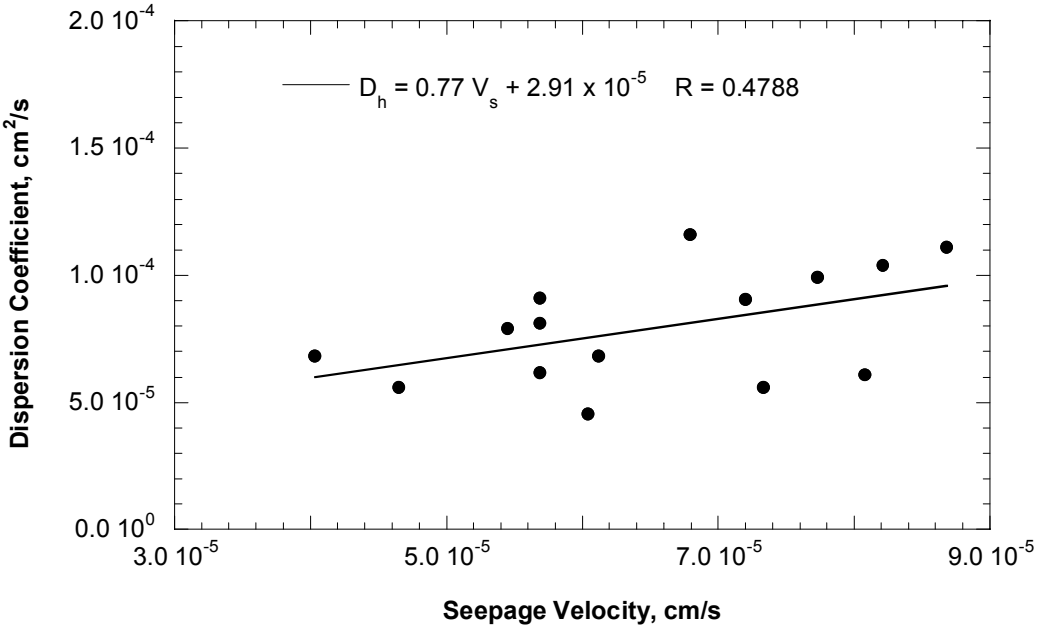

Fig. 5.11. Effect of Seepage Velocity on Hydrodynamic Dispersion Coefficient.

A second approach was to assume tortuosities within a typical range (0.1 to 0.5) for compacted clay (Kim et al. 1997). Dispersivities estimated using tortuosities of 0.1 and 0.5 (the two ends of the typical range) are shown in Table 5.7. The dispersivities differ by no more than 5% for this range of tortuosities, which suggests that the effect of tortuosity on dispersivity is insignificant for the column tests in this study.

The dispersivity varies between 0.05 L and 0.24 L for the soil-fly ash mixtures (Table 5.7). In general, the longitudinal dispersivity typically varies between 0.01 L and 1 L, and 0.1 L is commonly assumed (Gelhar et al. 1992). Neuman (1990) and Ayra (1986) have introduced empirical relationships for scaling dispersivities based on the length of the domain. For the column leaching tests, the estimated dispersivity from Neuman's empirical relationship is 0.38 L, and from Ayra's relationship it is 0.31 L. The dispersivities measured using the column leaching tests are comparable to these estimates, as well as the estimates in Gelhar et al. (1992).

5.2.1.5 Initial Instantaneous Effluent Concentration

The initial instantaneous effluent concentration of different species represents the initial pore water concentration of the soil-fly ash matrix, and is necessary for estimating the release of contaminants to groundwater, because it. The concentration of a species in the first leachate sample collected from the column leaching tests was assumed to be the initial instantaneous effluent

concentration of that species. A summary of the initial effluent concentration is shown in Table 5.3.

The initial effluent concentrations are shown in Figs. 5.12 and Fig. 5.13 as a function of fly ash content. The initial effluent concentration of Cd is lower from soil-fly ash mixtures prepared with Columbia fly ash than from soil alone, except for sand (Fig 5.12a). In the WLTs (see Table 5.1), a lower aqueous concentration of Cd was obtained from soil-fly ash mixtures prepared with the same fly ash than those for all soils, except for sand.

Generally, the initial effluent concentration increases with the increasing fly ash content, especially for metals that have higher concentrations in fly ash than in soil. This effect is evident in Fig. 5.12b, which shows that the initial effluent concentration of Ag increases slowly as the fly ash content increases. A similar finding for Ag was found from the WLTs on soil-fly ash mixtures prepared with Dewey fly ash. The initial effluent concentrations of Se and Cr increase more rapidly as the fly ash content increases (Fig 5.13), because the Se and Cr are much more abundant in fly ash than soil.

Similar to the WLTs results, the increase in initial effluent concentration is not linear with the fly ash content and the rate of increase diminishes as the fly ash content increases. As the fly ash content increases, the mass of metals in soil-fly ash mixtures increases approximately linearly. The diminishing return occurs because the pH is higher at higher fly ash content (Fig. 5.9). Higher pH leads to a higher partition coefficient, and less metals in the effluent.

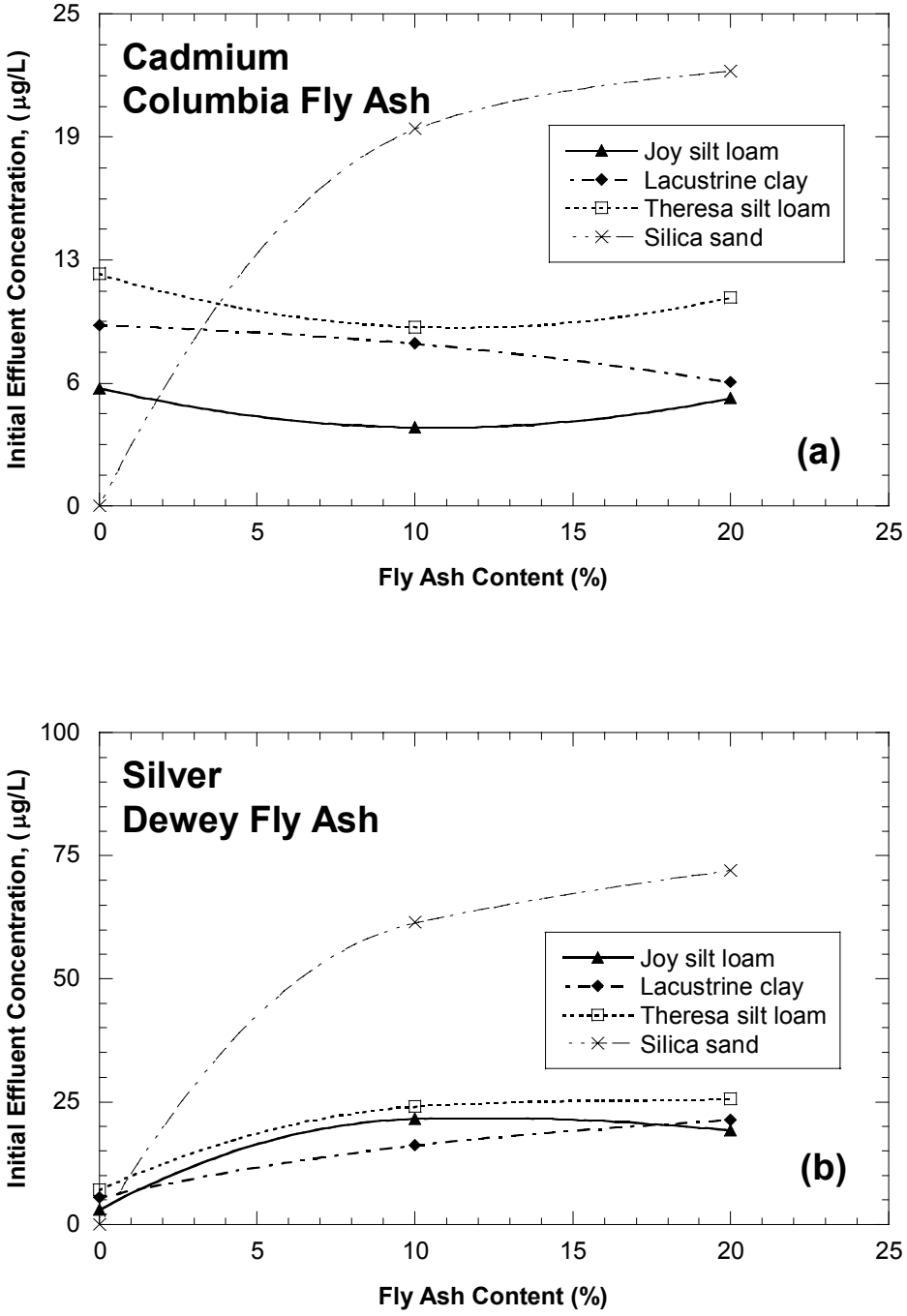

Fig. 5.12. Initial Effluent Concentrations from Column Leaching Tests for (a) Cadmium from Soil-Fly Ash Mixtures Prepared with Columbia Fly Ash and (b) Silver from Soil-Fly Ash Mixtures Prepared with Dewey Fly Ash.

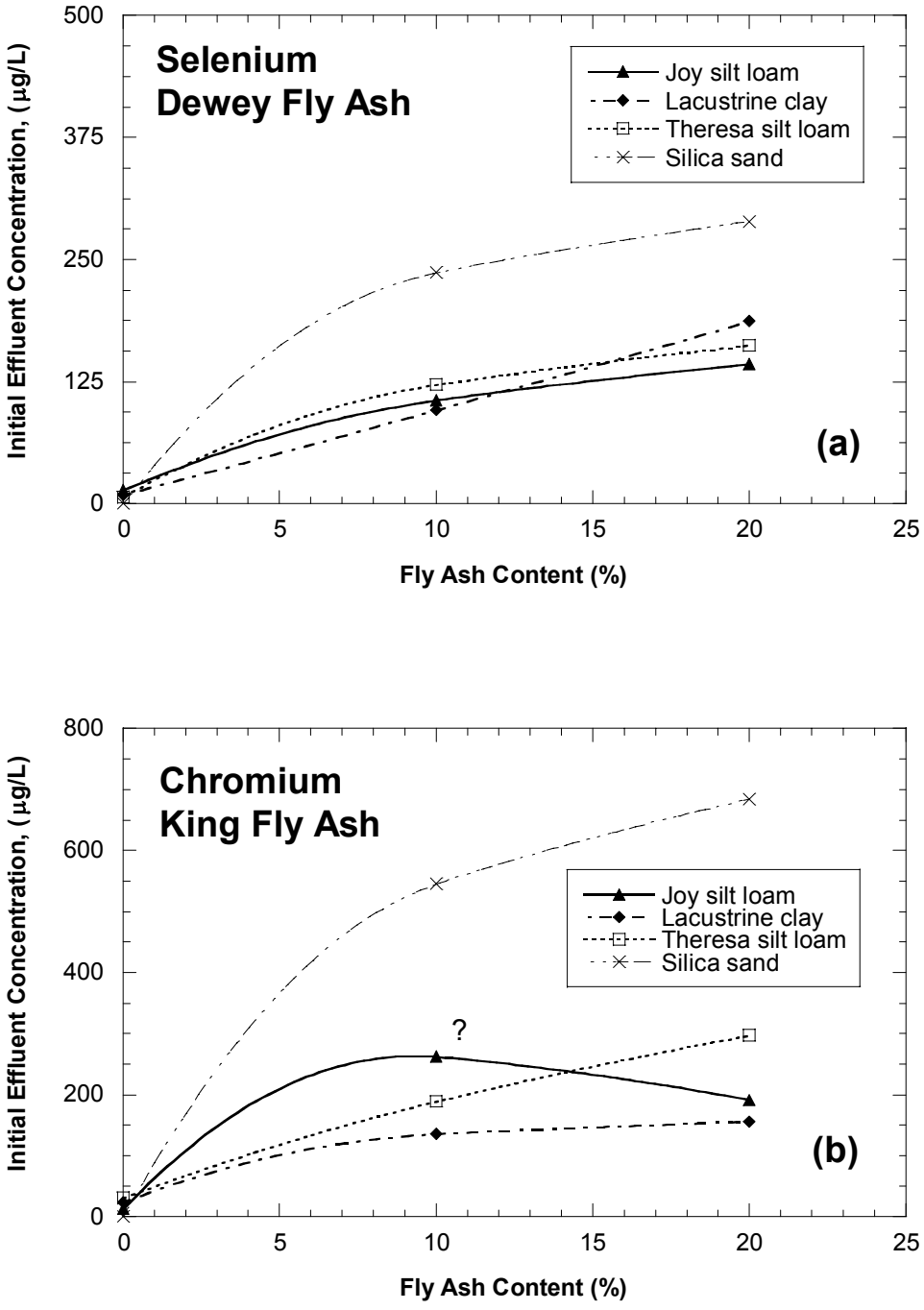

Fig. 5.13. Initial Effluent Concentrations from Column Leaching Tests for (a) Selenium from Soil-Fly Ash Mixtures Prepared with Dewey Fly Ash and (b) Chromium from Soil-Fly Ash Mixtures Prepared with King Fly Ash.

The initial effluent concentration is inversely proportional to the CEC of the soil in most of the cases. The initial effluent concentration is the highest for silica sand because of its lowest CEC, and in most cases, is the lowest for Lacustrine clay because of its highest CEC. The initial effluent concentration is slightly higher for Theresa silt loam than that for Joy silt loam. Theresa silt loam has a higher CEC than Joy silt loam. However, the pH of the effluent for Theresa silt loam was always slightly lower than that for Joy silt loam (Fig. 5.9), which permits more release of metals.

Initial effluent concentrations of Se from the column leaching tests on soil-fly ash mixtures are shown in Fig. 5.14. The initial effluent concentrations from different soil-fly ash mixtures vary within a narrow range for a particular fly ash (Fig. 5.14a), and vary over a broader range for a given fine-grained soil (Fig. 5.14b). Since the concentration of Se varies significantly for different fly ashes, and is much higher in fly ashes than in soils, the initial effluent concentration of Se depends more on the fly ash than the soil used to prepare the soil-fly ash mixtures.

5.2.1.6 Relationship Between Initial Effluent Concentration and WLT Concentration

Initial effluent concentrations from the column leaching tests on soil-fly ash mixtures are graphed against concentrations from the WLTs in Figs. 5.15 – 5.18. Relationships are provided for concentrations from WLTs conducted with soil-fly ash mixtures (Figs. 5.15a, 5.16a, 5.17a, and 5.18a), and WLTs conducted with bulk fly ash (Figs. 5.15b, 5.16b, 5.17b, and 5.18b).

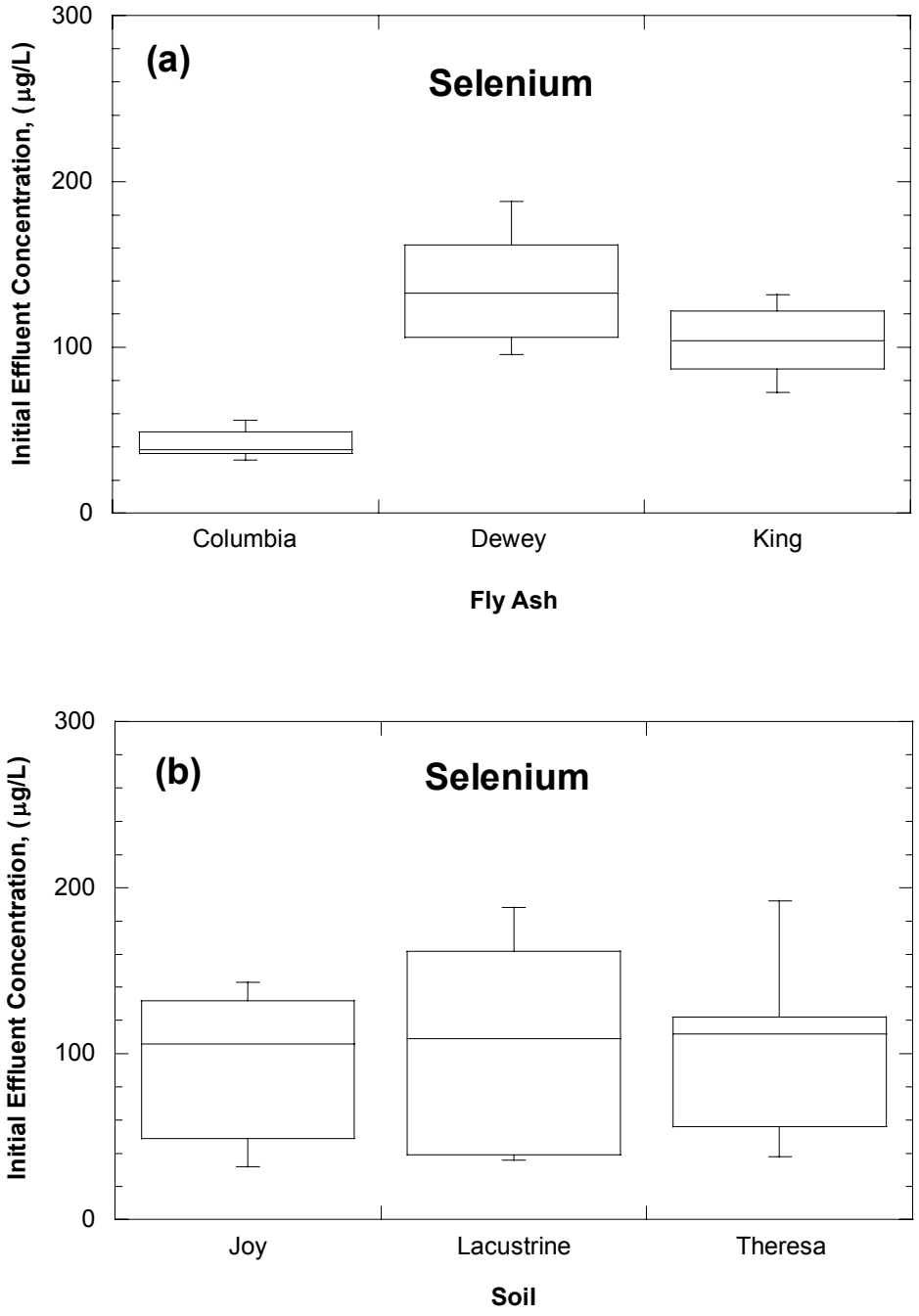

Fig. 5.14. Initial Effluent Concentration of Selenium from Soil-Fly Ash Mixtures Based on Fly Ashes Used (a) and Based on Soil Used (b) to Prepare the Soil-Fly Ash Mixtures.

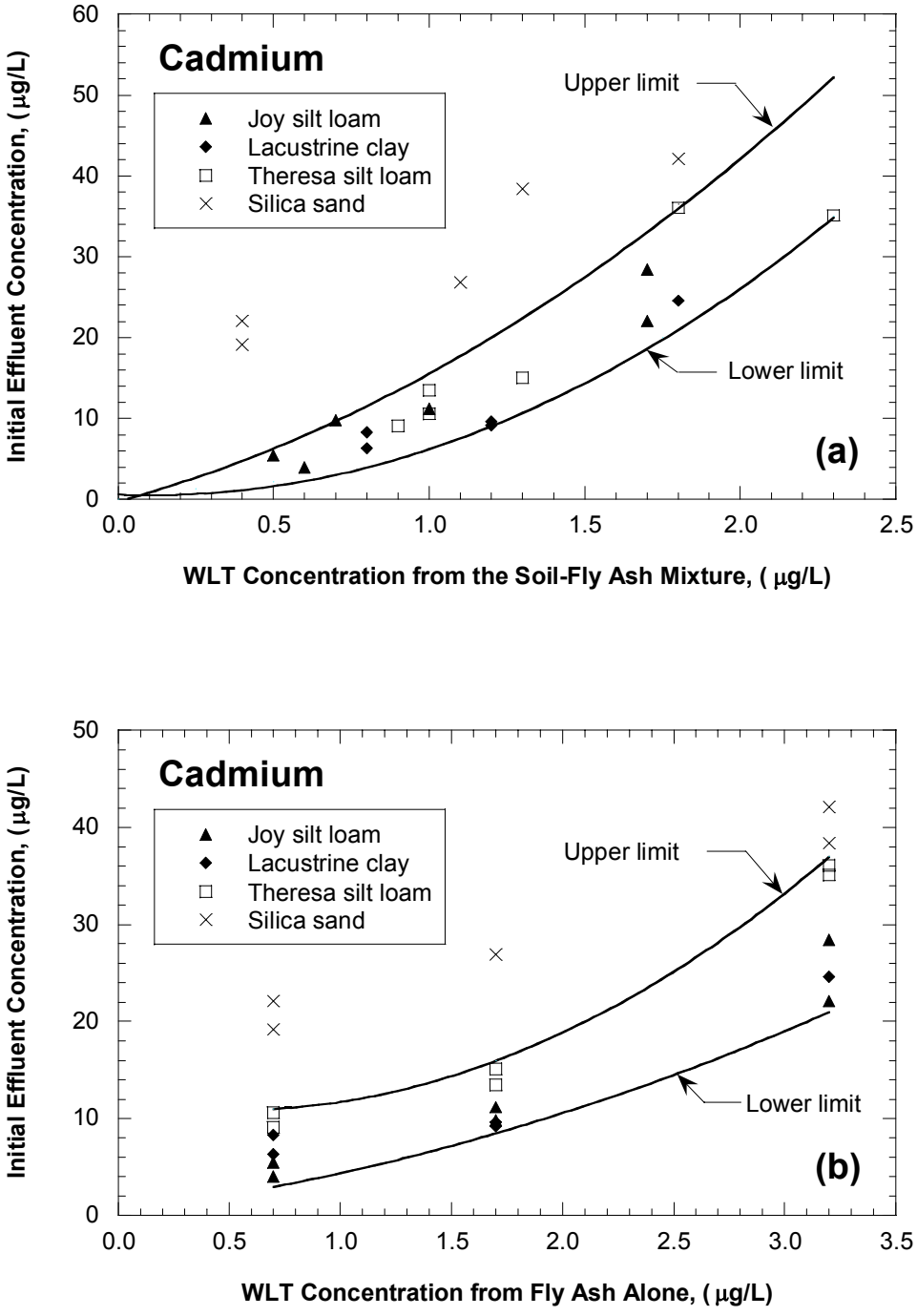

Fig. 5.15. Relationship Between Initial Effluent Concentration of Cadmium from Soil-Fly Ash Mixture with (a) Concentration from Water Leach Tests on Similar Soil-Fly Ash Mixture and (a) Concentration from Water Leach Tests on Bulk Fly Ash that was Used to Prepare the Mixture.

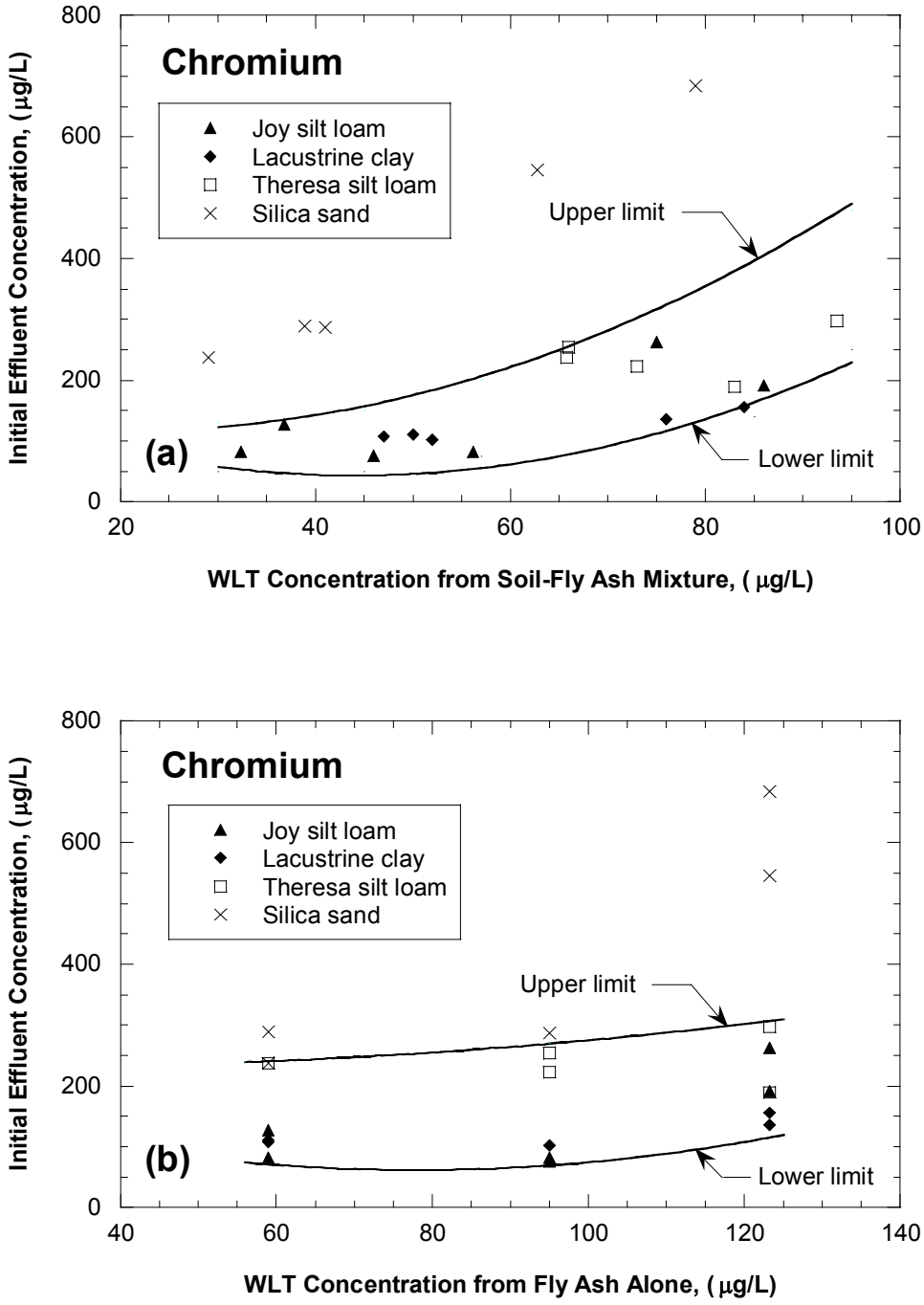

Fig. 5.16. Relationship Between Initial Effluent Concentration of Chromium from Soil-Fly Ash Mixture with (a) Concentration from Water Leach Tests on Similar Soil-Fly Ash Mixture and (a) Concentration from Water Leach Tests on Bulk Fly Ash that was Used to Prepare the Mixture.

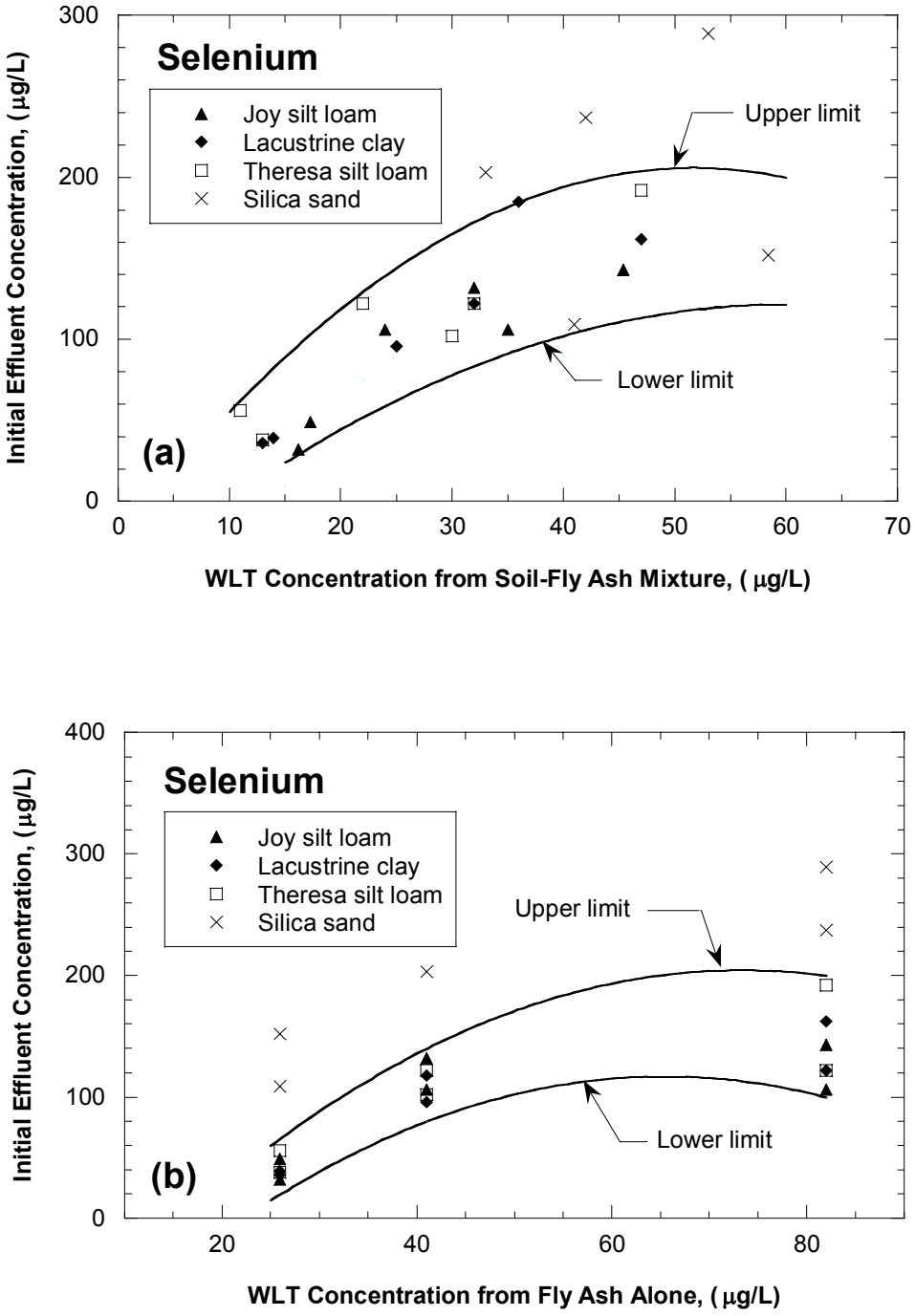

Fig. 5.17. Relationship Between Initial Effluent Concentration of Selenium from Soil-Fly Ash Mixture with (a) Concentration from Water Leach Tests on Similar Soil-Fly Ash Mixture and (a) Concentration from Water Leach Tests on Bulk Fly Ash that was Used to Prepare the Mixture.

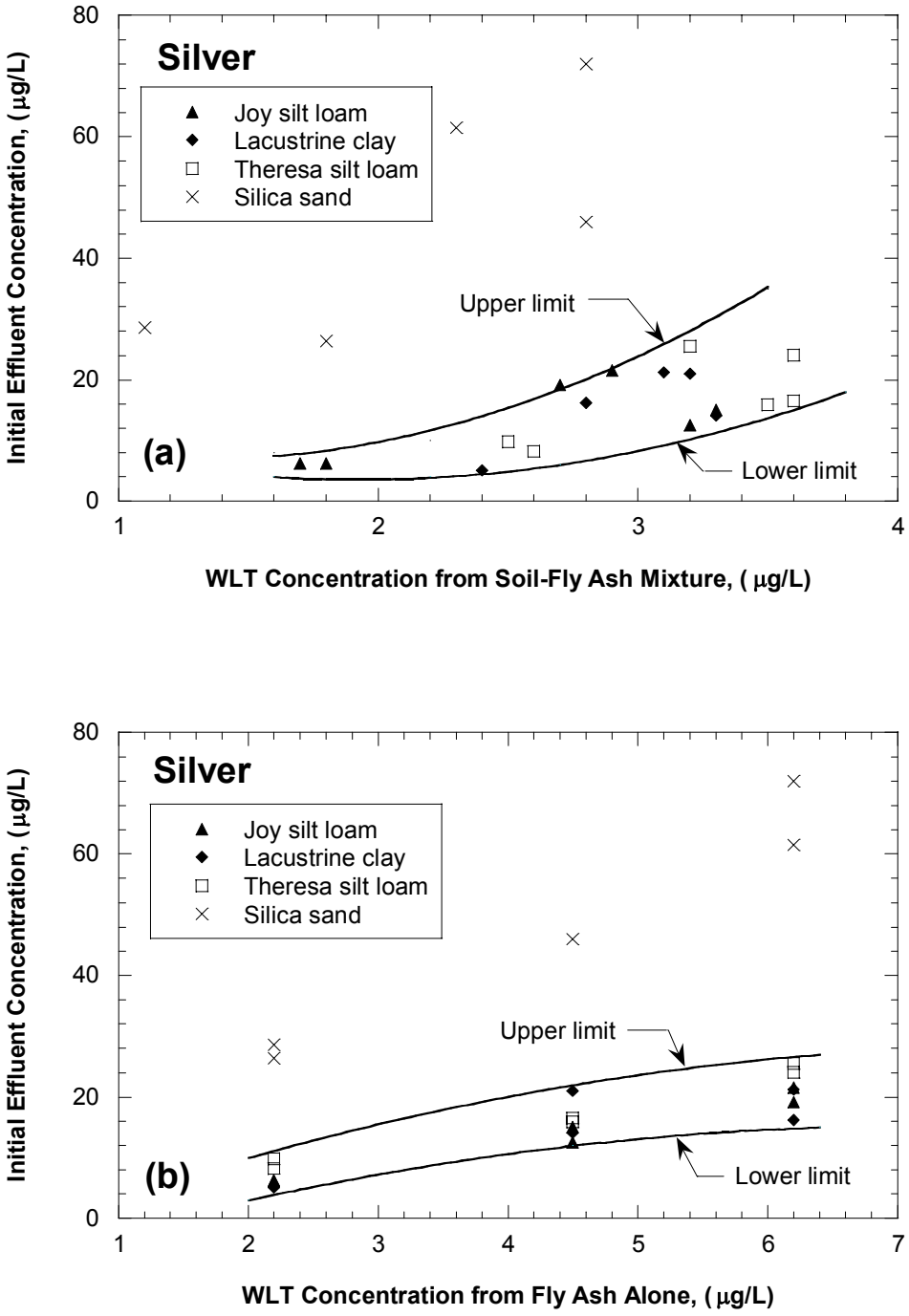

Fig. 5.18. Relationship Between Initial Effluent Concentration of Silver from Soil-Fly Ash Mixture with (a) Concentration from Water Leach Tests on Similar Soil-Fly Ash Mixture and (a) Concentration from Water Leach Tests on Bulk Fly Ash that was Used to Prepare the Mixture.

In general, initial effluent concentration increases with the concentration obtained from WLTs conducted on soil-fly ash mixtures and bulk fly ashes. However the relationships are non-linear and non-unique (i.e., a range of initial effluent concentrations can be realized for a given WLT concentration). The validity of using the relationships shown in Figs. 5.15 - 5.18 for a broad range of fly ashes currently is unknown. Tests on a broader range of fly ashes needs to be conducted to assess their generality. Nonetheless, they can be used for the fly ashes that were studied and a wide range of fine-grained soils that need to be stabilized for highway construction.

Initial effluent concentrations can be estimated conservatively from WLTs concentrations from the upper limit curves in Figs. 5.15-5.18). The data for silica sand were not included when developing the upper limit curves because sand generally does not require stabilization. However, the data for sand are included in the graphs to show that the initial effluent concentration would be much higher if the metals were not adsorbed by the fine-grained soil.

5.2.1.7 Retardation Factor and Partition Coefficient

Retardation factors and partition coefficients for the metals in different soil-fly ash mixtures are shown in Tables 5.4 and 5.5. The retardation factors were estimated by fitting Eqn. 4.2 to the elution data from the column leaching tests. The effective porosity and dispersivity obtained from the breakthrough curve for bromide were used when estimating the retardation factors. Typical elution curves for the metals are shown in Fig. 5.19. All of the elution curves are in Appendix E.

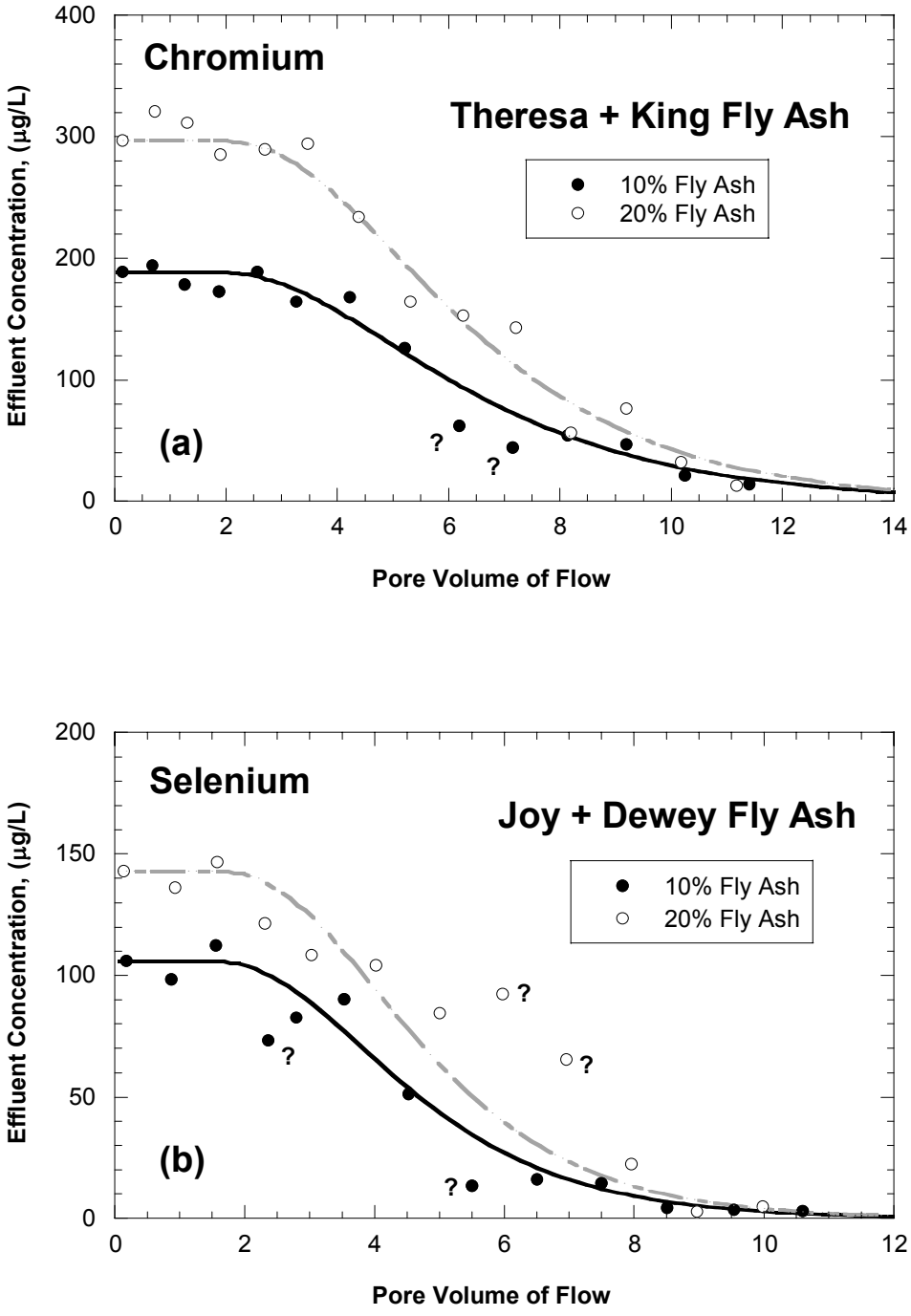

Fig. 5.19. Elution Curves for Chromium from Soil-Fly Ash Mixtures Prepared with Theresa Silt Loam and King Fly Ash (a) and for Chromium from Soil-Fly Ash Mixtures Prepared with Joy Silt Loam and Dewey Fly Ash (b). Curves Correspond to Fit of the Analytical Solution Shown in Eqn. 4.2.

The retardation factor in soil-fly ash mixtures was lowest for Se (R = 3.2 to 4.2) and was similar for Cd, Cr, and Ag (R = 4.4 to 6.1). Retardation factors for the metals of concern in soil-fly ash mixtures were not found in the literature survey. However, the retardation factors for Cd (R = 4.4 to 6.1) are comparable to those for sand-bentonite-fly ash mixtures (R = 5.5) reported by Shackelford and Glade (1997). Similarly, the retardation factor for Se (R = 3.2 to 4.2) is also comparable to that for Se in compacted clay (R = 3.0) as reported by Garcia et al. (1999).

Box plot of the retardation factors for the metals are shown in Fig. 5.20 for mixtures prepared with given soil and all three fly ashes. The retardation factor does not vary significantly for soil-fly ash mixtures prepared with a specific soil even though the type of fly ash varied. The soil is the major component (80-90%) of the mixture, and is primarily responsible for retarding solutes during transport. Thus, the retardation factor of a soil-fly ash mixture depends mainly on the type of soil rather than the fly ash used in the mixture.

Partition coefficients (k_p) were estimated from the retardation factor (R), the porosity (n), and dry density of soil-fly ash mixture (ρ_d) using the conventional relationship (Freeze and Cherry 1979):

$$R = 1 + \frac{\rho_d}{n} k_p \qquad (5.5)$$

The partition coefficients are tabulated in Table 5.5, and reflects only the partitioning involved in linear, reversible, and instantaneous sorption. As with the retardation factor, the partition coefficients do not vary significantly for different soil-fly ash mixtures prepared with a specific soil (Fig. 5.21).

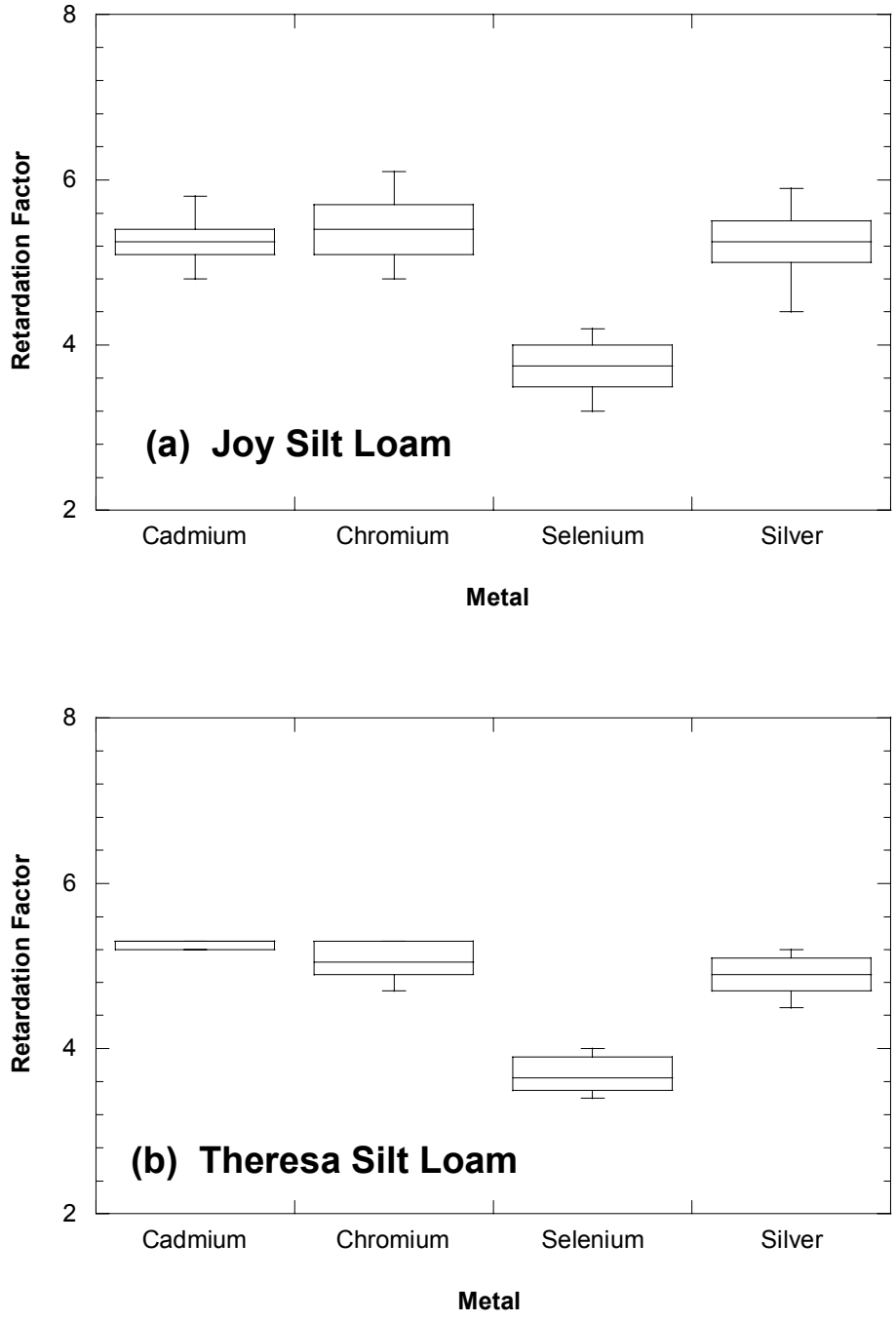

Fig. 5.20. Retardation Factor for Different Metals in Soil-Fly Ash Mixtures Prepared with Different Fly Ashes and (a) Joy silt loam (b) Theresa Silt Loam.

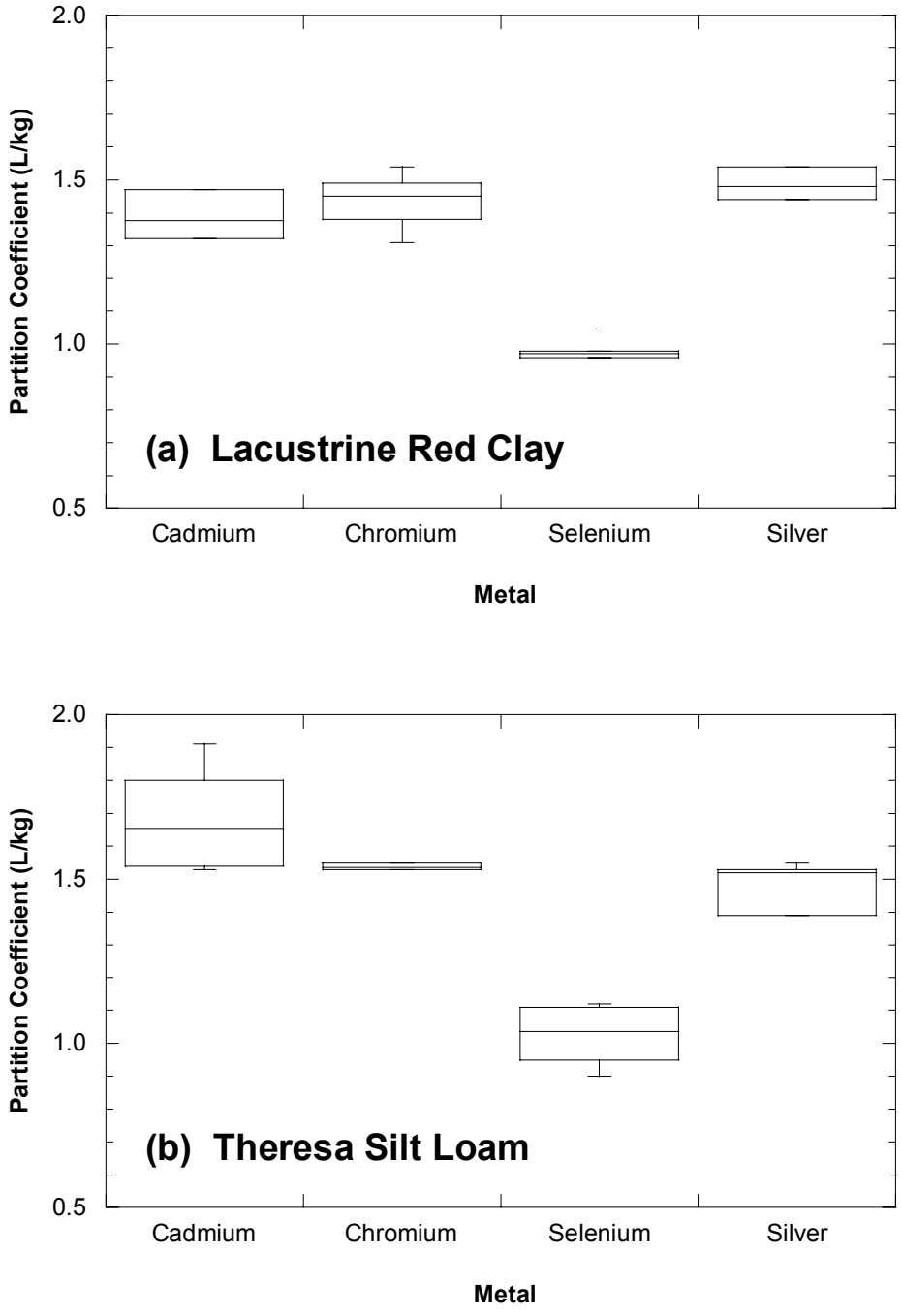

Fig. 5.21. Partition Coefficient for Different Metals in Soil-Fly Ash Mixtures Prepared with Different Fly Ashes and (a) Lacustrine Red Clay (b) Theresa Silt Loam.

5.2.2 Column Leaching Test on Soil-Spiked Fly Ash Mixtures

Four column leaching tests were conducted on soil-fly ash mixtures prepared with Joy silt loam and spiked Columbia fly ash (10%) to determine the initial effluent concentrations as a function of metal loading. The pH of the effluent for all four tests with spiked fly ash (i.e., 9.5) was similar to that for the test with unspiked Columbia fly ash at 10%. The release pattern of metals was also examined.

5.2.2.1 Relationship Between Initial Effluent Concentration and WLT Concentration

Initial effluent concentrations from the column leaching tests on soil-fly ash mixtures (10%) are graphed against concentrations from the WLTs in Fig. 5.22 and 5.23. Concentration of metals in leachate from the WLTs on both bulk fly ash and soil-fly ash mixtures (10%) are shown. A linear relationship exists between the initial effluent concentrations from the column leaching tests and the concentration from the WLTs. Since the pH was constant for each type of test and the partitioning is linear, a linear relationship can be expected. The relationship between initial effluent concentration from column leaching tests on soil-fly ash mixtures prepared with Joy silt loam and Columbia fly ash (spiked and unspiked) and concentration from WLTs on similar soil-fly ash mixtures that used for column leaching tests is:

$$C_i = a\, C_{S\text{-}FA} + b \qquad (5.6)$$

where C_i = initial effluent concentration, $C_{S\text{-}FA}$ = concentration from WLTs on soil-fly ash mixtures and a and b are coefficients that depend on the species being considered. Values of a and b for different species are also shown in Table 5.8.

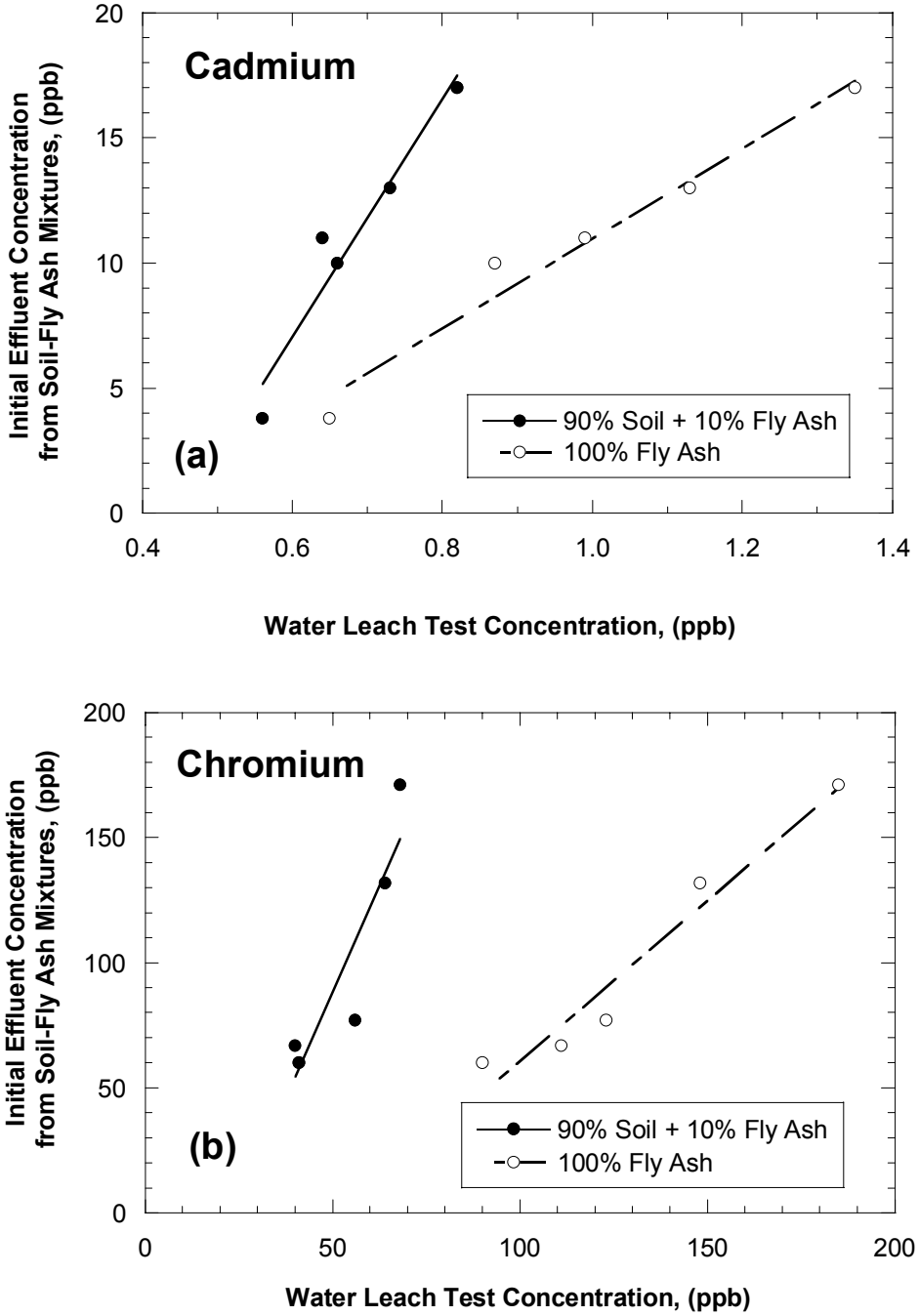

Fig. 5.22. Relationship Between Initial Effluent Concentration from Column Leaching Tests on Soil-Fly Ash Mixtures Prepared with Joy Silt Loam and Columbia Fly Ash (10%) and Concentration from WLTs on Similar Soil-Fly Ash Mixtures, and Joy Silt Loam Alone for (a) Cadmium and (b) Chromium.

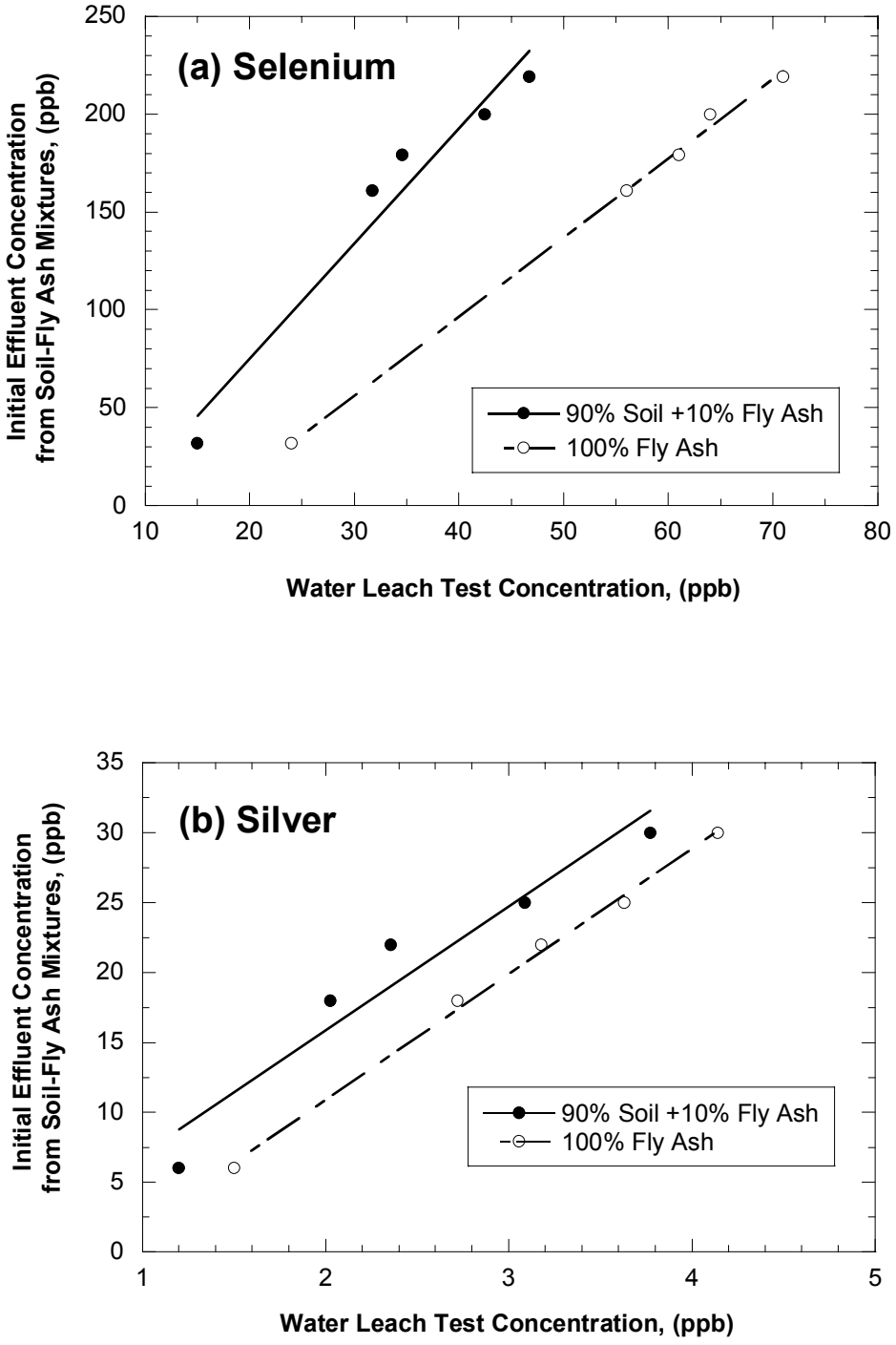

Fig. 5.23. Relationship Between Initial Effluent Concentration from Column Leaching Tests on Soil-Fly Ash Mixtures Prepared with Joy Silt Loam and Columbia Fly Ash (10%) and Concentration from WLTs on Similar Soil-Fly Ash Mixtures, and Joy Silt Loam Alone for (a) Selenium and (b) Silver.

Table 5.8. Coefficients for the Relationship Between Initial Effluent Concentration from Column Leaching Test on Soil-Fly Ash Mixtures (10% Fly Ash) Prepared with Joy Silt Loam and Columbia Fly Ash and Concentration from WLTs on Similar Soil-Fly Ash Mixtures and Joy Silt Loam Alone.

Species	Coefficients			
	Soil-Fly Ash Mixture		Bulk Fly Ash	
	a	b	d	e
Cadmium	47.5	-21.4	18.0	-7.0
Chromium (T)	3.4	-80.8	1.3	-67.1
Selenium	5.9	-42.4	4.0	-64.7
Silver	8.9	-1.8	9.0	-7.1

T = Total chromium

Similarly, the relationship between initial effluent concentration from column leaching tests on soil-fly ash mixtures prepared with Joy silt loam and Columbia fly ash (spiked and unspiked) and concentration from WLTs on bulk fly ash (spiked and unspiked) can be expressed with the following general expression:

$$C_i = d\ C_{bfa} + e \qquad (5.7)$$

where C_{bfa} = concentration from WLTs on bulk fly ash, and d and e are coefficients that depend on the species being considered. Values of d and e for different species are also shown in Table 5.8.

The ratio of average initial effluent concentration from column leaching tests on soil fly ash mixtures (10%) to average concentration from WLTs on similar soil-fly ash mixtures that were used for column leaching tests is the highest for Cd (20) followed by Ag (8), Se (5), and Cr (2). Similar trends were also found for the ratio of average initial effluent concentration from the column leaching tests on soil-fly ash mixtures (10% fly ash) to the average concentration from WLTs on bulk Columbia fly ash. The ratio for Cd (11) is the highest, followed by Ag (6), Se (3), and Cr (1.2). The difference of the ratio of concentrations for different species may be due to relative variation of partition coefficients of the species at different pH for the column leaching test (pH = 9.9), WLTs on fly ash alone (pH = 11.8), and WLTs on soil-fly ash mixtures (pH = 11.0).

5.2.2.2 Release Pattern

Three types of releases are usually associated with leaching from fly ash (Garavaglia and Caramuscio 1994): (a) rate-limited release, (2) solubility-controlled

release, and (3) adsorption-controlled release. When the release is controlled by the dissolution rate of the precipitated metal compounds, then it is called rate-limited release. Rate-limiting release occurs in non-equilibrium situations. For rate-limiting release, the concentration of the leachate depends on the rate of dissolution, and leachate concentrations remain unchanged over time unless the precipitated compounds are fully dissolved or the rate of release changes.

Solubility-controlled release also occurs in non-equilibrium situations when the dissolution rate is infinite, and dissolution is controlled by solubility. The concentration of the leachate depends on the solubility of a compound in pore water and remains at the solubility limit of the compound.

For adsorption-controlled release, the concentration of metals in pore fluid continually changes, because the metal concentrations in the solid and liquid phase are controlled by the partition coefficients. Adsorption-controlled release corresponds to an equilibrium condition where desorption occurs instantaniously.

The elution curves for Cr and Se from the soil-fly ash specimen having the highest metal concentrations (Spike D) are shown in Fig. 5.24. The concentrations from the column leaching tests decrease with time and agree well with the analytical solution of the ADRE, which corresponds to adsorption-controlled release. In fact, none of the elution curves exhibited rate-limited release or solubility-controlled release even after adding extra amounts of metals. Thus, the release pattern for soil-fly ash mixtures appears to be adsorption-controlled.

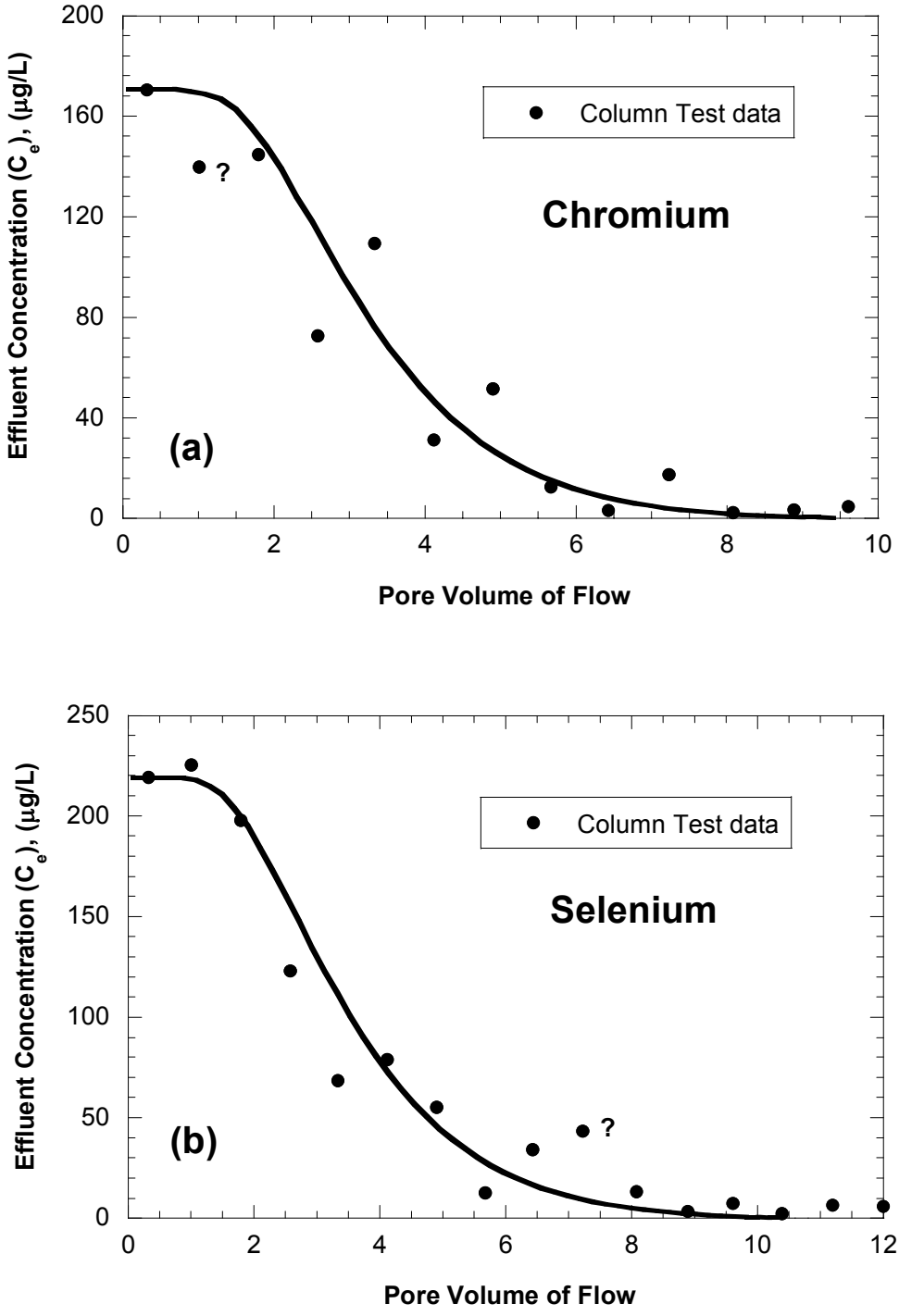

Fig 5.24. Elution Curves from Column Leaching Tests on Soil-Fly Ash Mixtures (10%) Prepared with Joy Silt Loam and Spiked Columbia Fly Ash (Spike-D) for (a) Chromium and (b) Selenium.

5.2.3 Column Tests on Subgrade Soil

Transport parameters for the subgrade soil are necessary to estimate the concentration of metals that would enter groundwater from a fly ash stabilized layer in a pavement system. Thus, column tests were conducted on subgrade soils to determine transport parameters for the metals released from the soil-fly ash mixtures. The fine-grained soils used to prepare the soil-fly ash mixtures were used in the column tests as representative subgrade soils. A synthetic leachate simulating the typical initial leachate from soil-fly ash mixtures was used as the influent solution. This solution was prepared by adding metals (Cd = 20 μg/L, Cr = 200 μg/L, Se = 100 μg/L, Ag = 20 μg/L) to a 0.1 M LiBr solution.

Concentrations of metals and bromide in the effluent of the soil column were analyzed following the methods described in Sec. 4.4. Effective porosity and dispersivity of the soil specimens were estimated from the breakthrough curves for bromide, whereas retardation factors for the metals were estimated by fitting Eqn. 4.1 to the breakthrough data for the metals. A summary of the transport parameters obtained from the column tests on the subgrade soils is shown in Table 5.9.

5.2.3.1 pH of the Effluent

pH of the effluent from the column tests was measured and recorded immediately after collecting the leachate samples. The pH of the influent solution was maintained at 9.5 using calcium hydroxide and hydrochloric acid to simulate the leachate from soil-fly ash mixtures. pH of the effluent from the column tests

Table 5.9. Transport Parameters for Subgrade Soils.

Soil Type	Chemical Species	Retardation Factor	Partition Coefficient (L/kg)	Dispersion Coefficient (cm^2/sec)	Peclet Number	Longitudinal Dispersivity
Joy silt loam	Bromide	1.0	0.00	9.93×10^{-5}	8.9	0.11 L
	Cadmium	5.3	1.07	9.61×10^{-5}	9.2	0.11 L
	Chromium (T)	5.4	1.10	9.58×10^{-5}	9.2	0.11 L
	Selenium	3.7	0.67	9.60×10^{-5}	9.2	0.11 L
	Silver	5.3	1.07	9.85×10^{-5}	9.0	0.11 L
Plano silt loam	Bromide	1.0	0.00	2.82×10^{-5}	12.2	0.07 L
	Cadmium	5.2	1.18	2.50×10^{-5}	13.7	0.07 L
	Chromium (T)	5.0	1.12	2.47×10^{-5}	13.9	0.07 L
	Selenium	3.8	0.78	2.49×10^{-5}	13.8	0.07 L
	Silver	4.1	0.87	2.73×10^{-5}	12.5	0.07 L
Lacustrine red clay	Bromide	1.0	0.00	9.06×10^{-5}	9.9	0.10 L
	Cadmium	5.5	1.46	8.74×10^{-5}	10.3	0.10 L
	Chromium (T)	5.1	1.33	8.70×10^{-5}	10.3	0.10 L
	Selenium	4.6	1.17	8.73×10^{-5}	10.3	0.10 L
	Silver	5.6	1.49	8.97×10^{-5}	10.0	0.10 L
Theresa silt loam	Bromide	1.0	0.00	6.82×10^{-5}	9.1	0.09 L
	Cadmium	5.3	1.61	6.50×10^{-5}	9.6	0.09 L
	Chromium (T)	4.3	1.24	6.47×10^{-5}	9.6	0.09 L
	Selenium	3.8	1.05	6.49×10^{-5}	9.6	0.09 L
	Silver	5.0	1.50	6.73×10^{-5}	9.2	0.09 L

Note: 1. T = Total chromium, L = Length of the specimen.

2. Detection limits are: Cd = 0.1 μg/L, Cr = 2.0 μg/L, Se = 2.0 μg/L, Ag = 0.2 μg/L, and bromide = 10 μg/L.

3. Molecular diffusion coefficients in free water (at 25^0C) are: Cd = 7.17×10^{-6} cm^2/s, Cr = 5.94×10^{-6} cm^2/s, Se = 6.79×10^{-6} cm^2/s, Ag = 16.6×10^{-6} cm^2/s, and Br = 20.1×10^{-6} cm^2/s (Lerman 1979).

decreased slightly at the beginning of the test and then remained similar to that of the influent solution.

5.3.3.2 Effective Porosity

Breakthrough curves for bromide from Joy silt loam and Lacustrine clay are shown in Fig. 5.25. Effective porosity of soil specimens was estimated using the same method used for soil-fly ash mixtures (described in Sec. 5.2.1.3).

The effective porosities are shown in Table 5.10, along with the dry unit weight, water content, and total porosity. The effective porosity is slightly lower than the total porosity for all soils, except for Theresa silt loam, and varies between 0.36 and 0.50. The effective-to-total porosity ratio of the subgrade soils varies between 0.89 and 1.02, which is typical for compacted clays (Kim el al.1997).

5.2.3.3 Dispersion Coefficient and Dispersivity

The dispersion coefficient, longitudinal dispersivity, and Peclet number for different species are shown in Table 5.9. The Peclet number for the column tests on subgrade soils varies within a narrow range (8.9 to 13.9). As shown in Sec. 5.2.1.4, the tortuosity has a negligible effect on dispersivity for this range of Peclet numbers. Thus, as in Sec. 5.2.1.4, the dispersivity was calculated considering a typical tortuosity (0.25) for fine-grained soil (Kim et al. 1997) and is expressed non-dimensionally in-terms of a fraction of the length (L) of the specimen. The longitudinal dispersivity for bromide varies between 0.06 L and 0.11 L. For the

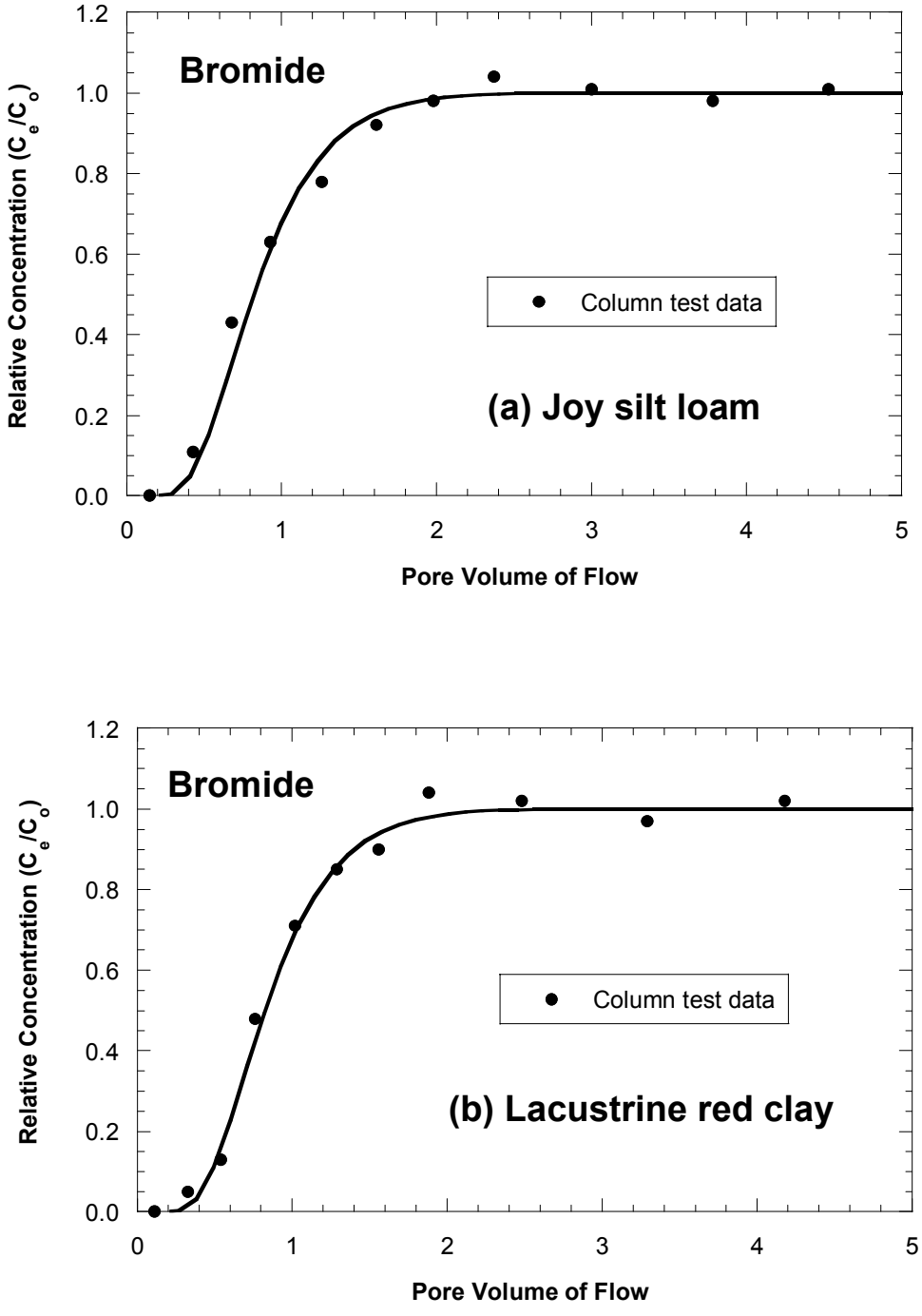

Fig. 5.25. Breakthrough Curves for Bromide from Column Leaching Tests on Subgrade Soil (a) Joy Silt Loam (b) Lacustrine Red Clay. Curves Correspond to the Fit of Analytical Solution Shown in Eqn. 4.1.

Table 5.10. Porosity and Related Properties of Specimens Used for Column Tests on Subgrade Soils.

Soil Type	Total Porosity	Effective Porosity	Effective-to-Total Porosity Ratio	Dry Unit Weight (kN/m^3)	Water Content (%)
Joy silt loam	0.38	0.35	0.92	16.2	17.2
Plano silt loam	0.44	0.39	0.89	14.7	17.3
Lacustrine red clay	0.50	0.47	0.94	13.4	21.2
Theresa silt loam	0.49	0.50	1.02	11.3	24.1

Note: Effective porosity is estimated by fitting the analytical model (Eqn. 4.1) with the data for bromide from the column tests. Total porosity is calculated from the weight-volume phase relationship.

metals, the longitudinal dispersivity varies between 0.09 L and 0.2 L for all soils. These longitudinal dispersivities are within typical ranges reported by Kim et al. (1997).

5.2.3.4 Retardation Factor and Partition Coefficient

Retardation factors for the subgrade soils were computed using the methods described in Sec. 5.2.1.7. The effective porosity and dispersivity obtained from the breakthrough curve for bromide were used when estimating the retardation factors. Typical breakthrough curves for metals from soil specimens are shown in Fig. 5.26. Breakthrough curves for other metals can be seen in Appendix F. Partition coefficients for the metals were calculated from the retardation factor, as described in Sec. 5.2.1.7.

Retardation factors and partition coefficients for different metals in subgrade soils are shown in Tables 5.9. Similar to the soil-fly ash mixtures, the retardation factor is lowest for Se (R = 3.7 to 4.6) and is comparable for Cr, Cr, and Ag (R = 4.1 to 5.6) for all soils. The retardation factors are also comparable to these reported by others (Shackelford and Glade 1997, Garcia et al. 1999).

The retardation factors and partition coefficients for the subgrade soils are shown in Fig. 5.27. The retardation factor for a particular species is similar for all four soils (Fig. 5.27a). The partition coefficients for Lacustrine red clay and Theresa silt loam are slightly higher than those for Joy silt loam and Plano silt loam (Fig. 5.27a), which is consistent with the CEC of these soils (see Table 3.2).

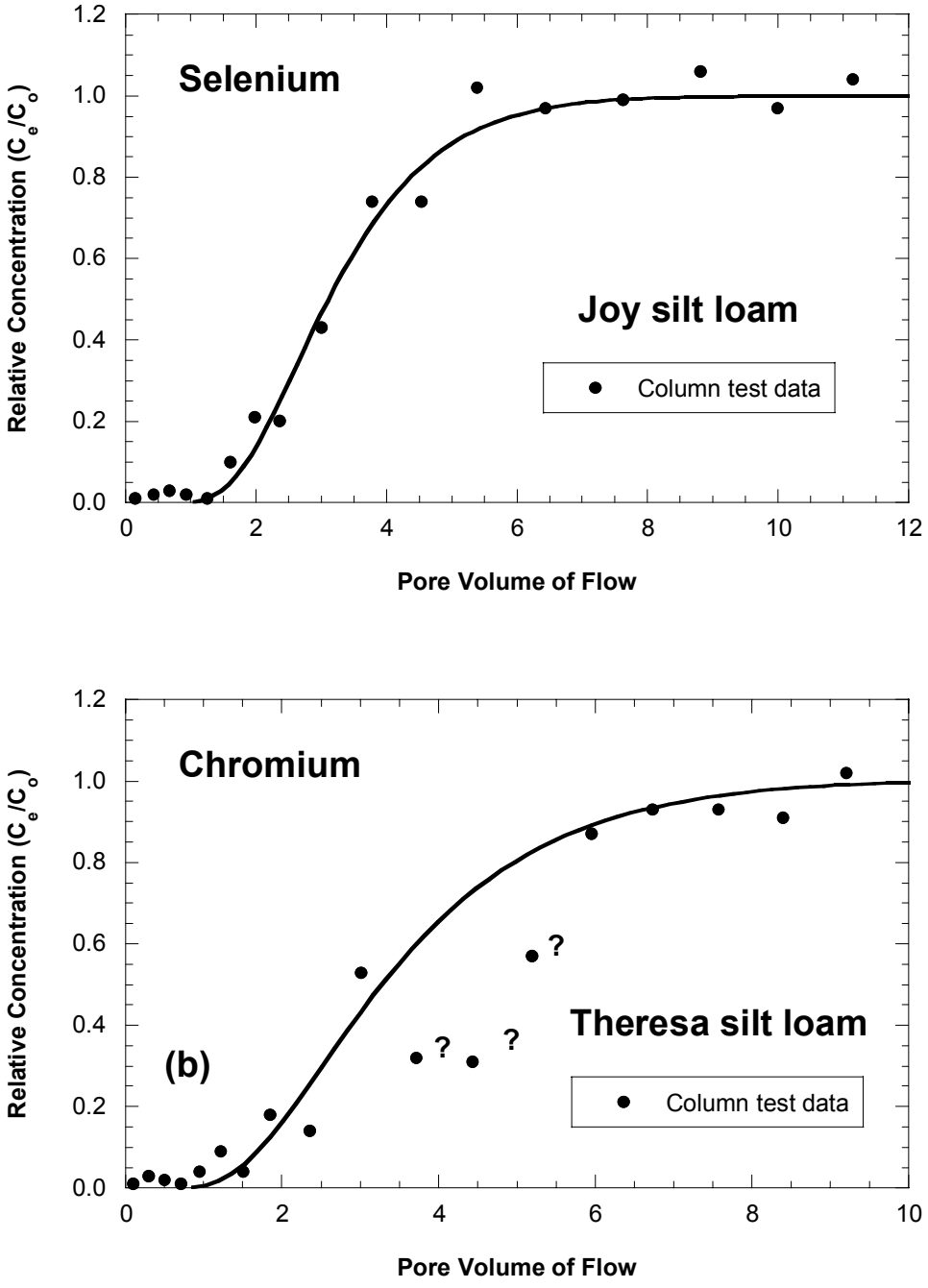

Fig. 5.26. Breakthrough Curve for (a) Selenium from Joy Silt Loam and (b) Chromium from Theresa Silt Loam. Curves Correspond to the Fit of the Analytical Solution Shown in Eqn. 4.1.

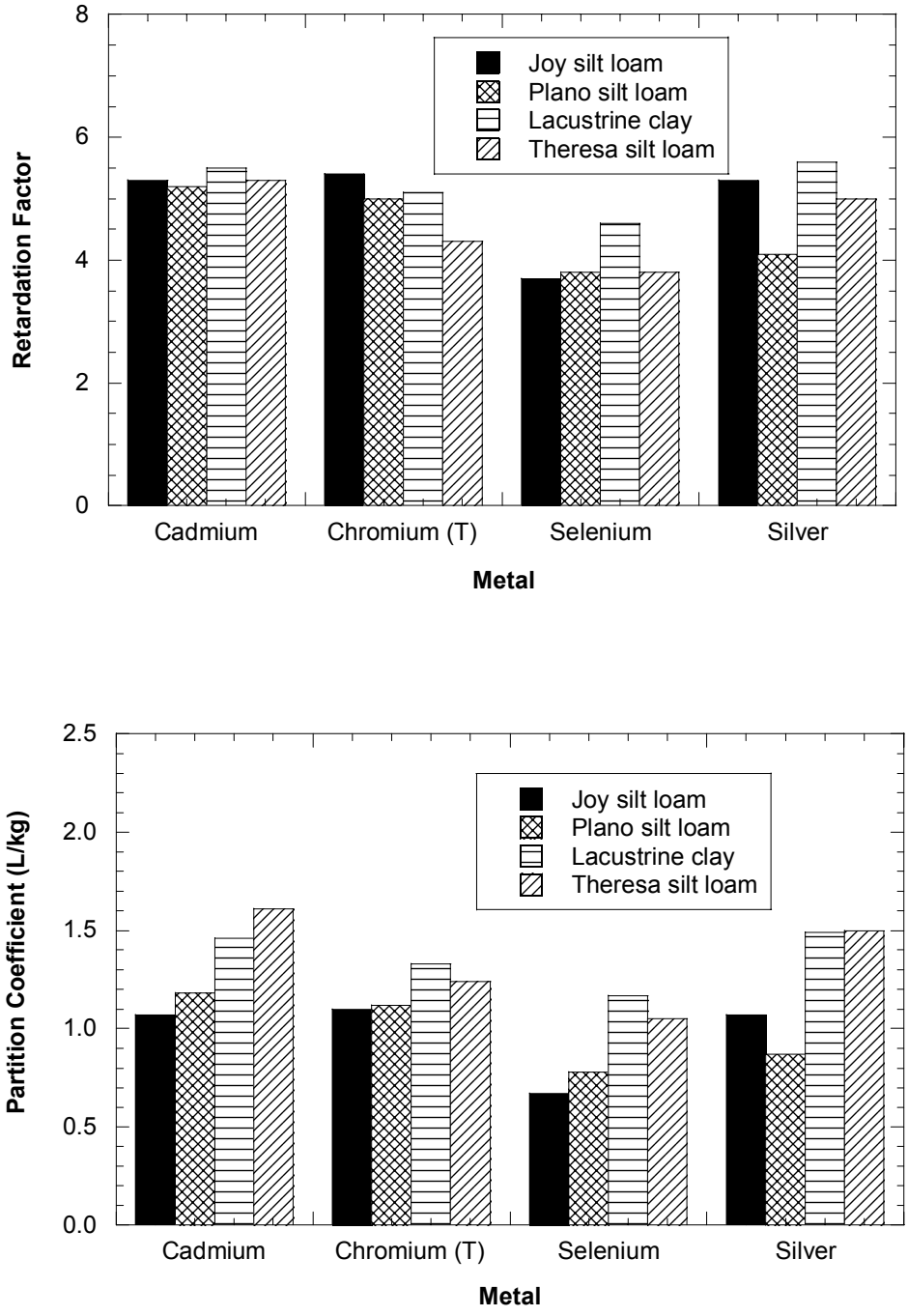

Fig. 5.27. Retardation Factors (a) and Partition Coefficients (b) of metals for Different Subgrade Soils.

Retardation factors and partition coefficients are shown in Fig. 5.28 as a function of fly ash content. Both the retardation factor and partition coefficient vary little with fly ash content. Thus, from a practical perspective, the retardation factor and partition coefficient of soil-fly ash mixtures can be assumed similar to that of the soil alone.

5.3 FIELD TESTS

5.3.1 STH 60 Site

5.3.1.1 Leachate Flux

The Darcy flux of leachate collected by the lysimeters in the control and fly ash stabilized subbase sections at STH 60 is shown in Fig. 5.29. Once the highway was paved during the first week of October 2000, the leachate flux decreased dramatically from 0.9 mm/d to 0.2 mm/d. The minimum leachate flux occurred during Winter 2001 (0.02 mm/d), because the stabilized subbase layer was frozen (Edil et al. 2002). The Darcy flux increased after the winter and was the maximum in Spring 2001 (0.27 mm/d). The annual average flux after paving was 0.15 mm/d (5% of average annual precipitation) for fly ash stabilized section and 0.20 mm/d for control section (6% of average annual precipitation) for the two-year monitoring period.

Lateral flow around lysimeters can cause a under estimation of the Darcy flux. Lateral flow can occur as a result of differences in the soil-water characteristic curve and unsaturated hydraulic conductivities between the fine grained subgrade soil and the geocomposite drainage layer (Chiu and Shackelford, 2000). However,

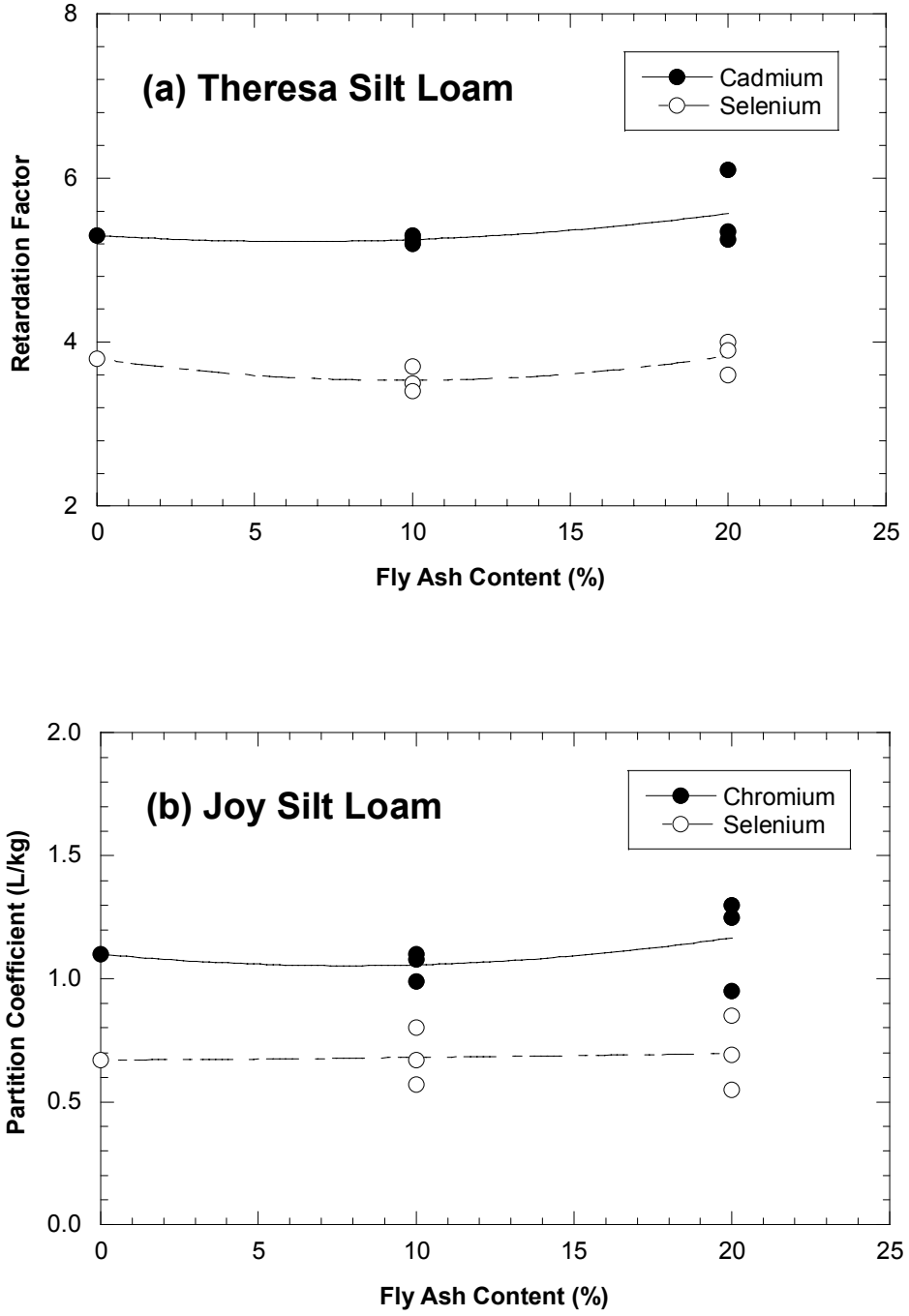

Fig. 5.28. Retardation Factor for Metals and Soil-Fly Ash Mixtures Prepared with Theresa Silt loam (a) and Partition Coefficient for Metals and Soil-Fly Ash Mixtures Prepared with Joy Silt loam (a) at Various Fly Ash Contents.

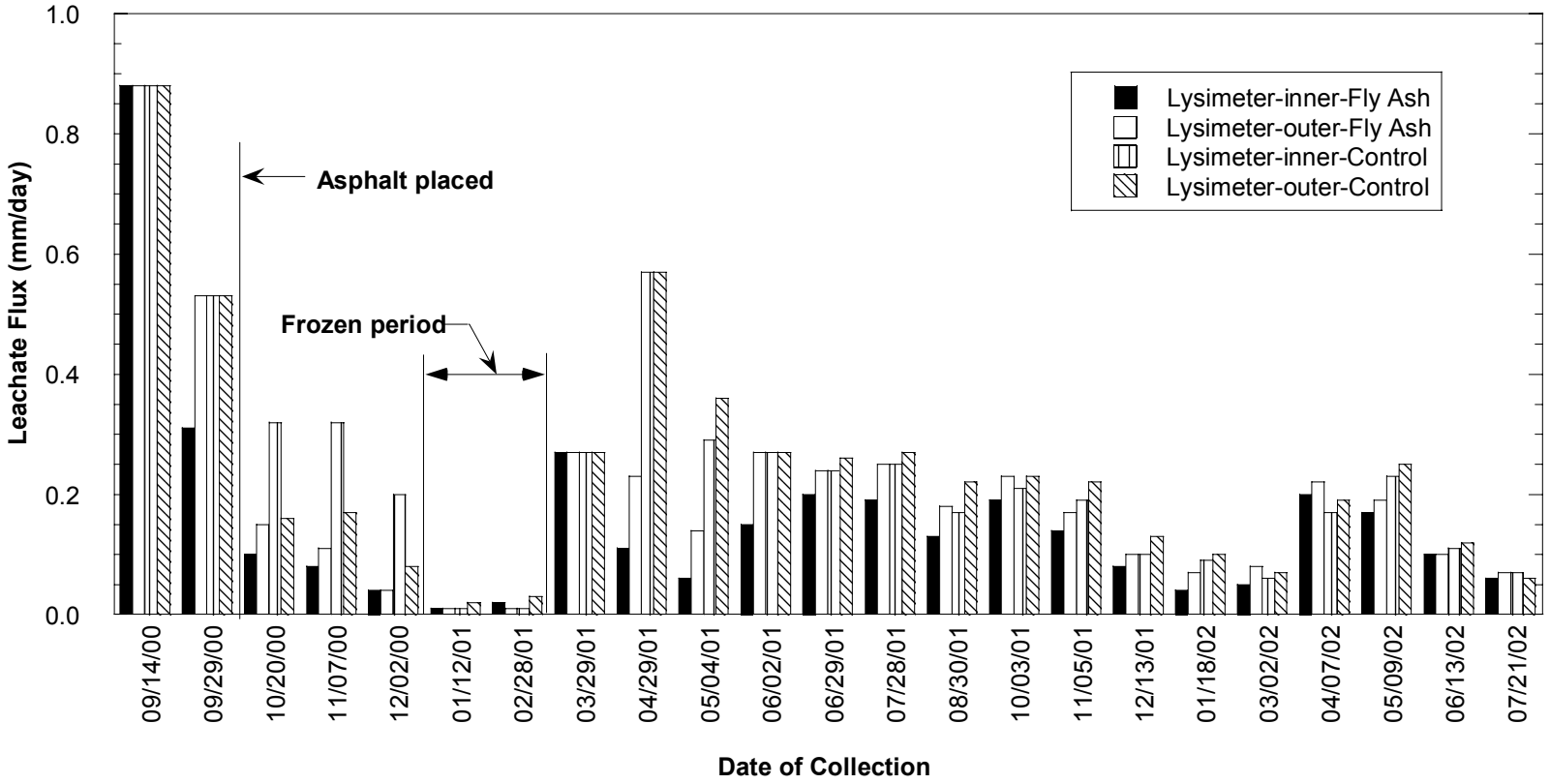

Fig. 5.29. Leachate Flux From Bottom of the Stabilized Subbase Layer at STH 60 Site.

flow bypassing is insignificant when the width of the lysimeter is at least five times the depth of the overlaying layer. The width-to-depth ratio for the lysimeters is 12. Thus, flow bypassing of the lysimeters is expected to be insignificant.

5.3.1.2 Leachate Concentrations

Concentrations of different species in the leachate from the fly ash stabilized section and the control section are shown in Fig. 5.30 and 5.31. The concentration of Se is highest among all metals for both the fly ash (~28 μg/L) and control sections (~11 μg/L), whereas the concentration of Cd is the lowest for the fly ash section (~2 μg/L) and Cr for the control section (<2 μg/L). Concentrations of Cr were below the detection limit (2 μg/L) for most of the leachate samples collected from the control section. The concentration of all species decreased slightly over time for both sections. The volume of water passing through the stabilized section (<2 pore volumes) and control section (<2.5 pore volumes) has been small. Thus, the change in concentration was minimal.

Concentrations of metals in the leachate collected during the first sampling event (September 14, 2000) are shown in Fig. 5.32. The concentration of Cd is slightly higher for the control section (5 μg/L) than for the fly ash stabilized section (2.4 μg/L), which is consistent with the concentration measured in the water leach tests (see Table 5.1). In contrast, the concentrations of Cr, Se, and Ag for the control section are lower than those for the fly ash stabilized section.

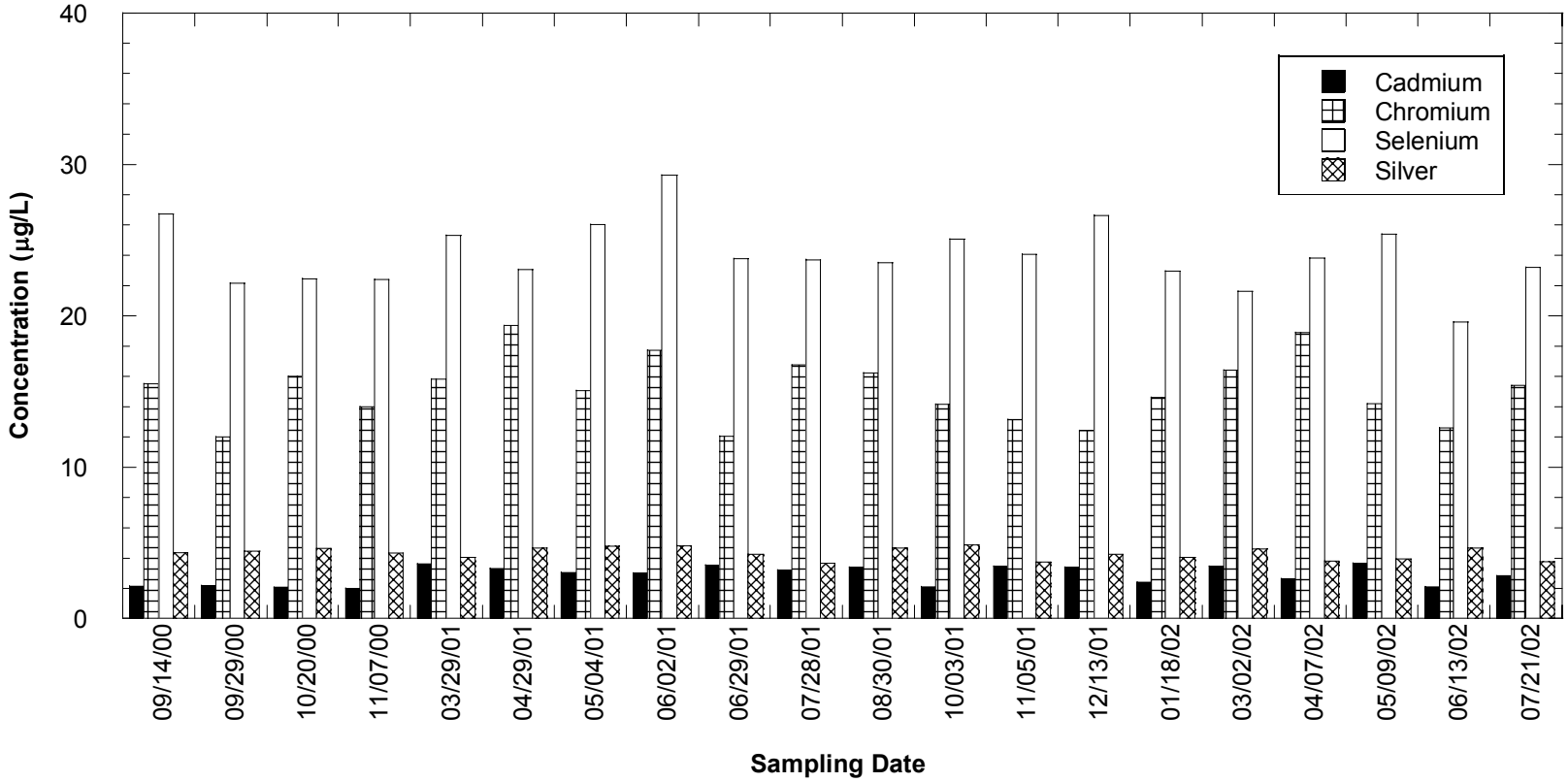

Fig. 5.30. Concentration of Metals in the Leachate from the Lysimeters in the Fly Ash Section at STH 60 Site. Detection Limits are: Cd = 0.1 µg/L, Cr = 2.0 µg/L, Se = 2.0 µg/L, and Ag = 0.2 µg/L.

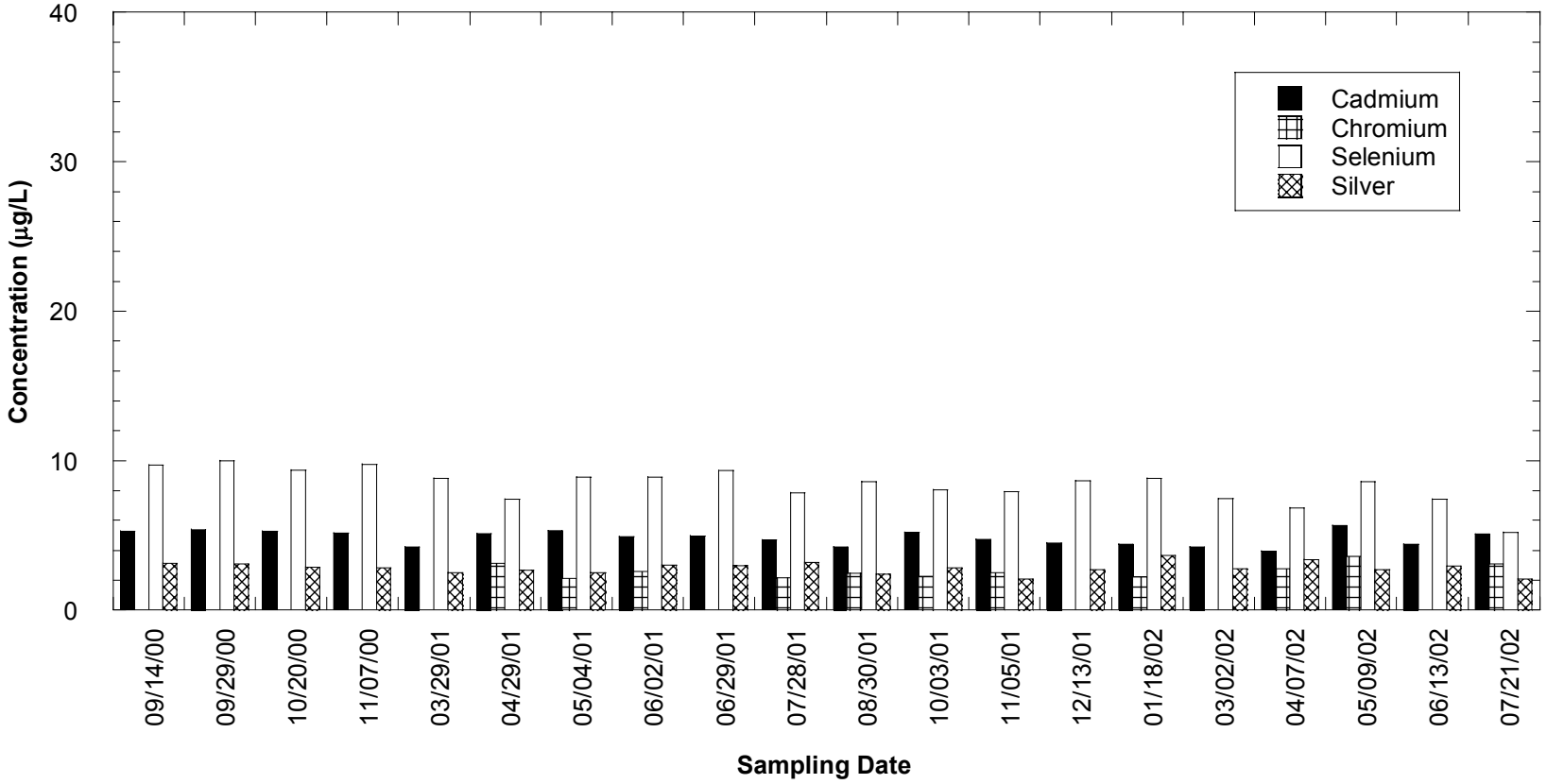

Fig. 5.31. Concentration of Metals in the Leachate from the Lysimeters in the Control Section at STH 60 Site. Detection Limits are: Cd = 0.1 μg/L, Cr = 2.0 μg/L, Se = 2.0 μg/L, and Ag = 0.2 μg/L.

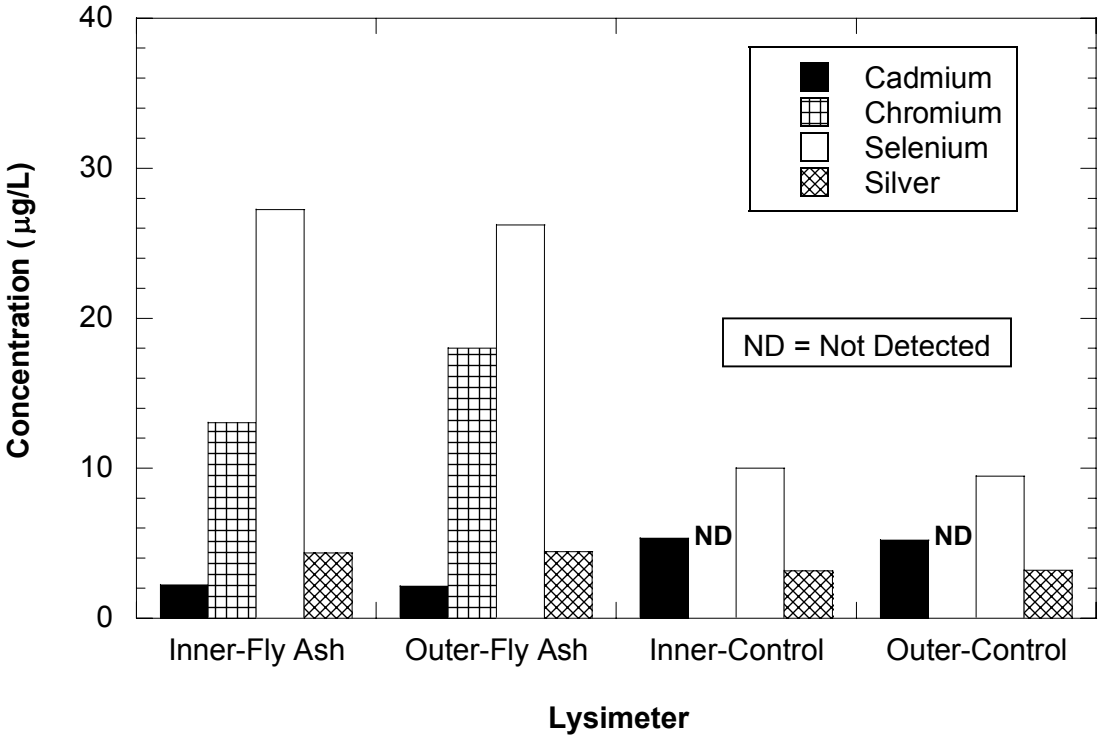

Fig. 5.32. Concentration of Metals in Leachate Samples Collected During First Sampling Event (Sept. 14, 2000) from the Four Lysimeters at the STH 60 Site. Detection Limits are: Cd = 0.1 μg/L, Cr = 2.0 μg/L, Se = 2.0 μg/L, and Ag = 0.2 μg/L.

5.3.2 Scenic Edge Site

5.3.2.1 Leachate Flux

The Darcy flux of leachate collected by the lysimeter at the Scenic Edge site is shown in Fig. 5.33. Construction of the lysimeter was completed at the end of October 2000. During the first two sampling events (Nov. 2000 and Jan. 2001), there was no leachate (NF in Fig. 5.33). Leachate was first observed after winter, and a maximum flux of 0.23 mm/d was observed in April 2001. The average leachate flux through the stabilized layer was 0.11 mm/d in 2001 (4% of average annual precipitation), which is comparable to the flux recorded at the STH 60 site.

5.3.2.2 Leachate Concentrations

Concentrations of different species in the leachate collected from the lysimeter at the Scenic Edge site are shown in Fig. 5.34. As was observed for the STH 60 site, the concentration of Se is highest (35 μg/L) and the concentration of Ag is lowest (0.2 μg/L). The concentration of Cr varies between 13 μg/L and 18 μg/L and the concentration of Cd varies between 1.8 μg/L and 1 μg/L. The concentrations of all metals decreased slightly over time. As in STH 60 site, the volume of water passing through the stabilized subbase was small (<2 pore volumes), and thus the change in concentration was also small.

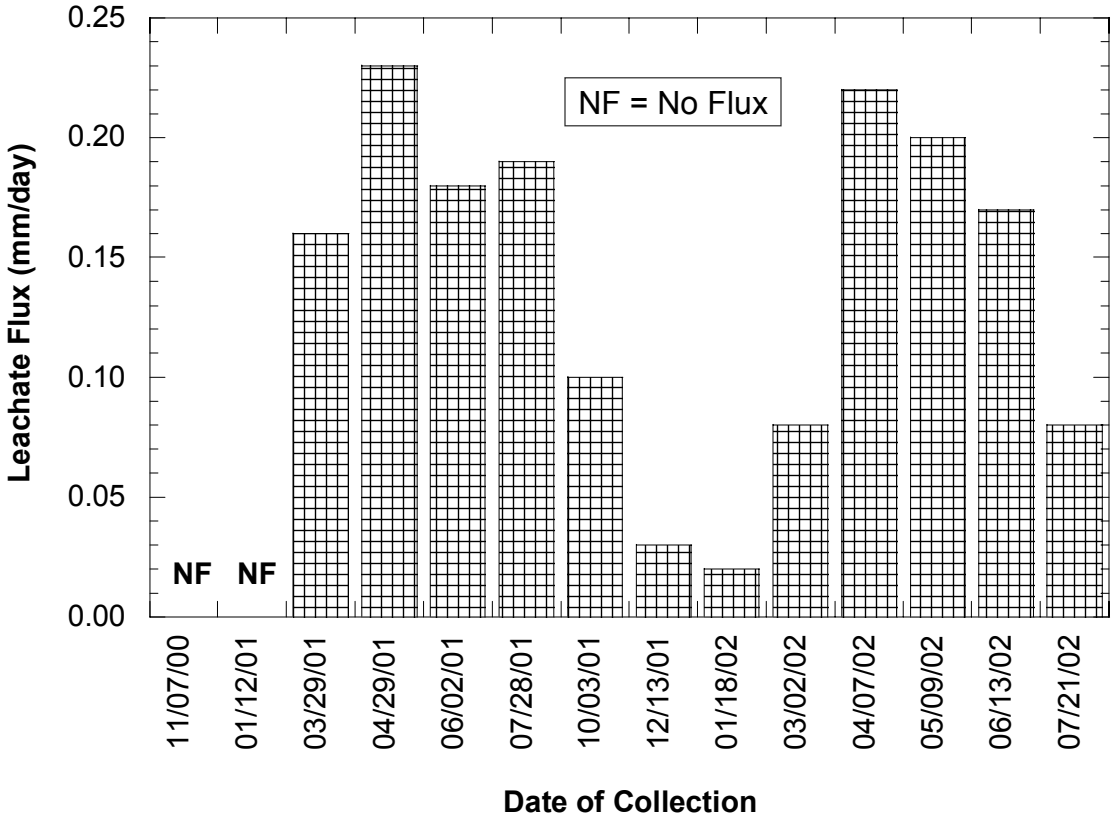

Fig. 5.33. Leachate Flux at the Bottom of the Stabilized Subbase Layer at Scenic Edge Site.

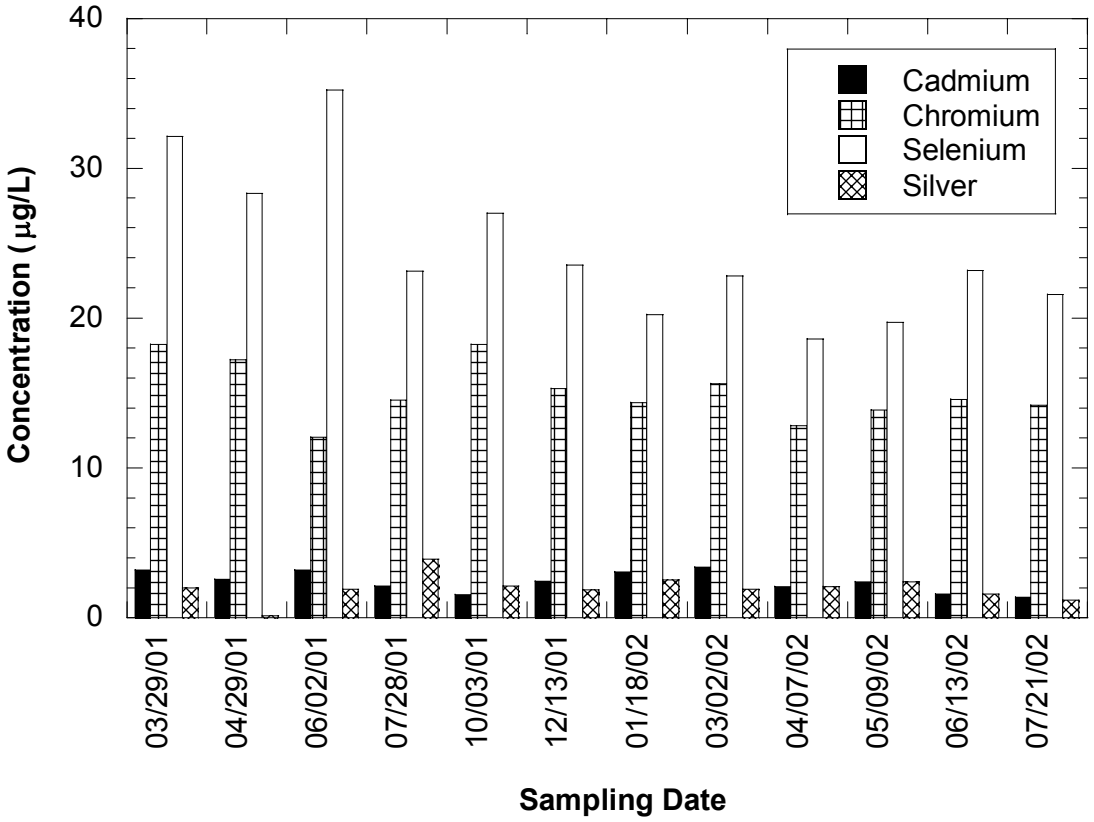

Fig. 5.34. Concentration of Metals in the Leachate Samples from the Lysimeter at Scenic Edge Site. Detection Limits are: Cd = 0.1 μg/L, Cr = 2.0 μg/L, Se = 2.0 μg/L, and Ag = 0.2 μg/L.

5.4 COMPARISON OF LEACHATE CONCENTRATIONS

5.4.1 Field Sites

Concentrations of metals in leachate collected during the first sampling event from the fly ash stabilized section at STH 60 (Sep.14, 2000) and the Scenic Edge site (Mar. 29, 2001) are shown in Fig. 5.35. Concentrations of metals in the leachate from Scenic Edge are slightly higher than those from the STH 60 site, except for Ag. The concentration of Ag in the leachate from Scenic Edge is slightly lower than that from the STH 60 site. The fly ash content for soil stabilization was 12% at Scenic Edge and 10% at STH 60. The slightly higher concentration of metals may be due to higher fly ash content that was used for stabilization at Scenic Edge site.

5.4.2 STH 60 Site and Column Leaching Test Data

Concentrations of different species obtained from leachate from the column leaching tests are compared with concentrations of leachate collected from the lysimeters installed in STH 60 in Fig. 5.36. For clarity, only curves obtained by fitting the leaching model (Eqn. 4.2) to the column leaching test data of Joy silt loam (the soil from the STH 60 site) are shown in Figs. 5.36 and 5.37. Additionally, comparisons are only made with curves from the column leaching tests conducted on soil-fly ash mixtures with 10% fly ash content and the soil alone, since only these conditions were tested in the field. In the control section, the leachate also passed through a crushed rock subbase layer before entering into the subgrade layer. This condition was not simulated in the column leaching tests.

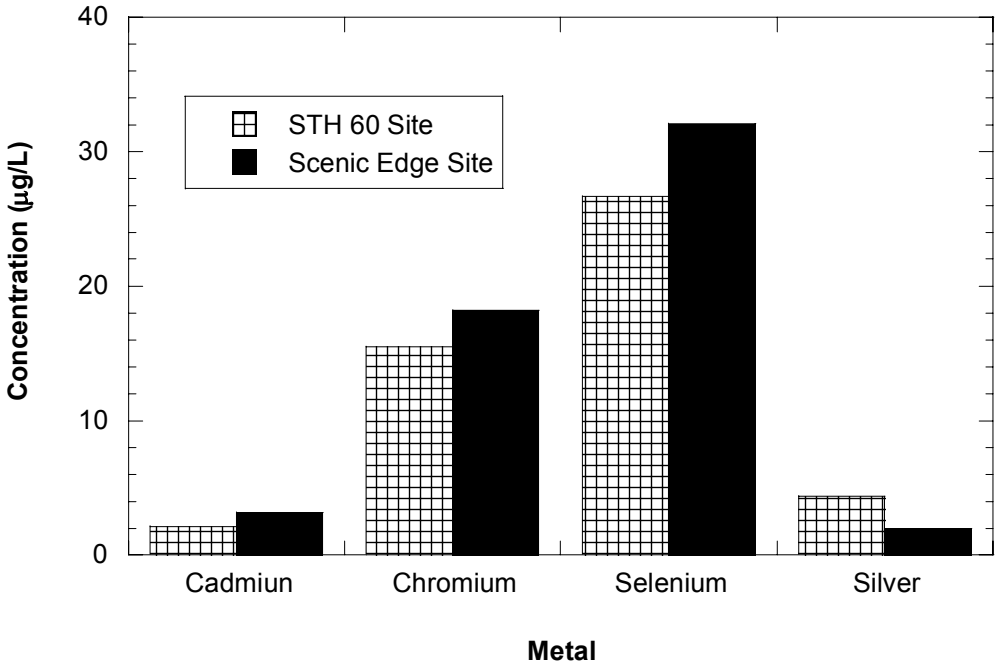

Fig. 5.35. Comparison of Metal Concentrations in Leachate Samples Collected During First Sampling Event at the STH 60 Site (Sept. 14, 2000) and Scenic Edge Site (March 29, 2001). Detection Limits are: Cd = 0.1 μg/L, Cr = 2.0 μg/L, Se = 2.0 μg/L, and Ag = 0.2 μg/L.

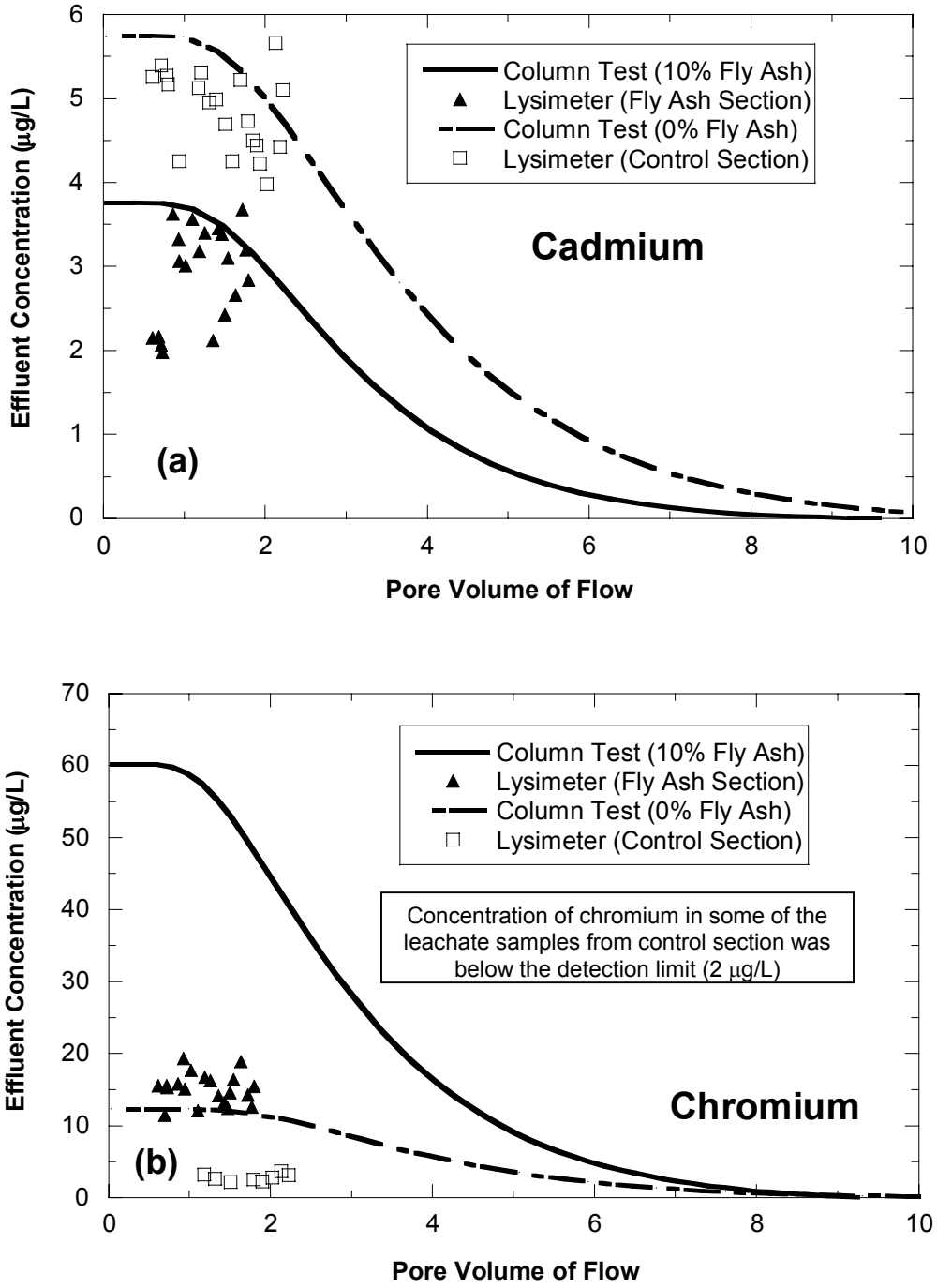

Fig. 5.36. Comparison of Concentration of Cd (a) and Cr (b) in Leachate from Lysimeter in the Stabilized Section at STH 60 and in Leachate from Column Leaching Tests on Similar Stabilized Soil Prepared with Joy Silt Loam and Columbia Fly Ash (10%).

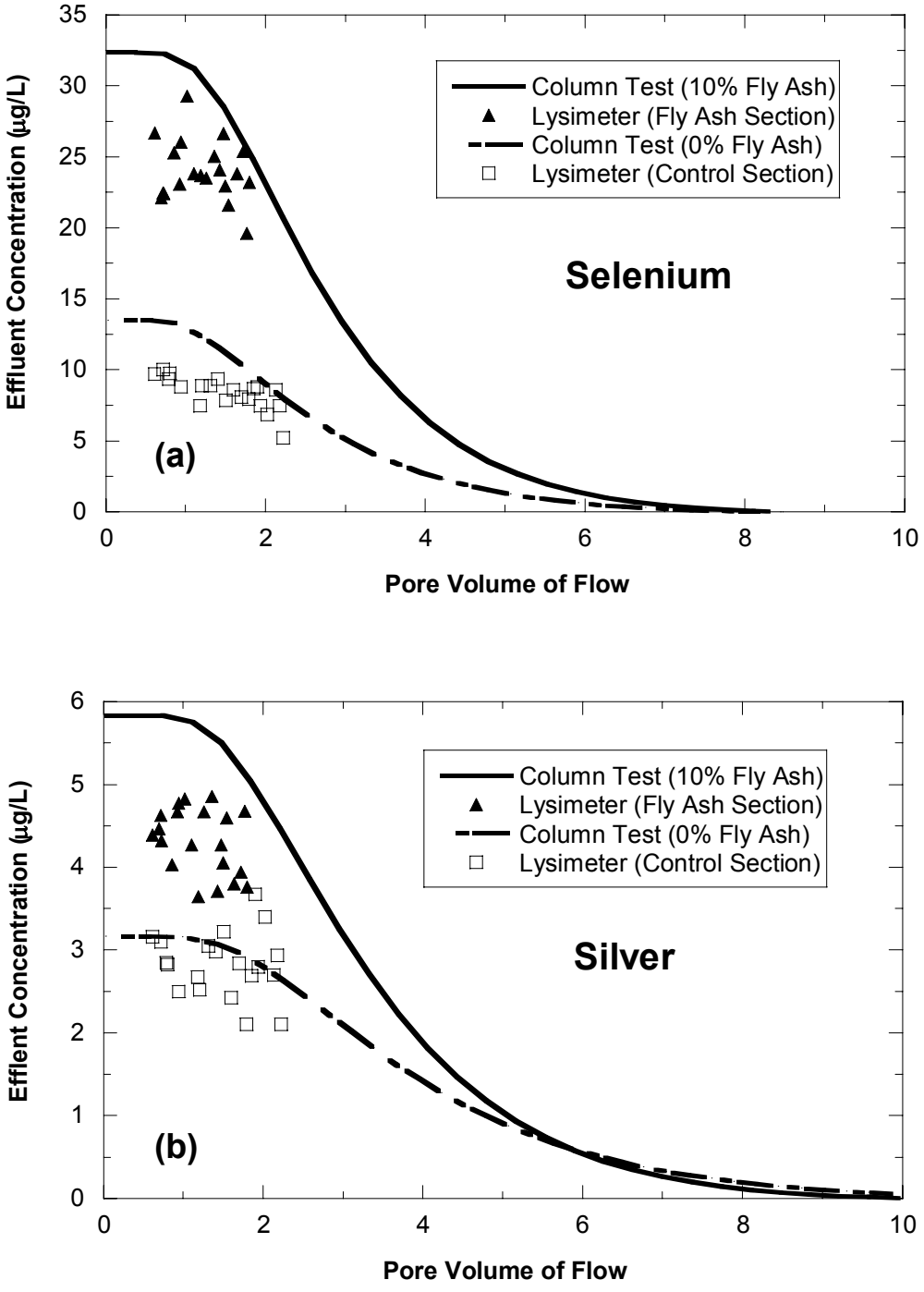

Fig. 5.37. Comparison of Concentration of Se (a) and Ag (b) in Leachate from Lysimeter in the Stabilized Section at STH 60 and in Leachate from Column Leaching Tests on Similar Stabilized Soil Prepared with Joy Silt Loam and Columbia Fly Ash (10%).

The lysimeters were connected to the collection tanks three weeks after stabilization. Weather data close to the field sites show that 80 mm of rain was received between the time when the soil was stabilized and the time when the tanks were connected. Additionally, the surface was unpaved during this period. If 50-60% of precipitation is assumed to have infiltrated during this period, then approximately 0.5 pore volumes of leachate escaped before the tanks were installed. Thus, the initial concentrations were assumed to correspond to 0.5 pore volumes of flow.

Concentrations of all species, except Cr, from the column leaching tests with 10% fly ash content are comparable with the concentrations obtained from the leachate of the fly ash stabilized section. The concentration of Cr from the column leaching test was four times higher than the concentration from the field.

Comparable Cd, Se, and Ag concentrations between the leachate samples obtained from the control section and those from the column leaching tests suggest that the presence of the crushed rock subbase layer did not affect leaching of these metals from the subgrade soil placed over the lysimeters in the control section. Concentrations of Cr in the leachate samples obtained from the field are at least five times lower than those from the column leaching tests, and are below the detection limit (2 μg/L) both for the fly ash and the control section.

In general, concentrations of metals in leachate from the column leaching tests are in good agreement, or over estimate concentrations in leachate from the lysimeters. Thus, transport parameters obtained from column leaching tests can be used reliably as input to models used to simulate field scenarios.

SECTION 6

CHEMICAL TRANSPORT MODELING

6.1 NUMERICAL MODEL

Transport of contaminants from a stabilized subbase to groundwater was simulated using HYDRUS2D, a windows-based software package for simulating water, heat, and solute movement in two-dimensional variably saturated media (Simunek et al. 1999). HYDRUS2D uses the finite element method to solve Richards' equation for two-dimensional variably saturated water flow and the advection-dispersion equation for solute transport. The solute transport equations consider advective-dispersive transport in the liquid phase, as well as diffusion in the gas phase. Only isothermal simulations were conducted in this study.

6.1.1 Flow Simulation

HYDRUS2D considers two-dimensional isothermal Darcian flow of water in a rigid variably saturated porous medium. The air phase is assumed to have no effect on liquid flow. Flow equation for these conditions can be described by the following modified form of Richards' equation:

$$\frac{\partial \theta}{\partial t} = \frac{\partial}{\partial x_i}\left[K\left(K_{ij}^{A} \frac{\partial h}{\partial x_j} + K_{ij}^{A} \right) \right] - S \qquad (6.1)$$

where θ is the volumetric water content [-], h is pressure head [L], S is a sink term [1/T], x_i (i = 1, 2) are the spatial coordinates [L], t is time [T], K_{ij}^{A} are components of

a dimensionless anisotropy tensor K^A, and K is the unsaturated hydraulic conductivity function [L/T], which is given by

$$K(h, x, z) = K_s(x, z)\, K_r(h, x, z) \tag{6.2}$$

In Eq. 6.2, K_r is the relative hydraulic conductivity and K_s is the saturated hydraulic conductivity [L/T]. The anisotropy tensor K_{ij}^A is used to account for an anisotropic medium. For an isotropic media, the diagonal entries of K_{ij}^A equal one and the off-diagonal entries are zero. If Eq. 6.1 is applied to planar flow in a vertical cross-section, $x_1 = x$, which is the horizontal coordinate and $x_2 = z$, which represents the vertical coordinate.

6.1.2 Contaminant Transport Simulation

HYDRUS2D assumes that solutes can exist in all three phases (liquid, solid, and gas), and that the decay and production processes can be different in each phase. The interaction between the solid and liquid phases may be described by non-linear non-equilibrium equations, while interactions between the liquid and gas phases are assumed to be linear and instantaneous. Zero-order production and two first-order degradation reactions (one is independent of other solutes, and the other provides coupling between solutes involved in sequential first-order decay reactions) can be simulated. In addition, physical non-equilibrium solute transport can be simulated using a two-region dual-porosity type formulation, which partitions the liquid phase into mobile and immobile regions. Solutes are transported by advection and dispersion in the liquid phase, and by diffusion in the gas phase.

The governing equation for solute transport solved by HYDRUS2D is:

$$-\theta R\frac{\partial c}{\partial t}-q_i\frac{\partial c}{\partial t}+\frac{\partial}{\partial x_i}\left(\theta D_{ij}\frac{\partial c}{\partial x_j}\right)+Fc+G=0 \qquad (6.3)$$

where θ is the volumetric water content [-], R is the retardation factor, c is the solute concentration [M/L^{-3}], t is the time [T], q_i is the Darcy velocity [L/T], x_i (i = 1, 2) are the spatial coordinates [L], D_{ij} [L^2/T] is an effective dispersion coefficient tensor, F [L^2 or L^3] is the coefficient matrix in the global matrix equation for water flow, and G [L^2/T or L^3/T] is the coefficient matrix in the global matrix equation for solute transport.

6.2 MODEL VALIDATION

The contaminant transport algorithm in HYDRUS2D was validated by comparison with analytical solutions for leaching over a range of system Peclet numbers and retardation factors that might be encountered when simulating leaching from a fly ash stabilized subbase. A simple case of leaching from column leaching tests was used for validation. A description of the analytical model, including the geometry, initial conditions, boundary conditions, and its solution are presented in the following sections. Derivation of the analytical solution is described in detail in Appendix G.

6.2.1 Conceptual Model

A schematic of the column that was simulated is shown in Fig. 6.1, along with the conceptual model implemented with HYDRUS2D. For flow, the boundary condition at the entry boundary of the domain was assigned a constant flux. The exit boundary condition was assigned a constant head (pressure head = 0). The side boundaries were assigned as "no flux" boundaries. For contaminant transport, the entry and side boundaries were "no mass flux" boundaries and the exit boundary was a third type (Cauchy type) boundary, which is mass conservative. The initial concentration in the aqueous phase was assumed to be C_o throughout the domain.

The analytical solution for this case described in the previous section is (van Genuchten 1981):

$$\frac{C_e(L,T)}{C_o} = 1 - \frac{1}{2}\left\{ \operatorname{erfc}\left(\frac{R-T}{2(TR/P_L)^{1/2}} \right) + \exp(P_L)\ \operatorname{erfc}\left(\frac{R-T}{2(TR/P_L)^{1/2}} \right) \right\} \qquad (6.4)$$

where C_e is the effluent concentration, R is the retardation factor, T is the pore volume leached (vt/RL), P_L (= vL/D) is the column Peclet number, erfc is the complimentary error function, v is the seepage velocity, t is the time, L is the length of the column, and D is the dispersion coefficient ($v\alpha + D_m$).

6.2.2. Comparison of the Analytical Solution with HYDRUS2D Simulations

A sensitivity analysis was initially conducted to assess the level of mesh and temporal refinement needed for the model validation. The mesh Peclet number was

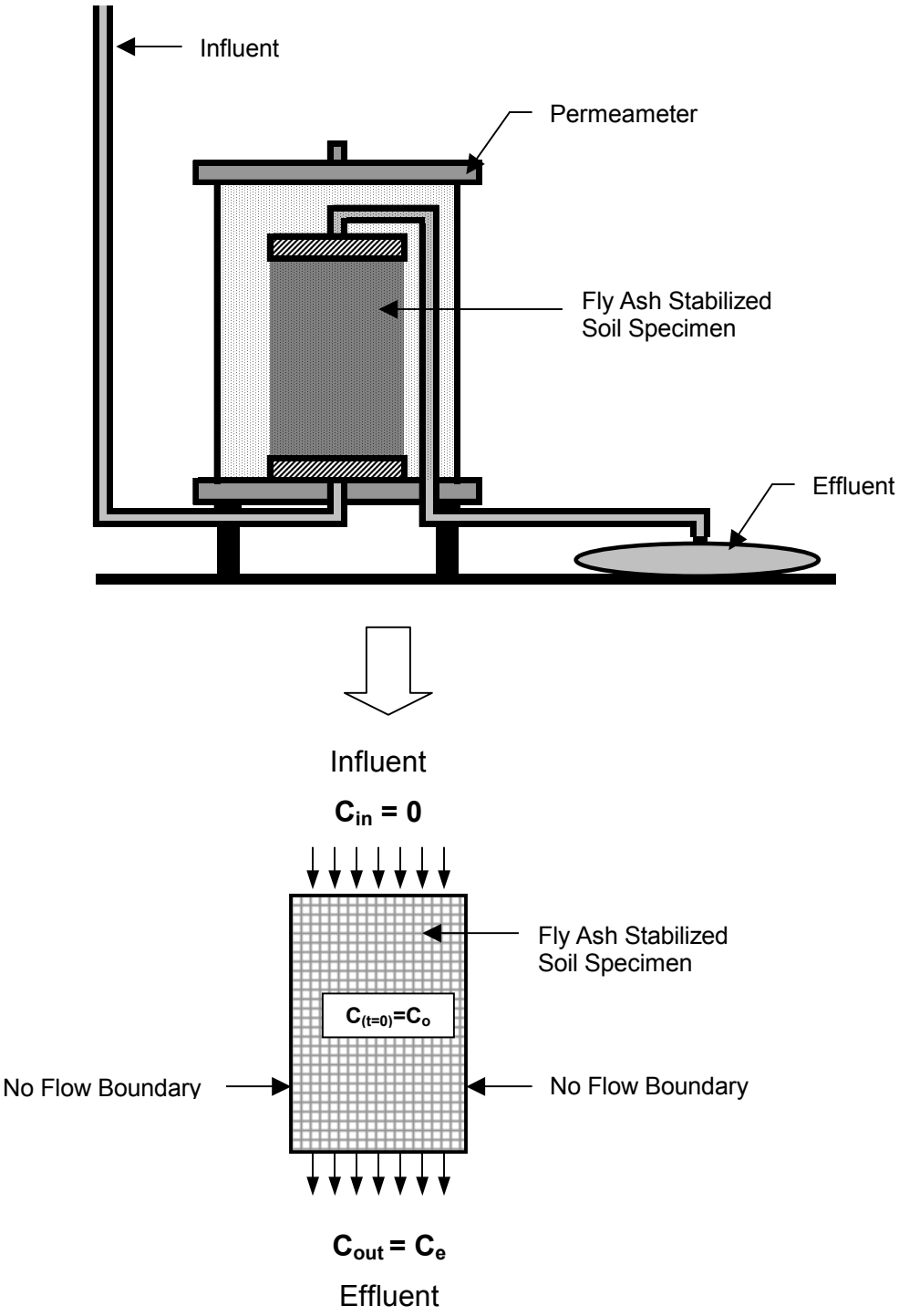

Fig. 6.1. Conceptual Model for Column Leaching Test.

varied from 0.05 to 1.24 by changing the mesh size from 1 mm to 23 mm, and the Courant number ($v \Delta t/R \Delta x$) was varied from 6.4×10^{-2} to 3.0×10^{-5} by varying the time step from 100 s to 50,000 s and varying the mesh size from 1 mm to 23 mm. Varying the mesh Peclet number from 0.05 to 1.24 did not affect the elution curve. However, the mass balance error increased from 0.06 to 0.21% as the mesh Peclet number increased. The elution curve obtained from HYDRUS2D remained unchanged for the range of Courant numbers that were tested. Thus, for the remaining validation tests, the mesh size was 5 mm x 5 mm (mesh Peclet number = 0.05) and the maximum time step was 100 s (Courant number = 0.001).

A series of simulations was conducted for a range of system Peclet numbers and retardation factors that might be used when simulating leaching from a fly ash stabilized subbase. The system Peclet number was varied between 2 and 100 by varying the seepage velocity between 1×10^{-4} mm/d to 1×10^{4} mm/d, and by varying the dispersivity from 0.01 L to 0.5 L. The range of Peclet number includes both advection and diffusion dominated systems. The retardation factor was varied between 1 and 14. Elution curves from the analytical solution and the HYDRUS2D simulations are shown in Fig. 6.2 for different system Peclet numbers and different retardation factors. The analytical solutions and HYDRUS2D simulations are identical for higher Peclet numbers (P_L>5), and deviate slightly for lower Peclet numbers (Fig. 6.2a). HYDRUS2D over-predicts concentrations compared to those from the analytical solution for low Peclet number. For a Peclet number of 2, concentrations from the numerical simulations are 5-7% higher than those obtained

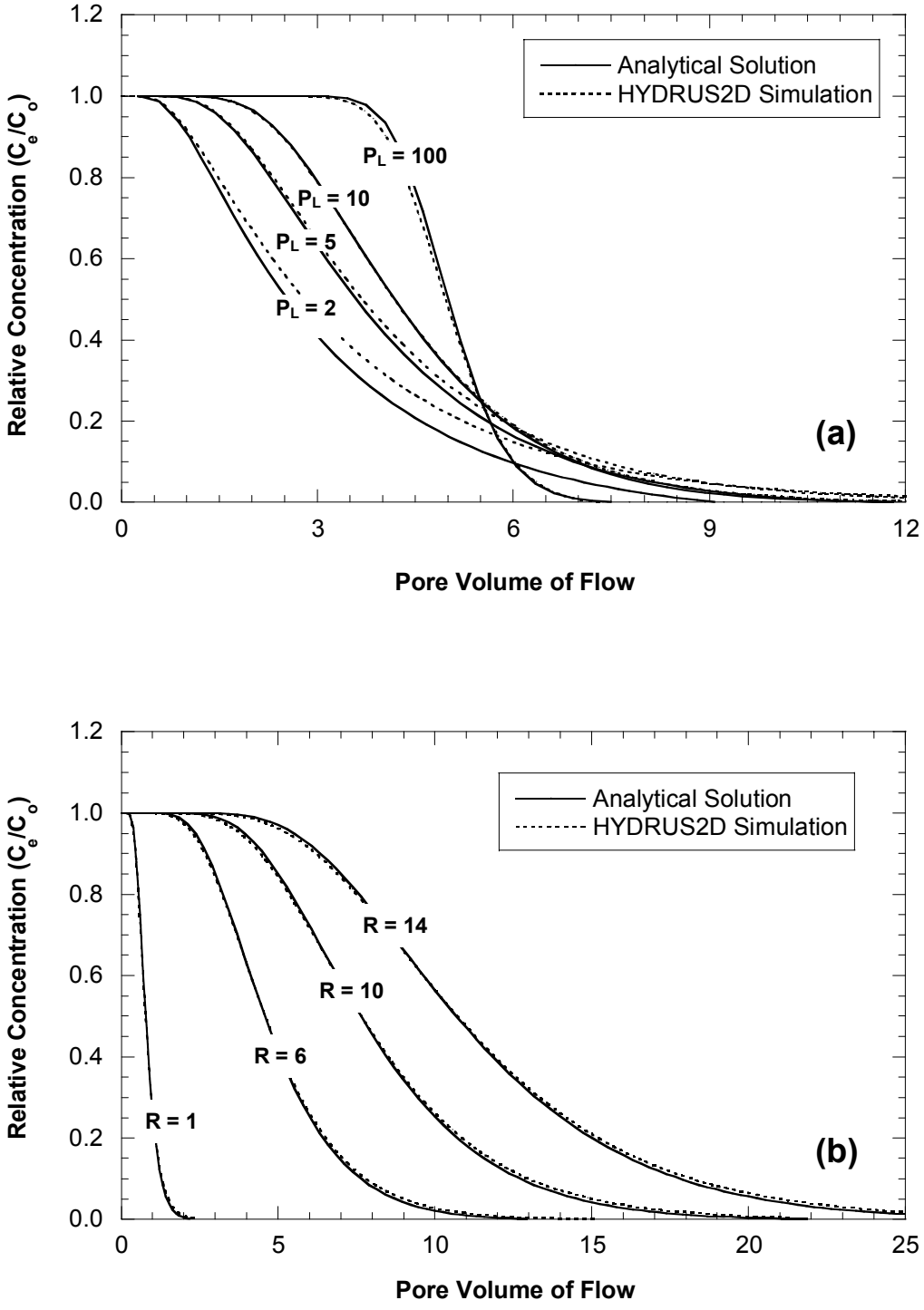

Fig. 6.2. Comparison of Elution Curves from Analytical Solutions and HYDRUS2D Simulations for Different (a) System Peclet Numbers and (b) Retardation Factors.

from the analytical solutions. The Peclet number for the field and column tests in this study varied between 4 and 25. Within this range, concentrations from the analytical solution and HYDRUS2D are essentially the same. Good agreement exists between the analytical and numerical solutions over the range of retardation factors that was considered (Fig. 6.2b).

Concentrations predicted with HYDRUS2D were also compared with concentrations from a column leaching test. The leaching test was conducted on a soil-fly ash mixture prepared with Joy silt loam and 10% Columbia fly ash. Transport parameters for this column leaching test were obtained by fitting the analytical solution (Eq. 6.4) to the effluent concentrations (C_o = 32 μg/L, q = 1.17 x 10^{-6} cm/s, α = 0.16 L, and R = 3.5, see Table 6.1). These transport parameters were used as input to HYDRUS2D for simulating the column test. The concentrations predicted with HYDRUS2D and measured during the column test are shown in Fig. 6.3. Good agreement exists between the measured and predicted concentrations. The predicted concentrations are typically within 3% of the measured concentrations.

6.3 MODEL OF FIELD SCENARIO

After validation, HYDRUS2D was used to develop a model simulating typical field scenarios where the subgrade was stabilized with fly ash. This model was used to conduct a series of simulations to estimate the highest metals concentrations that would occur when leachate from a stabilized subbase reaches groundwater, and

Table 6.1. Input Parameters for the Numerical Simulation.

Parameter	**Value**
Height of the Domain, cm	11.43
Width of the Domain, cm	10.16
Total Porosity, n	0.38
Effective Porosity, n_e	0.33
Darcy Velocity, v (cm/sec)	1.17×10^{-6}
Longitudinal Dispersivity, α (cm)	0.16 L
Retardation Factor, R	3.5
Influent Concentration, C_{in} (μg/L)	0
Initial Pore Fluid Concentration, C_o (μg/L)	32

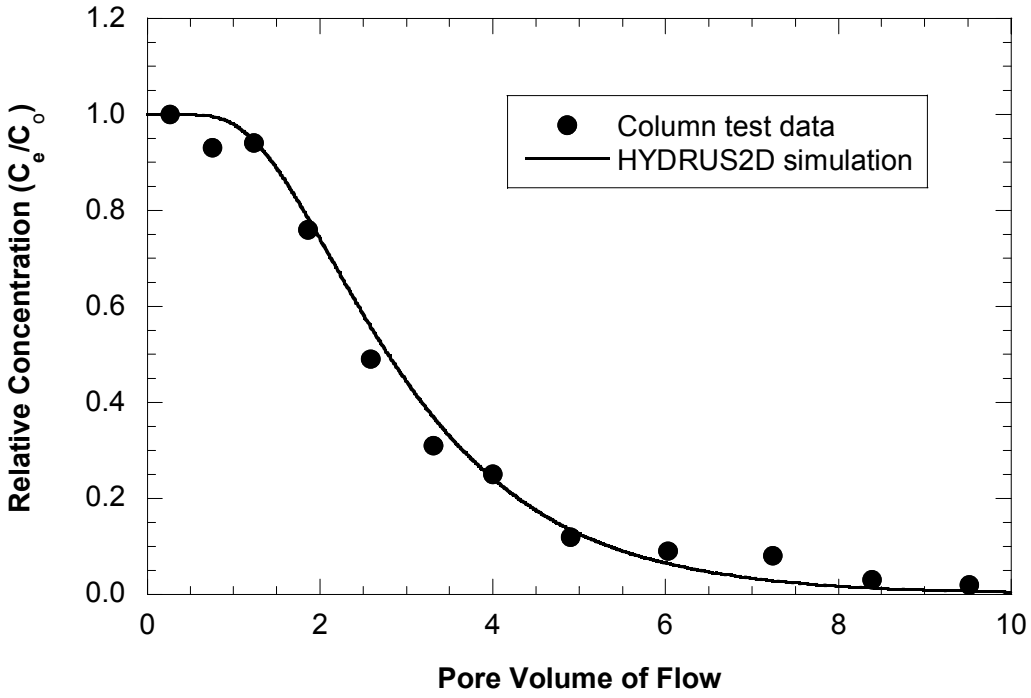

Fig. 6.3. Comparison of Column Leaching Test Data with the Elution Curve Obtained from the HYDRUS2D Simulation. Input Data are Summarized in Table 6.1. Column Leaching Test was Conducted on Soil-Fly Ash Mixture.

the time at which the highest concentration would occur. These simulations were conducted with transport parameters obtained from the column leaching tests and with Darcy fluxes measured in the field.

6.3.1 Conceptual Model

The conceptual model for the field scenario is shown in Fig. 6.4. Metals are leached from stabilized soil as rainwater or ice-melt water infiltrates through the asphalt layer and percolates downward through the base layer and the stabilized subbase layer. Metals in the stabilized subbase dissolve in the percolating water, and are transported towards the groundwater table. Transport was assumed to occur one dimensionally in the vertical direction. Thus, for both flow and transport, the vertical sides of the domain were no flux boundaries.

For flow, the boundary condition at the top of the domain was assigned as constant flux. The bottom boundary, which is the groundwater table, was set as a zero pressure head boundary. For contaminant transport, the top boundary was set as a no flux boundary and the bottom boundary was assumed to be a third type (Cauchy type) boundary.

The concentration of percolating water was assumed to be zero before entering the stabilized layer and the initial concentration of metals in pore water of the stabilized soil was set equal to unity. No degradation or biological activity was considered. Column tests showed that the partition coefficients of the stabilized soil and subgrade were essentially the same for a particular species (see Sec 5.2.1.3).

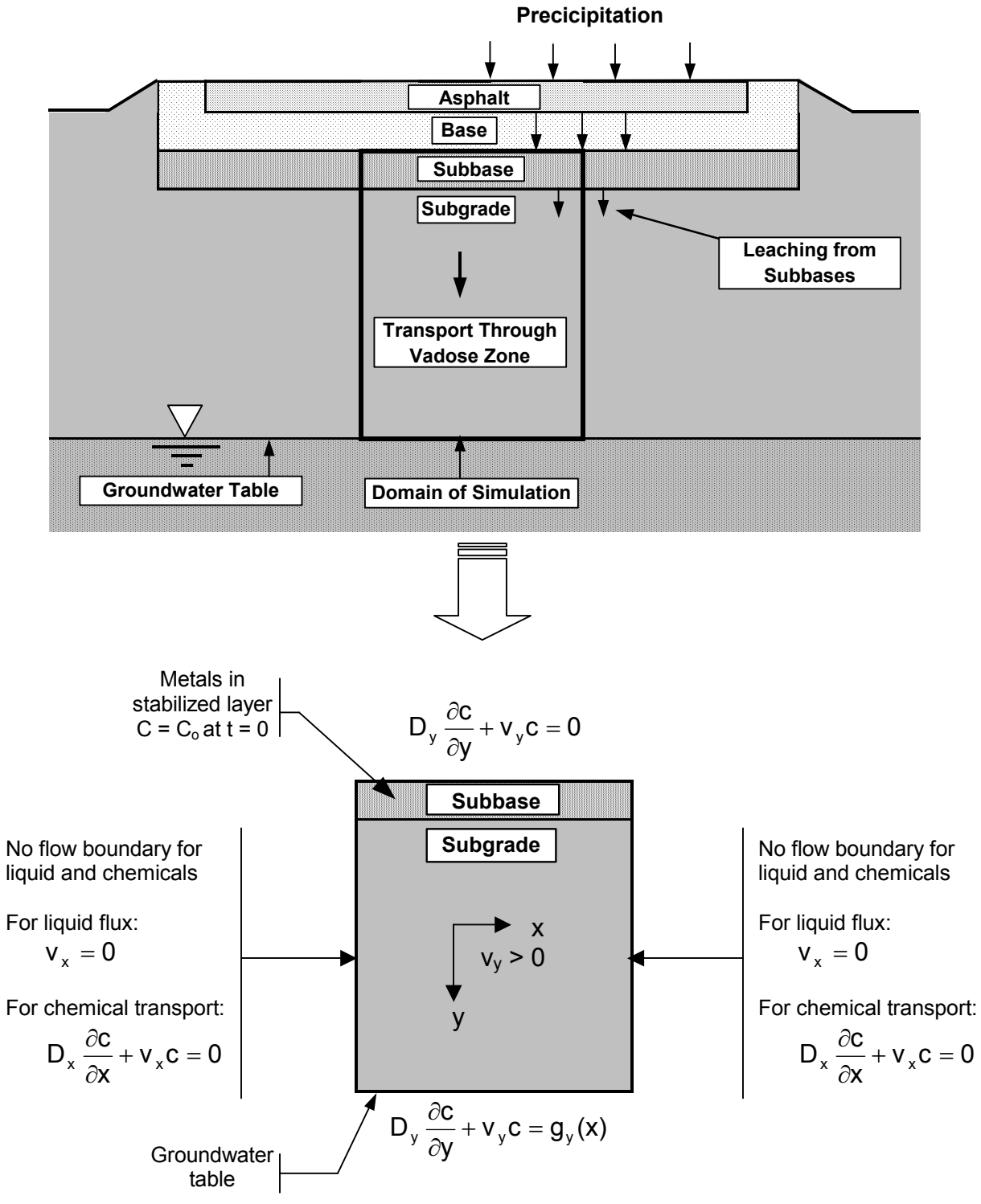

Fig. 6.4. Conceptual Model and Domain for the Numerical Simulation.

Thus, the retardation factors of the stabilized soil and subgrade were assumed to be the same.

The depth of the domain was set at 6 m, which corresponds to the deepest depth to groundwater for the portion of STH 60 where the field tests were conducted (Edil et al. 2002). The vertical extent of the domain extends from the top surface of the stabilized layer to the depth of the groundwater table. The stabilized subbase layer was assumed to be 0.3 m thick. The liquid flux in the field was measured at the base of the pavement structure (i.e., subbase) in the field, and is assumed to represent a steady flux through the pavement structure. For simplicity, the upper two layers (hot mixed asphalt and base layer) of the roadway were excluded from the model domain. Therefore, the domain consists of two different materials: the stabilized subbase and the subgrade. The material in each layer is assumed to be homogeneous and isotropic.

6.3.2 Spatial and Temporal Discretization

Several simulations were conducted with different mesh discretization to evaluate how mesh refinement affected the mass balance. The square mesh size was varied from 20 mm to 300 mm, while all other parameters remained the same. The geometry and input parameters used for these simulations are summarized in Table 6.2. All input parameters were obtained from a column leaching test, except Darcy velocity, which was measured from the field.

Table 6.2. Input Parameters for Spatial and Temporal Discretization.

Parameter	**Value**
Height of the Domain, m	6
Thickness of Stabilized Layer, m	0.3
Darcy Velocity, v (mm/d)	0.15
Concentration of Metals in Percolate Entering Stabilized Layer, C_{in} (μg/L)	0
<u>Fly Ash Stabilized Soil Properties</u>	
Initial Pore Fluid Concentration, C_o (μg/L)	32
Total Porosity, n	0.38
Effective Porosity, n_e	0.33
Saturated Hydraulic Conductivity (mm/d)	1.03
Longitudinal Dispersivity, α (m)	0.1L
Retardation Factor, R	3.5
van Genuchten parameter, α_{vG}	0.02
van Genuchten parameter, n_{vG}	1.41
<u>Subgrade Properties</u>	
Initial Pore Fluid Concentration, C_o (μg/L)	0
Total Porosity, n	0.38
Effective Porosity, n_e	0.35
Saturated Hydraulic Conductivity (mm/d)	0.68
Longitudinal Dispersivity, α (m)	0.1 L
Retardation Factor, R	3.5
van Genuchten parameter, α_{vG}	0.02
van Genuchten parameter, n_{vG}	1.41

Note: van Genuchten parameters, α_{vG} and n_{vG} are obtained from Rosetta database on HYDRUS 2D.

Solute mass balance errors for different mesh Peclet numbers are summarized in Table 6.3. An appreciable reduction in mass balance error was obtained when the mesh size was reduced from 300 mm to 100 mm, and then from 100 mm to 50 mm. However, reducing the mesh size from 50 mm to 30 mm resulted only a small (0.001%) reduction in the mass balance error. A non-uniform mesh was also evaluated where finer spatial resolution was used in the stabilized layer and at the interface between the two layers (20 mm x 20 mm near the stabilized layer and 30 mm x 30 mm for the remainder). This mesh had a slightly (0.01%) higher mass balance error. Therefore, a uniform mesh of 50 mm x 50 mm was used for the remainder of the simulations.

Sensitivity to temporal discretization was evaluated by varying the minimum time steps from 0.001 to 0.1 d and the maximum time steps from 0.5 to 5 d. The mass balance errors for these simulations are summarized in Table 6.4. Reducing the time-step had little effect on the mass balance error. This insensitivity is most likely due to the small Courant numbers being used. The Courant number varied between 1.2×10^{-2} and 1.2×10^{-3}, which is much smaller than the upper bound of 1 that is typically recommended for HYDRUS2D (Simunek et al. 1999). Therefore, a time-step ranging between 0.01 and 2 d was used for all simulations.

6.3.3 Verification With Field Data

Concentrations predicted with the model were compared with concentrations measured in the leachate collected from the lysimeters at STH 60 beneath the

Table 6.3. Spatial Discretization Based on Mass Balance Error.

Mesh Size (W x D) (mm x mm)	Time Step (days)		Peclet Number	Mass Balance Error (%)
	Minimum	Maximum		
300 x 300	0.01	2	0.50	2.914
100 x 100	0.01	2	0.17	0.315
50 x 50	0.01	2	0.08	0.107
30 x 30	0.01	2	0.05	0.106
20 x 20 near stabilized layer, 30 x 30 over remainder	0.01	2	0.05	0.117

Table 6.4. Temporal Discretization Based on Mass Balance Error.

Mesh Size (W x D) (mm x mm)	Time Step (days)		Courant Number	Mass Balance Error (%)
	Minimum	Maximum		
300 x 300	0.01	2	0.0008	2.914
300 x 300	0.001	1	0.0004	2.911
50 x 50	0.1	5	0.0120	0.108
50 x 50	0.01	2	0.0048	0.107
50 x 50	0.01	1	0.0024	0.106
50 x 50	0.001	0.5	0.0012	0.106

stabilized soil. Concentrations of selenium are shown in Fig. 6.5. The input parameters that were used for field model were obtained from a column leaching test and are summarized in Table 6.2. The column leaching test was conducted on a soil-fly ash mixture prepared with Joy silt loam and 10% Columbia fly ash similar to the field case. Concentrations of selenium in the leachate are in good agreement with the predicted concentrations. The predicted concentrations are typically within 5% of the measured concentrations.

6.4 PARAMETRIC SIMULATION RESULTS

A series of simulations was conducted using different parameters that might be realized in a field scenario. The primary objective of these simulations was to estimate the maximum leachate concentration at a particular depth, and the time to reach the maximum concentration at a particular depth. A summary of the geometry and input parameter is shown in Table 6.5. Hydraulic properties of the stabilized subbase and subgrade measured in column tests were used as input. The retardation factor was varied between 3 and 6, and the dispersivity was varied between 0.05 L and 0.2 L to bracket the range of dispersivities anticipated in the field. Thickness of the stabilized subbase layer was varied from 0.15 m to 0.3 m. The Darcy velocity was assumed to be steady, but was varied between 0.02 mm/d and 0.72 mm/d.

The concentration of metals in percolate entering the stabilized subbase from the overlying layers was assumed to be zero. A unit concentration was used to

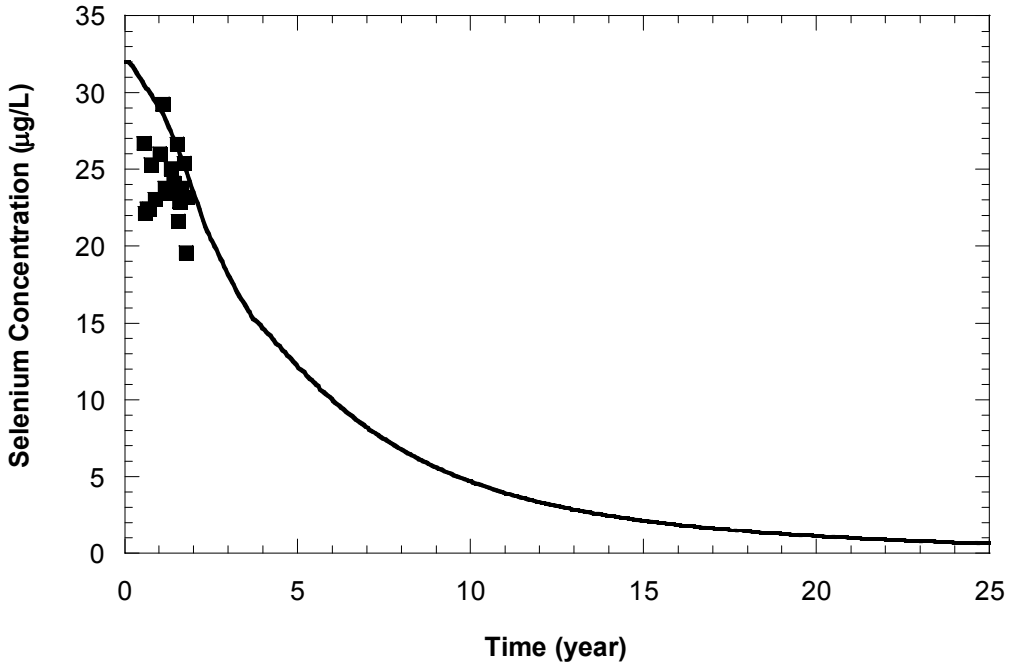

Fig. 6.5. Comparison of Concentrations Predicted by Model and Measured in Leachate Collected from Lysimeters at STH 60 Field Site. Input Data are Summarized in Table 6.2, which was Adopted from a Column Leaching Test Conducted on Soil-Fly Ash Mixture.

Table 6.5. Input Parameters for Parametric Simulations.

Parameter	Value
Height of the Domain, m	6
Thickness of Stabilized Layer, m	0.15 - 0.3
Darcy Velocity, v (mm/d)	0.02 - 0.72
Concentration of Metals in Percolate Entering Stabilized Layer, C_{in} (μg/L)	0
<u>Fly Ash Stabilized Soil Properties</u>	
Initial Pore Fluid Concentration, C_o (μg/L)	1
Total Porosity, n	0.38
Effective Porosity, n_e	0.33
Saturated Hydraulic Conductivity (mm/d)	1.03
Longitudinal Dispersivity, α (m)	0.05 L – 0.2 L
Retardation Factor, R	3 - 6
van Genuchten parameter, α_{vG}	0.02
van Genuchten parameter, n_{vG}	1.41
<u>Subgrade Properties</u>	
Initial Pore Fluid Concentration, C_o (μg/L)	0
Total Porosity, n	0.38
Effective Porosity, n_e	0.35
Saturated Hydraulic Conductivity (mm/d)	0.68
Longitudinal Dispersivity, α (m)	0.05 L – 0.2 L
Retardation Factor, R	3 - 6
van Genuchten parameter, α_{vG}	0.02
van Genuchten parameter, n_{vG}	1.41

Note: van Genuchten parameters, α_{vG} and n_{vG} are obtained from Rosetta database on HYDRUS 2D.

describe the initial condition of the pore fluid in the stabilized subbase layer. Use of a unit concentration allows the results to be scaled to other initial pore fluid concentrations by multiplying the concentration obtained from the simulation by the actual initial concentration of the pore water. The initial concentration of metals in the pore fluid of subgrade was assumed to be zero.

6.4.1 Darcy Velocity

Darcy fluxes measured using the lysimeters were reported in Sec. 5.2.1. For 2001, the Darcy flux was minimum in winter (0.02 mm/d) and maximum in spring (0.27 mm/d). The annual average flux in 2001 was 0.15 mm/d. The equivalent saturated hydraulic conductivity (harmonic mean weighted based on layer thicknesses) of the subbase and subgrade layer (for a total depth of 6 m) is 0.72 mm/d, which is approximately five times higher than the average flux. Thus flow probably occurred under unsaturated conditions during most of 2001.

Four simulations were run to determine the effect of Darcy flux on the chemical transport from stabilized subbase. The following fluxes were used: the minimum field flux (0.02 mm/d), the average field flux (0.15 mm/d), the maximum field flux (0.27 mm/d), and a flux equal to the equivalent saturated hydraulic conductivity (0.72 mm/d).

Breakthrough curves at the groundwater table (6 m below the subbase surface) for these fluxes are shown in Fig. 6.6. For the Darcy fluxes that were used, the maximum concentration was independent of the Darcy flux (Fig. 6.6.a).

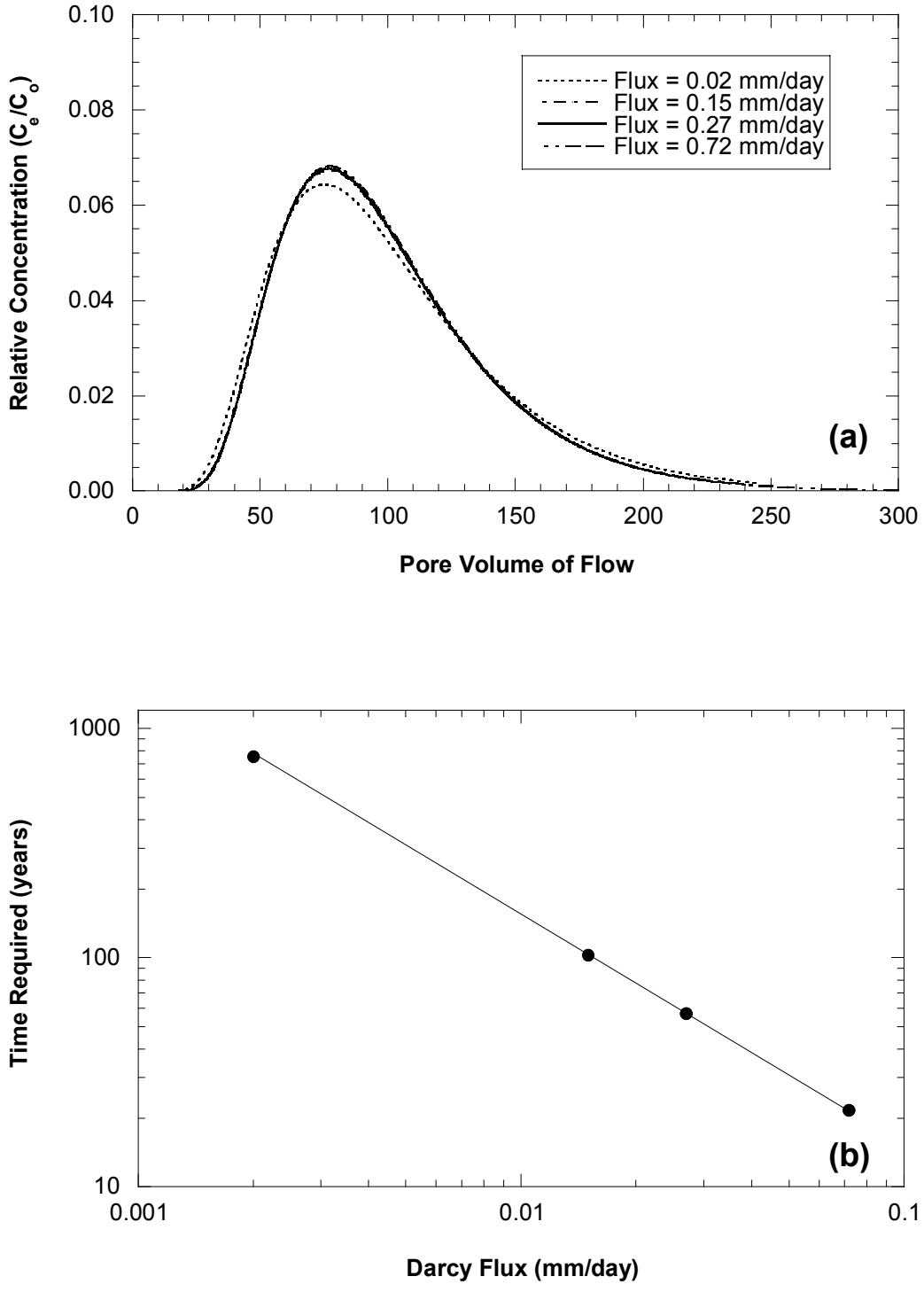

Fig. 6.6. Breakthrough Curves at Various Darcy Fluxes (Varied from 0.02 mm/d to 0.72 mm/d): (a) Breakthrough Curve Presented with Pore Volumes of Flow and (b) Time to Reach the Maximum Concentration.

Similarly, the time for the maximum concentration is proportional to the Darcy flux (Fig. 6.6b). That is, transport is dominated by advection for the field scenario being simulated. Accordingly, the simulation results can be scaled by the flux to simulate other field scenarios, provided they are advection dominated.

Scaling of the results is not valid when the advective component is small, and transport is controlled by diffusion. To define when scaling is no longer valid and the maximum concentration is no longer independent of the Darcy flux, a series of simulations was conducted for system Peclet numbers ranging from 0.15 to 50 by varying the Darcy flux between 2×10^{-4} and 7.2 mm/d.

The maximum concentrations at the groundwater table are shown in Fig. 6.7a as a function of the system Peclet number. The maximum concentration is independent of the Darcy flux provided the Peclet number higher is than 10 (i.e., transport is dominated by advection). Similarly, the maximum concentration is independent of the Darcy flux when the system Peclet number is lower than 1, because transport is dominated by diffusion. However, the transition from advection to diffusion dominated transport has only a small effect on the maximum concentration at the water table. The maximum concentration decreases by only 1.5% when transport becomes fully dominated by diffusion. As the Peclet number decreases from 10 to 1, the maximum concentration also decreases smoothly, since an advection dominated transport scenario is changing toward a diffusion dominated transport scenario.

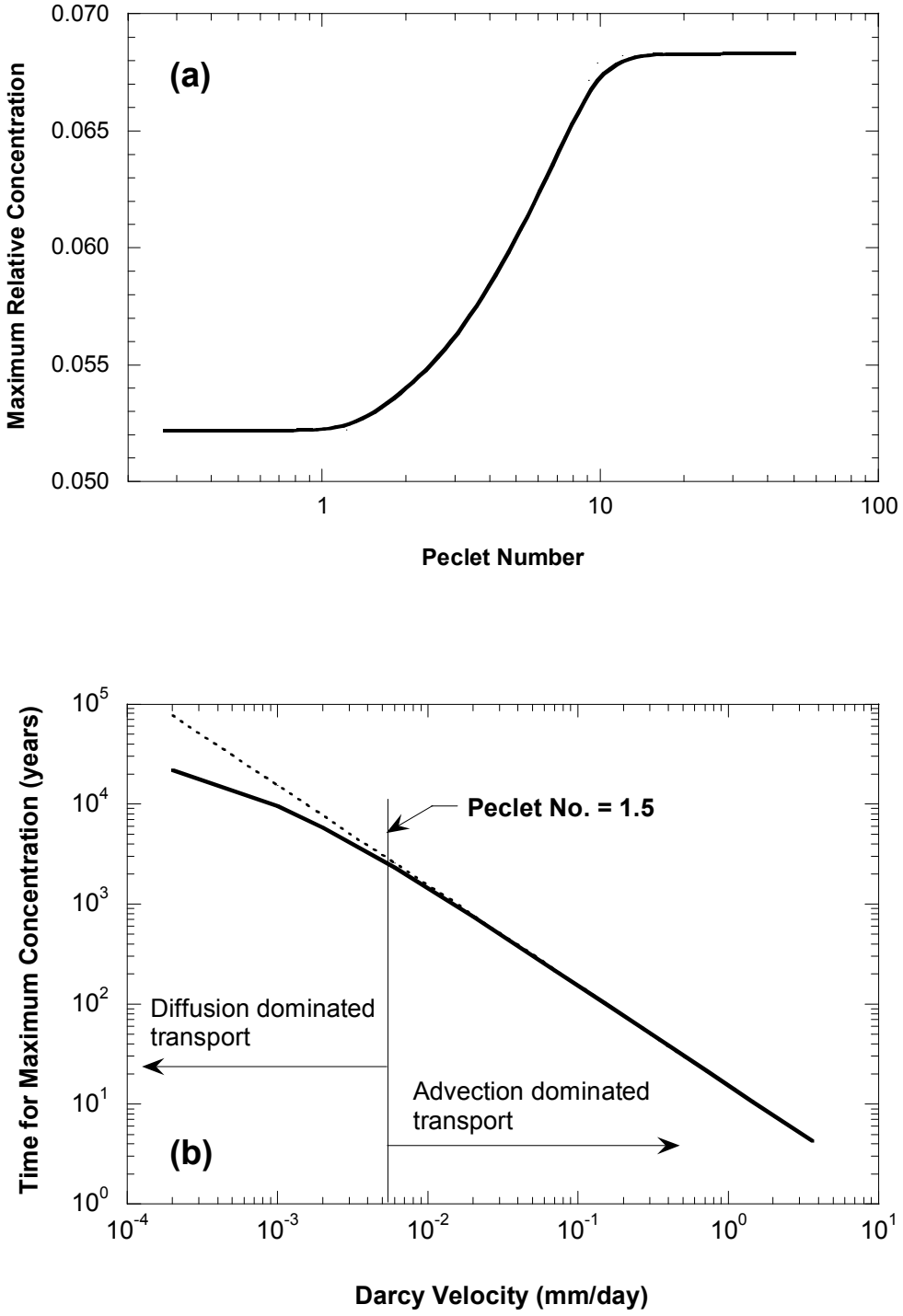

Fig. 6.7. The Maximum Concentrations at the Groundwater Table as a Function of System Peclet Number (a) and the Time for the Maximum Concentration at the Groundwater Table for Different Darcy Fluxes.

The time to reach the maximum concentration at the groundwater table for different Darcy fluxes is shown in Fig. 6.7b. The time to reach the maximum concentration is proportional to the Darcy flux provided the Darcy flux is higher than 0.005 mm/d (Peclet number = 1.5). At Darcy fluxes lower than 0.005 mm/d, transport is dominated by diffusion and scaling is no longer valid. In the diffusion dominated transport scenario, the time to reach the maximum concentration is less than the scaled time from a flux that causes advection dominated transport.

6.4.2 Retardation Factor

The maximum relative concentration is shown as a function of depth below the subbase in Fig. 6.8a for retardation factors of three and six. The maximum relative concentration decreases with depth due to adsorption and re-distribution of mass in the subgrade, and is independent of the retardation factor. The maximum relative concentration decreases abruptly from 1.0 to 0.2 in the first meter, and then decreases more gradually at deeper depths (e.g., from 0.2 to 0.07 as the depth increases from 2 to 6 m).

The time required to achieve the maximum relative concentration at different depths is shown in Fig. 6.8b. The time to reach the maximum concentration increases with the retardation factor for all depths. Similarly, the time to reach the maximum concentration increases linearly with depth, since the flux is constant. The time to reach the maximum concentration at a particular depth for a given retardation factor usually changes with the Darcy flux, and the changes are

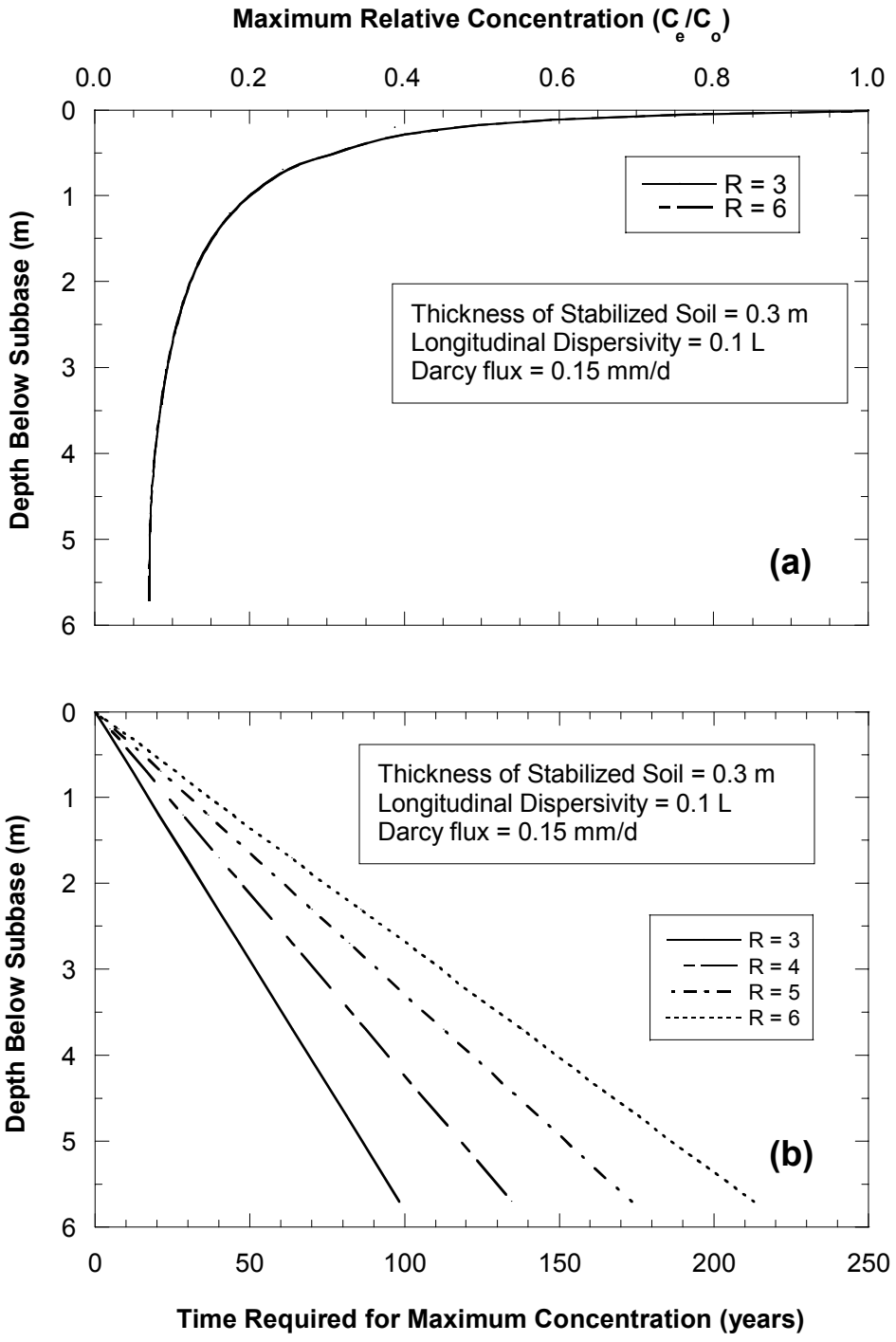

Fig. 6.8. Maximum Relative Concentration vs. Depth (a) and Time to Reach for Maximum Concentration at Different Depths (b) Simulations Conducted with Retardation Factor Ranging Between 3 and 6.

proportionate with Darcy flux when the transport is dominated by advection. A similar effect was shown in Fig. 6.6, where the time required to achieve the maximum concentration was proportional to the Darcy flux for the advection dominated flow scenario. However, for both advection-controlled and diffusion-controlled transport situations, the time to reach the maximum concentration increases linearly with depth, as the Darcy flux or diffusion is steady.

6.4.3 Dispersivity

The effect of longitudinal dispersivity on the maximum relative concentration at different depths and the time required to achieve the maximum concentration is shown in Fig. 6.9. The maximum relative concentration at a particular depth and the time required to achieve the maximum concentration decrease with increasing dispersivity. The elevated spreading and dilution associated with higher dispersivity causes a slightly lower maximum concentration and the time required to reach the maximum concentration.

6.4.4 Thickness of the Stabilized Layer

Effect of thickness of the stabilized subbase layer on the maximum relative concentration and the time required to achieve the maximum concentration is shown in Fig. 6.10. Lower maximum relative concentrations are obtained when the stabilized subbase layer is thinner (Fig. 6.10a) because less chemical mass is present in a thinner stabilized layer, whereas, the ability of the subgrade to adsorb and re-distribute contaminants remains unchanged.

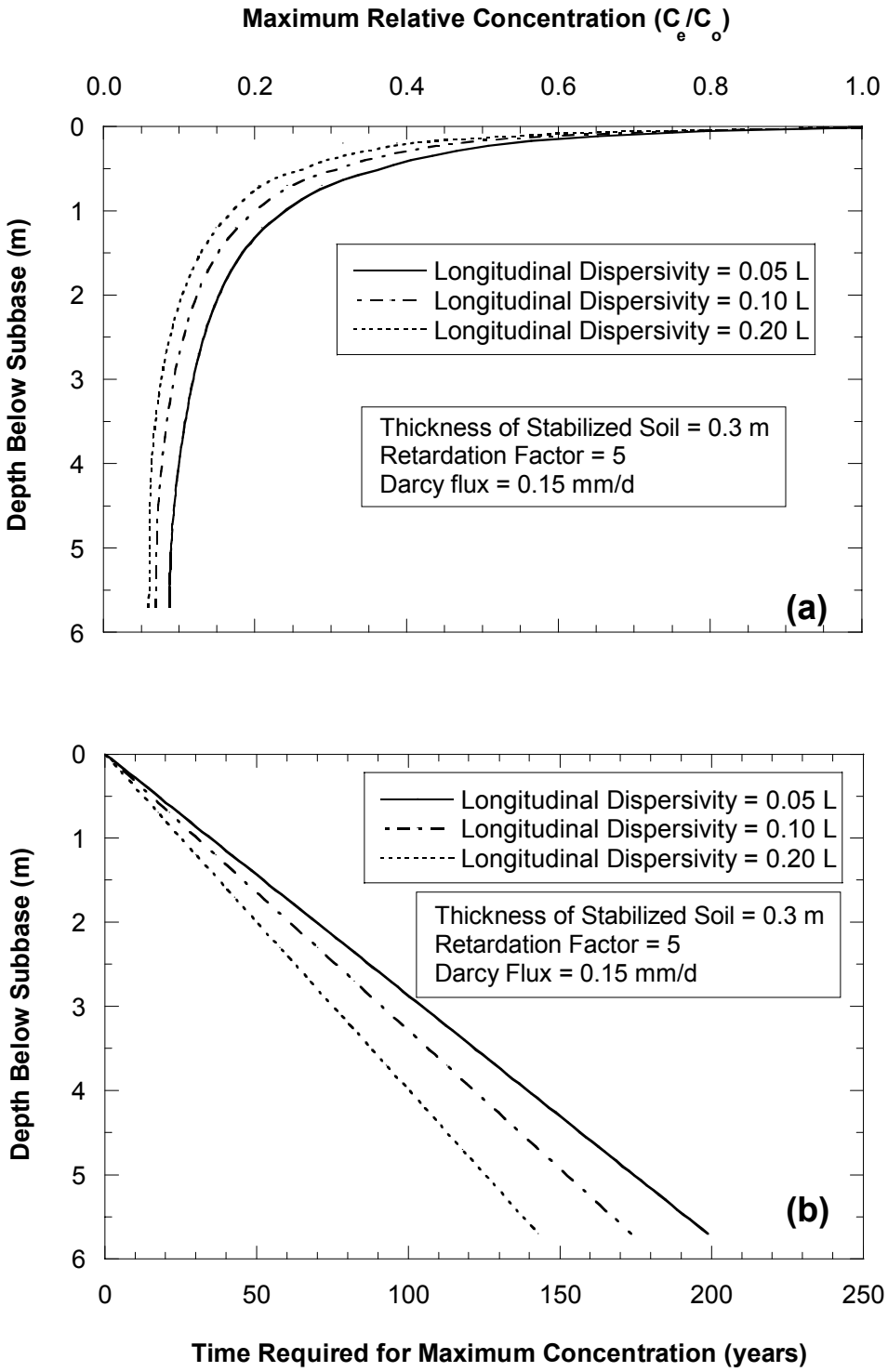

Fig. 6.9. Maximum Effluent Concentration (a) and Time to Reach Maximum Concentration (b) as a Function of Dispersivity Ranged from 0.05 L to 0.20 L.

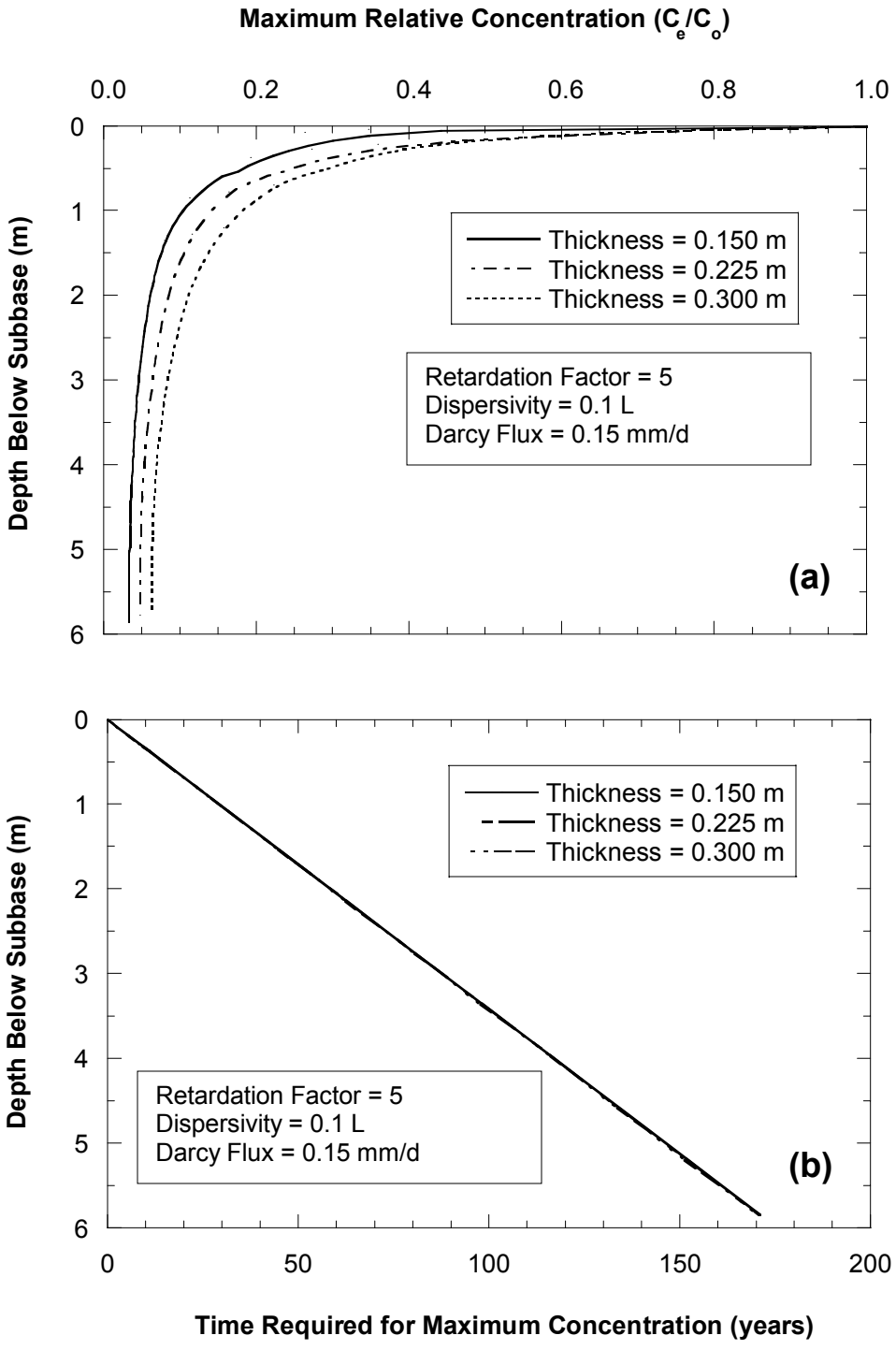

Fig. 6.10. Maximum Relative Concentration (a) and Time to Reach Maximum Concentration (b) as a Function of Depth for Stabilized Subbase Layers Ranged from 0.15 m to 0.30 m.

The time required to achieve the maximum relative concentration is essentially independent of the thickness of the subbase layer (Fig. 6.10b). Thickness of the stabilized subbase does not affect the time for the maximum concentration because the time for maximum concentration is controlled by the rate at which mass is discharged from the stabilized subbase and transported through the subgrade. The rate of both the discharge and transport is directly proportional to Darcy flux, and is influenced by the retardation factor and dispersivity of the subbase and subgrade layer. Since the Darcy flux, and the retardation factor and dispersivity of both layers were not varied in the simulations, the time required to achieve the maximum relative concentration is not expected to be a function of thickness of the stabilized layer.

SECTION 7

CONCLUSIONS

The primary objective of this study was to conduct an in-depth assessment of leaching of heavy metals from fly ash stabilized soil used in highway construction. An additional objective was to estimate the potential for groundwater contamination in a typical highway containing a stabilized layer. To achieve these objectives, four different tasks were undertaken: (1) water leach testing (WLT), (2) laboratory column testing, (3) field lysimeter testing, and (4) numerical modeling. Testing was conducted on fly ash stabilized soils that were prepared with three locally available fly ashes and four subgrade soils representing a range of subgrade soil conditions that might be encountered in Wisconsin.

7.1 Water Leach Testing

Concentrations of metals in leachate from soil-fly ash mixtures prepared with various soil and fly ashes at different fly ash content tend to be lower (1.5 to 2.5 times) than those from fly ash alone. The concentrations of metals in the leachate from soil-fly ash mixtures varies non-linearly with fly ash content and cannot be estimated based on a simple dilution calculation. The non-linear behavior is attributed to the variation in pH with fly ash content, and the effect of pH on the partition coefficient.

Leaching potential of a metal from a soil-fly ash mixture depends on the metal concentration in the fly ash as well as in the soil, pH of the leachate, the

cation exchange capacity (CEC) of the soil, and the type of fly ash. The pH of the leachate increases as the lime content of the fly ash increases.

7.2 Laboratory Column Testing

Column leaching tests conducted on soil-fly ash mixtures showed that the hydraulic conductivity, pH of the effluent, and initial effluent concentration of the soil-fly ash mixture increase with increasing fly ash content, but the partition coefficient is essentially independent of fly ash content. For compacted soil-fly ash mixtures, the effective-to-total porosity varies between 0.65 and 1.08, and the longitudinal dispersivity varies between 0.05 L and 0.24 L, where L is the length of the column.

The initial effluent concentration from the column leaching tests on soil-fly ash mixtures prepared with various soils and fly ash at different fly ash contents is non-linearly related to the concentration obtained from WLTs on similar soil-fly ash mixtures and with the concentration from WLTs on fly ash alone. Non-linearity exist because the pH of the leachate varies with fly ash content, which affects adsorption of metals. In contrast, if the fly ash content is fixed, and the fly ash is spiked with different metal concentrations, initial effluent concentrations from column leaching tests on soil-fly ash mixtures are linearly related to the concentration obtained from the WLTs on soil-fly ash mixtures. A linear relationship exists for spiked fly ashes because the pH remains constant when the fly ash content is fixed.

The release pattern of metals from the soil-fly ash mixtures appears to be adsorption-controlled. Adsorption of metals is highly dependent on the pH of the pore fluid. However, the pH of the soil-fly ash mixtures appears to be persistent for

at least 30 pore volumes of flow, which corresponds to at least 30-yrs of flow in the field.

Column tests conducted on subgrade soils (i.e., soil without fly ash) with synthetic fly ash leachate used as the permeant liquid showed that the partition coefficient of metals for soil-fly ash mixtures is similar to that of the soil alone, and is slightly higher for soils with higher CEC. That is, the partition coefficient depends primarily on the type of soil rather than the fly ash. The column tests also showed that the effective-to-total porosity ratio varies between 0.89 and 1.02, and the longitudinal dispersivity varies between 0.06 L and 0.11 L for compacted fine-grained subgrade soils.

7.3 Field Tests

Lysimeters installed at two field sites were used to monitor the water flux and concentration of metals in leachate from fly ash stabilized soil layer and a control section. The average annual flux through the stabilized sections is approximately 4-6% of the average annual precipitation, and is comparable to that from the control section. Concentrations of most of metals of concern are higher in the fly ash stabilized section than the control section. The concentrations have decreased slightly over time as water has passed through the fly ash stabilized layer.

Concentrations of metals in leachate collected in the lysimeters usually are higher (2 times) than those from WLTs. The concentrations are slightly higher at the Scenic Edge site, where the fly ash content is higher. Concentrations of metals in leachate from the field agree well with concentrations in the effluent from the

column leaching tests, which suggests that the transport parameters obtained from the column leaching tests can be used to predict field conditions.

7.4 Numerical Modeling

A numerical model was developed to simulate leaching and contaminant transport for typical field scenarios where the subgrade is stabilized with fly ash. Simulations conducted using transport parameters obtained from the column tests and Darcy fluxes measured in the field showed that the maximum concentration decreases by a factor of five within the first meter beneath the fly ash stabilized layer, and then decreases gradually at deeper depths. The maximum concentration at a given depth is independent of the retardation factor, and decreases as the dispersion coefficient of subgrade soil increases and the thickness of the stabilized layer decreases.

For an advection-dominated transport scenario, the maximum concentration is independent of Darcy flux, and the time to reach the maximum concentration is inversely proportional to the Darcy flux. The time to reach the maximum concentration increases linearly with depth when the flow is uniform. The time to reach maximum concentration at a particular depth is independent of the thickness of the stabilized layer, and increases as the dispersion coefficient of the subgrade soil decreases and the retardation factor of the subgrade soil increases.

Graphs generated from the results of the numerical simulations are presented that can be used to quantify the maximum relative concentration at a particular depth and the time required to achieve the maximum concentration. The

only required parameter is the initial effluent concentration, which depends primarily on the type of fly ash and can be estimated from a water leach test. To determine the time required to achieve the maximum concentration at a given depth, the Darcy flux and the retardation factor are required. The retardation factor depends primarily on the type of soil being stabilized, but does not vary significantly for fine-grained soils. Thus, quick and reasonable predictions can be made using a conservative estimate of the retardation factor and Darcy flux.

7.5 Practical Implications

According to NR 538 Section of the Wisconsin Administrative Code, the potential for leaching of heavy metals from fly ash stabilized soil is estimated from a water leach test on bulk fly ash. However, the leaching potential of heavy metals is lower for fly ash stabilized soil than for bulk fly ash. Water leach tests on soil-fly ash mixtures intended for use in field construction may provide more realistic estimates of the leaching potential.

Concentration of metals in leachate collected from the lysimeters installed beneath the fly ash stabilized soils were significantly higher than those in leachate from the water leach test. However, prediction made with the numerical model of contaminant transport show that the concentration of metals that exists when the leachate reaches the groundwater table depends significantly on field conditions, and generally is much lower than the concentration measured at the base of the stabilized layer. Thus to evaluate the impact on groundwater, an index test is not sufficient. A systematic evaluation must be conducted to assess each case. The

design charts presented in Sec. 6 of this report can be used to make such an evaluation. A conservative, yet realistic evaluation can be made with this procedure using only the result of a water leach test performed on the intended soil-fly ash mixture.

SECTION 8

REFERENCES

ACAA (1999). "Soil and Pavement Base Stabilization with Self-Cementing Coal Fly Ash," *American Coal Ash Association*, Alexandria, Virginia.

Allen, H. E., Perdue, E. M., and Brown, D. S. (1993). *Metals in Groundwater*. Lewis Publishers, Chelsea, MI, pp. 1-36.

ASTM (1992). "Standard Test Method for Shake Extraction of Solid Waste with Water," *Annual Book of ASTM Standards*, Vol. 04.01, D 3987-85.

Ayala, J., Blanco, F., Garcia, P., Rodriguez, P., and Sancho, J. (1998). "Asturian Fly Ash as a Heavy Metals Removal Material," *Fuel,* Vol. 77, pp. 1147-1154.

Baker, W. T. (1987). "Production and Properties of Fly Ash," *Utilization of Ash Workshop*, University of North Dakota, Grand Forks, May 13-15.

Bilski, J. J. and Alva, A. K. (1995). "Transport of Heavy Metals and Cations in a Fly Ash Amended Soil", *Bulletin of Environmental Contamination and Technology*, Vol. 55, pp. 502-509.

Binner, S., Galeotti, L., Lombardi, F., Mogensen, E., and Sirini, P. (1997). "Mass Balance and Heavy Metals Distribution in Municipal Solid Waste Incineration," *J. of Solid Waste Technology and Management*, Vol. 24 (1), pp. 45-52.

Boles, W. F. (1986). "Fly Ash Facts for Highway Engineers: Technology Transfer," *Federal Highway Administration, FHWA-DP-59-8*, Washington, D.C.

Brunori, C., Balzamo, S., and Morabito, R. (1999). "Comparison Between Different Leaching/Extraction Tests for the Evaluation of Metal Release from Fly Ash," *International J. of Environ. Anal. Chem.,* Vol. (1-2), pp. 19-31.

Brusseau, M. L. (1996). "Evaluation of Simple Methods for Estimating Contaminant Removal by Flushing." *Ground Water*, Vol. 34 (1), pp. 19-22.

Buchter, B., Davidoff, B., Amacher, M. C., Hinz, C., Iskandar, I. K., and Selim, H. M. (1989). "Correlation of Freundlich K_d and n Relation Parameters with Soils and Elements," *Soil Science*, Vol. 148 (5), pp. 370-379.

Canter, L. W., and Knox, R. C. (1985). *Ground Water Pollution Control*. Lewis Publishers, Inc., Chelsea, Michigan.

Chichester, D. L. and Landsberger, S. (1996). "Determination of Leaching Dynamics of Metals from Municipal Solid Waste Incinerator Fly Ash Using a Column Test," *Journal of the Air and Waste Management Association*, Vol. 46, pp. 643-649.

Chiu, T. F. and Shackelford, C. D. (2000). "Laboratory Evaluation of Sand Underdrains," *J. of Geotech. and Geoenvir. Engrg*., Vol. 126 (11), pp. 990-1001.

Chu, S. C. and Kao, H. S. (1993). "A Study of Engineering Properties of a Clay Modified by Fly Ash and Slag," *Fly Ash for Soil Improvement-Geotechnical Special Publication*, Vol. 36, pp. 89-99.

Cockrell, C. F. and Leonard, J. W. (1970). "Characterization and Utilization Studies of Limestone Modified Fly Ash," *Coal Research Bureau*, Vol. 60.

Collins, R. J. and Ciesielski, S. K. (1992). "Highway Construction Use of Wastes and By-products," *Utilization of Waste Materials in Civil Engineering Construction*, ASCE, New York, pp.140-152.

Conner, J. R., (1990). *Chemical Fixation and Solidification of Hazardous Waste*, Van Nostrand Reinhold, New York.

Creek, D. N. and Shackelford, C. D. (1992). "Permeability and Leaching Characteristics of Fly Ash Liner Materials," *Transportation Research Record* 1345.

Das, H. A., Van Der Sloot, H. A., and Wijkstra, J. (1989). "Measurement of the Leaching Behavior of Granular Solid Waste," *Toxicological and Environmental Chemistry,* Vol. 19, pp. 109-118.

DiGioia, A. M. and Nuzzo, W. L. (1972). "Fly Ash as Structural Fill," *J. Power Div.,* ASCE, New York, Vol. 98 (1), pp. 77-92.

DiTorro, D. M., Mahony, J. D., Kirchgraber, P. R., O'Byrne, A. L., Pasquale, L. R., and Piccirilli, D. C. (1986). "Effect of Nonreversibility, Particle Concentration, and Ionic Strength on Heavy Metal Sorption," *Environ. Sci. and Technol*., Vol. 20 (1), pp. 55-61.

Edil, T. B., Sandstorm, L. K. and Berthouex, P. M., (1992). "Interaction of Inorganic Leachate with Compacted Pozzolanic Fly Ash," *J. of Geotech. Engrg.*, ASCE, New York, Vol.118 (9), pp. 1410-1430.

Edil, T. B., Benson, C. H., Bin-Shafique, M. S., Tanyu, B. F., Kim, W., and Senol, A. (2002). "Field Evaluation of Construction Alternatives for Roadway over Soft Subgrade," *Transportation Research Record, 1786 pp. 36-48*.

Evans, J. and Williams, P. T. (2000). "Heavy Metals Adsorption onto Fly Ash in Waste Incineration Flue Gases," *Institution of Chemical engineers (IChemE)*, Vol. 78, pp. 40-46.

Ferguson, G., (1993). "Use of Self-Cementing Fly Ash as a Soil Stabilizing Agent," *Geotechnical Special Publication* No. 36, ASCE, New York, N.Y.

Fetter, C. W. (1993). *Contaminant Hydrogeology*, Macmillan Publishing Company, New York.

Fleming, L. N., Abinteh, H. N., and Inyang, H. I. (1996). "Leachant pH Effect on the Leachability of Metals from Fly Ash," *Journal of Soil Contamination*, Vol. 5 (1), pp. 53-59.

FHWA (1995). "Fly Ash Facts for Highway Engineers", *Federal Highway Administration, FHWA – SA – 44 – 081*, Washington, D.C.

Ganguly, C., Matsumoto, M. R., Rabideau, and Van Benchosten, J. E. (1998). "Metal Ion Leaching from Contaminated Soils: Model Calibration and Application," *J. of Envir. Engrg.*, Vol. 124 (12), pp.1150-1158.

Garavaglia, R. and Caramuscio, P. (1994). "Coal Fly-Ash Leaching Behavior and Solubility Controlling Solids," *Environmental Aspects of Construction with Waste Materials*, Elsevier Science, pp. 87-101.

Garcia, G. M., Missana, T., Molinero, J., and Mingarro, M. (1999). "Migration Experiments in Compacted Ca-bentonite," *Symposium Proceedings*, Materials Research Society, Vol. 556, pp. 695-701.

Gelhar, L. W., Welty, C., and Rehfeldt, K. R. (1992). "A Critical Review of Data on Field-Scale Dispersion in Aquifers," *Water Resources Research*, Vol. 28 (7), pp. 1955-1974.

Ghodrati, M., Sims, J. T., and Vasilas, B. L. (1995). "Evaluation of Fly Ash as a Soil Amendment for the Atlantic Coastal Plain: I. Soil Hydraulic Properties and Elemental Leaching," *Water, Air, and Soil Pollution,* Vol. 81, pp. 349-361.

Ghosh, A., and Sobbarao, C. (1998). "Hydraulic Conductivity and Leachate Characteristics of Stabilized Fly Ash," *J. of Envir. Engrg.* ASCE, New York, Vol. 24 (9), pp. 812-820.

Goh, A. T. C., and Tay, J. H. (1993). “Municipal Solid Waste Incinerator Fly Ash for Geotechnical Applications,” *J. of Geotech. Engrg.*, ASCE, New York, Vol. 119 (5), pp. 811-825.

Gray, D. H., and Lin, Y. K. (1972). “Engineering Properties of Compacted Fly Ash,” *J. of Soil Mech. and Found. Engrg.*, ASCE, New York, Vol. 98 (4), pp. 361-380.

Gustin, F. H. and Thomes, M. R. (1997). “Environmental Aspects of Class C Fly Ash in Soil Stabilization,” *Twelfth International Symposium on Management & Use of Coal Combustion Byproducts*, Jan. 26-30, Orlando, Florida.

Huang, C., Lu, C., and Tzeng, J. (1998). “Model of Leaching Behavior from Fly Ash Landfills with Different Age Refuses,” *J. of Envir. Engrg.*, Vol. 124 (8), pp. 767-775.

Huang, W. H. (1993). *Pavement Analysis and Design*. Prentice-Hall, Englewood Cliffs, NJ.

Huang, W. H., and Lovell, C. W. (1990). “Bottom Ash as Embankment Material.” *Geotechnics of Waste Fills-Theory and Practice*,” ASTM, STP 1070, Philadelphia, PA, pp. 71-85.

Kaminiski, M. D. and Landsberger, S. (2000). “Heavy Metals in Urban Soil of East St. Louis, IL Part:II: Leaching Characteristics and Modeling,” *Journal of the Air and Waste Management Association*, Vol. 50, pp. 1680-1687.

Kanungo, S. B., and Mohapatra, R. (2000). “Leaching Behavior of Various Trace Metals in Aqueous Media from Two Fly Ash Samples,” *J. of Environ. Qual.* Vol. 29, pp. 188-196.

Karczewska, A. Chodak, T., and Kaszubkiewicz, J. (1996). “The Suitability of Brown Coal as a Sorbent for Heavy Metals in Polluted Soils,” *Applied Geochemistry*, Vol. 11, pp. 343-346.

Kim, J. Y., Edil, T. B., and Park, J. E. (1997). “Effective Porosity and Seepage Velocity in Column Tests on Compacted Clay,” *J. of Geotech. and Geoenvir. Engrg*., Vol. 123 (12), pp. 1135-1142.

Kirby, C. S. and Rimstidt, J. D. (1994). “Interaction of Municipal Solid Waste Ash with Water,” *Environ. Sci. and Technol.*, Vol. 28, pp. 443-451.

Kyper, T. N. (1992). “Institutional Constraints to the Use of Coal Fly Ash in Civil Engineering Construction,” *Utilization of Waste Materials in Civil Engineering Construction*, ASCE, New York, pp. 32-43.

Lerman, A. (1979). *Geochemical Processes in Water and Sediment Environments*, John Wiley and Sons, New York.

Lu, C. (1996). “A Model of Leaching Behavior from MSW Incinerator Residue Landfills,” *Waste Management and Research*, Vol. 14, pp. 51-70.

Malhotra, V. M. and Mehta, P. K. (1996). “Pozzolanic and Cementitious Materials,” *Published by Gordon and Breach Publishers*, Amsterdam, Netherlands.

McCarthy, G. J., Beaver, F. and Stevenson, R. J. (1987). “The Essential Role of Mineralogical Characterization in Utilization and Disposal of Coal Conversion Ashes,” *Utilization of Ash Workshop,* University of North Dakota, Grand Forks. May 13-15, 1987.

Means, J. L., Smith, L. A., Nehring, K. W., Gavaskar A. R., Sass, B. M., and Mashni, C. I. (1995). *The Application of Solidification/Stabilization to Waste Materials,* Lewis Publishers, Boca Raton, Florida.

Mitani, T., Nakajima, C., Sungkono, I. E., and Ishii, H. (1995). “Effects of Ionic Strength on the Adsorption of Heavy Metals by Swollen Chitosan Beads,” *J. of Environ. Sci. Health*, Vol. A30 (3), pp. 669-674.

Murarka, I. P., Rai, D., and Ainsworth C. C. (1991). “Geochemical Basis for Predicting Leaching of Inorganic Constituents from Coal-Combustion Residues,” *Waste Testing and Quality Assurance: Third Vol. ASTM STP 1075*, pp. 279-288.

Ogata, A. and Banks, R. B. (1961). “A Solution of the Differential Equation of Longitudinal Dispersion in Porous Media,” *US Geological Survey Profl. Paper 411-A*, US Geological Survey, Washington D. C.

Prammer, M. G, Drack, E. D, Bouton, J. C, Gardner, J. S, (1996). “Measurements of Clay-bound Water and Total Porosity by Magnetic Resonance Logging,” *Log-Analyst*. Vol. 37 (6), pp. 61-69.

Papini, M. P., Kahie, Y. D., Troia, B., and Majone, M. (1999). “Adsorption of Lead at Variable pH onto a Natural Porous Medium: Modeling of Batch and Column Experiments,” *Environ. Sci. and Technol.,* Vol. 33, pp. 4457-4464.

Reed, B. E. and Nonavinakere, S. K. (1992). “Metal Adsorption by Activated Carbon: Effect of Complexing Ligands, Competing Adsorbates, Ionic

Strength, and Background Electrolyte," *Separation Science and Technology*, Vol. 27 (14), pp. 1985-2000.

Ricou, P., Lecuyer, I., and Cloirec, P. L. (1998). "Influence of pH on Removal of Heavy Metallic Cations by Fly Ash in Aqueous Solution," *Environmental Technology, Vol*. 19 (10-11), pp. 1005-1016.

Ricou, P., Lecuyer, I., and Cloirec, P. L. (1999). "Removal of Cu^{+2}, Zn^{+2}, and Pb^{+2} by Adsorption onto Fly Ash and Fly Ash/Lime Mixing," *Wat. Sci. Tech.,* Vol. 39 (10-11), pp. 239-247.

Roy, D. M., Luke, K. and Diamond, S. (1985). "Characterization of Fly Ash and Its Reaction in Concrete," *Fly Ash and Coal Conversion By-Products: Characterization, Utilization, and Disposal I*, Materials Research Society, Vol. 43.

Sauve, S., Hendershot, W., and Allen, H. (2000). "Solid-Solution Partitioning of Metals in Contaminated Soils: Dependence on pH, Total Metal Burden and Organic Matter," *Envir. Sci. and Technol.*, Vol. 34 (7), pp. 1125-1131.

Selim, H. M. and Ma, L. (1995). "Transport of Reactive Solute in Soils: A Modified Two-Region Approach," *Soil Sci. Soc. Am. J*. Vol. 59, pp. 75-82.

Shackelford, C. D. (1994). "Critical Concepts for Column Testing," *J. of Geotech. Engrg.,* Vol.120 (10), pp. 1804-1828.

Shackelford, C. D. and Glade, M. J. (1997). "Analytical Mass Leaching Model for Contaminated Soil and Soil Stabilized Waste," *Ground Water*, Vol.34 (2), pp. 233-242.

Simunek, J., Sejna, M., and van Genuchten, M. Th. (1999). *Simulating Water Flow and Solute Transport in Two Dimensional Variably Saturated Media*, International Groundwater Modeling Center, Golden, Colorado.

Stewart, B. R., Daniels, W. L., Zelazny, L. W. and Jackson, M. L. (2001). "Evaluation of Leachates from Coal Refuse Blended with Fly Ash at Different Rates," *J. of Envir. Qual*, Vol. 30, pp. 1382-1391.

Stumm, W. and Morgan, J. J. (1995). *Aquatic Chemistry*, A Wiley-Interscience Publication, John Wiley and Sons, Inc., New York.

Theis, T. M. and Wirth, J. L. (1977). "Sorptive Behavior of Trace metals on Fly Ash in Aqueous Systems," *Envir. Sci. and Technol*., Vol. 11 (12), pp. 1096-1100.

TRB (1987). “Lime Stabilization: Reactions, Properties, Design, and Construction”, *State of the Art Report 5*. Transportation Research Board, National Research Council, Washington, D.C.

Torrey, S. (1978). *Coal Ash Utilization: Fly Ash, Bottom Ash and Slag*, Published by Noyes Data Corporation, Park Ridge, NJ.

Van Genuchten, M. Th. (1981). “Analytical Solutions for Chemical Transport with Simultaneous Adsorption, Zero-order Production, and First-order Decay,” *J. of Hydrology*, Vol. 49, pp. 213-233.

Walton, J. C., Bin-Shafique, M. S., Smith, R. W., Gutierrez, N., and Tarquin, A. J. (1997). “Role of Carbonation in Transient Leaching of Cementitous Wasteforms,” *Envir. Sci. and Technol.,* Vol. 32 (8), pp. 2345-2349.

Weber, J. T. and Adriano, D. C. (2001). “Influence of Fly Ash on Soil Physical Properties and Turfgrass Establishment,” *J. Envir. Qual.,* Vol. 30, pp. 596-601.

Weng, C. H. and Huang, C. P. (1990). “Removal of Trace Heavy Metals by Adsorption onto Fly Ash,” *J. of Envir. Engrg.*, pp. 923-925.

Yan, R., Gauthier, D., and Flamant, G. (2001). “Volatility and Chemistry of Trace Metals in a Coal Combustor”, *Fuel*, Vol. 80 (15), pp. 2217-2226.

Yeh, Y. J., Lee, C. H., and Chen, S. T. (2000). “A Tracer Method to Determine Hydraulic Conductivity and Effective Porosity of Saturated Clays Under Low Gradients,” *Ground Water*, Vol. 38 (4), pp. 522-529.